DESIGN AND SYNTHESES OF POLYMERIC MATERIALS FOR VISIBLE AND NEAR-INFRARED EMITTING APPLICATIONS

by

Sean Owen Clancy

A Dissertation Presented to the
FACULTY OF THE GRADUATE SCHOOL
UNIVERSITY OF SOUTHERN CALIFORNIA
In Partial Fulfillment of the
Requirements for the Degree
DOCTOR OF PHILOSOPHY
(CHEMISTRY)

May 2005

EPIGRAPH

Science is the tool of the Western mind and with it more doors can be opened than with bare hands. It is part and parcel of our knowledge and obscures our insight only when it holds that the understanding given by it is the only kind there is.

Carl Gustav Jung (1875 – 1961)

Science is a wonderful thing if one does not have to earn one's living at it.

Albert Einstein (1879 – 1955)

The really good idea is always traceable back quite a long way, often to a not very good idea that sparked off another idea that was only slightly better, which someone else misunderstood but in such a way that he then said something that really was quite interesting, which was picked up by someone else who combined it with an earlier idea, which most other people there had forgotten, all of which was reshaped by someone else, and so on and so on.

John Cleese (1939 –)

ACKNOWLEGMENTS

Last, but certainly not least, I want to thank my wife, Melissa, without whom none of what I am today would have been possible. She has been my inspiration and best friend. I cannot imagine life without her.

TABLE OF CONTENTS

LIST OF TABLES

LIST OF FIGURES

LIST OF SCHEMES

ABSTRACT

Several classes of polyphenylene-type polymeric materials were synthesized according to several different design parameters, with the end results of each being able to sensitize small molecule organics or lanthanide chelates as dopants which emit energy in the visible and/or near-infrared regions of the electromagnetic spectrum. The goal of this research was to create materials that would emit in the near-infrared. The first group of materials was *para-para* linked polyphenylene-type polymers doped with several small molecule organic dyes. The second group was *para-para* and *para-meta* linked polyphenylene-type polymers doped with a series of Coumarins and a couple metalloporphines. The third group was *para-meta* linked polyphenylene-type polymers with pendant terpyridine groups. The fourth group was *para-meta* linked polyphenylene-type polymers with various pendant *beta*-diketonates to which europium complexes were bound. The fifth group was *para-meta* linked polyphenylene-type polymers with various pendant *beta*-diketonates to which erbium-porphyrinate complexes were bound.

The first and second groups served as preliminary studies on the energy transfer properties of polymers to organic dyes. With a better understanding of how doped conjugated polymers behaved, other polymers were designed with specific structural properties that lead to the desired photophysical properties. This elaboration of structure-property relationships also lead to the pendant groups to which the

lanthanides would be datively or covalently bonded to the polymer, as was studied with the third and fourth groups, respectively. Upon this foundation, the fifth group of materials reached the goal of having polymeric-materials that emitted energy in the near-infrared region of the electromagnetic spectrum.

CHAPTER 1

INTRODUCTION

1.1 Historical overview.

Polymers may be the most important discoveries by man, and during the last few decades polymers have replaced metallic components in many applications ranging from car bumpers to building materials. However, the pioneering work of Nobel laureates Heeger, MacDiarmid and Shirakawa in 1977 inspired the use of polymers as conductors.[1] The transition of polymers from insulators to conductors opened up a variety of new functions. In 1990, Friend *et al.* added another valuable application to the already growing list for conjugated polymers.[2] A plastic sandwich made up of polymers produced light upon applying a voltage to it, which was previously seen in small molecule, aluminum *tris*(8-hydroxyquinolate) (Alq_3) devices.[3,4] Since then, conducting polymers have been used in polymeric light emitting devices (PLEDs)[5,6,7,8] and photovoltaic cells.[9,10,11,12] Polymeric devices are easy to process and can be produced in bulk at a low cost. They also have excellent luminescent properties such as; high brightness, high contrast, low power consumption, and being light weight. These properties make polymers suitable emissive materials for notebook computers, cell phone displays, and flexible displays. Polymeric OLEDs, or PLEDs, are fabricated by sandwiching a polymer layer with two electrodes, which are shown in Figure 1.1.
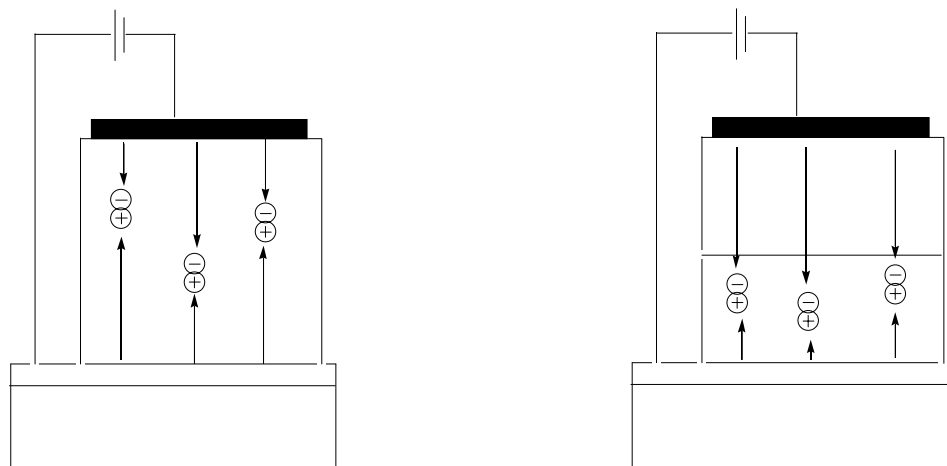
Figure 1.1. Configurations of typical single layer and double layer electroluminescent cells.

Organic conjugated polymers consist of a long carbon chain with alternating single and double carbon-carbon bonds. The carbon-carbon double bond consists of a strong σ bond formed by the sp^2 hybridized orbital, and a π bond formed by the overlap of the remaining P_z orbital. The π molecular orbitals spread along the polymer chain. Low energy bonding π orbitals form the valence band, whereas the high energy, anti-bonding, π^* orbitals form the conduction band. The separation between these two bands corresponds to the band gap. The band gap between the valence band (VB) and the conductance band (CB) of the material influence the behavior of the material as a semiconductor or an insulator. Insulators usually have a band gap of about 10 eV or higher, and most semiconductors have a band gap between 1.5 eV to 3.0 eV. General representations of these band gaps for insulators, semiconductors, and conductors are illustrated in Figure 1.2. The chemical composition and the polymer structure can be changed to obtain desired emission.
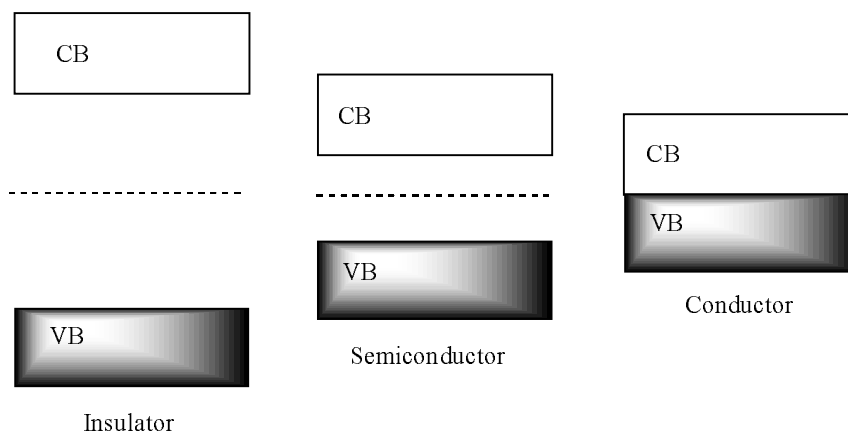
Figure 1.2. Schematic representations of the position of valence band and the conductance band for insulators, semiconductors, and conductors.

Conducting polymers can be obtained through chemical or electrochemical oxidation or reduction of an insulator. Doping converts an insulating polymer to a conducting polymer via introduction of a simple anionic or cationic species, known as dopants. Oxidation of the polymer causes a removal of electrons and introduction of negatively charged counter ions to preserve the charge neutrality. This is called p-type doping, and is usually achieved with I_2, PF_6, AsF_6. Conversely, upon reduction of the polymer, the addition of electrons and introduction of positively charged ions to the polymer occurs. This is called n-type doping, and is usually achieved with Na, K, Li, Ca. Figure 1.3 shows how doping relates to the band gap of the polymer, along with how optical excitation also moves an electron to the conduction band. An increase in doping concentration results in an increase in the conducting property of the polymer. Most doped conjugated polymers had conductivities as high as that of copper.
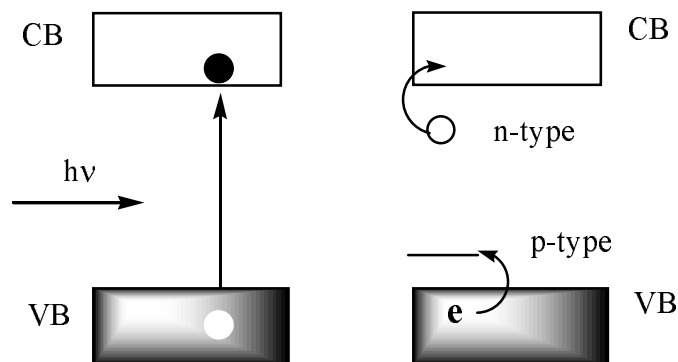
Figure 1.3. The creation of excited state via optical excitation of an undoped system, and a mechanism of doping in doped state.

The simplest form of a PLED device is made by using a thin layer of the polymer sandwiched by two electrodes. The negative electrode injects electrons to the polymer layer (reduction) and the positive electrode injects holes (oxidation). The recombination of the hole and the electron produces light. The organic materials provide a media for charge transport and a site for recombination. The nature of the materials used affects these charge transport properties and could affect overall device efficiency. The neutral bound state formed upon recombination of hole and electron is characterized in terms of it's spin wave function either as a singlet excited state (S = 0) or a triplet excited state (S = 1). Theoretical analysis indicates that electrical excitation produces only 25% singlet states.[13] Experimental studies indicate that the limit for external quantum efficiency of a small molecule based device is 0.25[14] and a polymeric device is 0.57.[15] Thompson and Forrest through their pioneering work have reported that electrophosphorescent devices have higher

efficiencies than electroluminescent devices.[16] The challenge in the future is to design and synthesize polymeric devices with higher external efficiencies.

1.2 Color tuning – band gap engineering

A major advantage of polymeric devices is the ease with which the device properties can be altered by varying the chemical composition and the structure of the polymer. To illustrate this phenomenon, polymers with different substitution groups are shown in Figure 1.4. The photophysical properties of the polymers are summarized in Table 1.1.
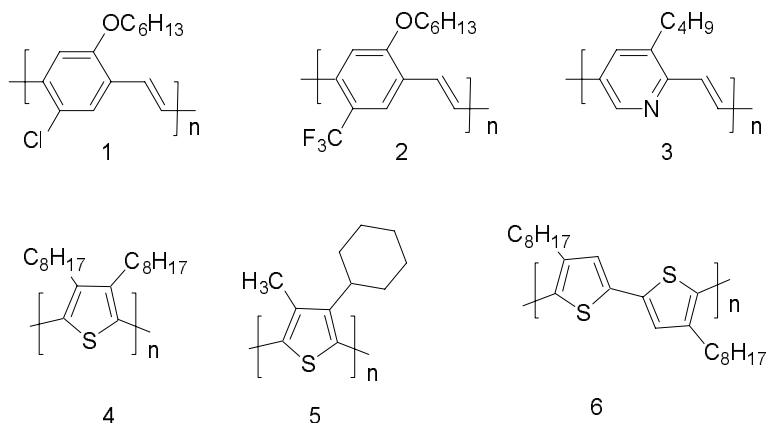
Figure 1.4. Chemical structures of polymers used to illustrate the structure-property relationship.

The red emission in Polymer **1** changes yellow, upon changing substitution in polymer **2**. PPV has an emission maximum in the green region where as **3**, the pyridine version of PPV has an emission in the blue region. Varying the substitution at the 3-position of poly(3-alkylthiophenes) changes the emission maxima and the

emission efficiency.[17] Polymers **4** (blue) and **6** (green) indicate the effect of the monomer on the emission properties of the polymer.

Table 1.1. Photophysical properties of polymers used to illustrate the structure-property relationship.

Compound	Color	Emission Max	Reference
1	Red	620-630 nm	Friend [18]
2	Yellow	540-570 nm	Friend [19]
3	Red	630 nm	Swager[20]
4	Blue	460 nm	Gill[21]
5	Blue	460 nm	Berggren[22]
6	Green	530 nm	Gill

1.3 Polymer photophysics

Interaction of matter with light produces an excited state which relaxes back to the ground state via different processes. Alternate pathways compete with each other to dissipate the energy of the molecule. The most dominant pathway is decided by factors such as structure, chemical environment, nature of the excited state, and experimental conditions. The processes available to an excited state can be represented in a Jablonski diagram, which is shown in Figure 1.5. Depending upon the energy of the incident light, different excited states with different energies can be populated. The time frame for an electronic transition (10^{-15} s) is less than that for a molecular vibration (10^{-13} s). Thus according the Franck-Condon principle, the molecule remains frozen during the production of an excited state. The electron does not have time to invert the spin. As a result optical excitation produces a singlet excited state.
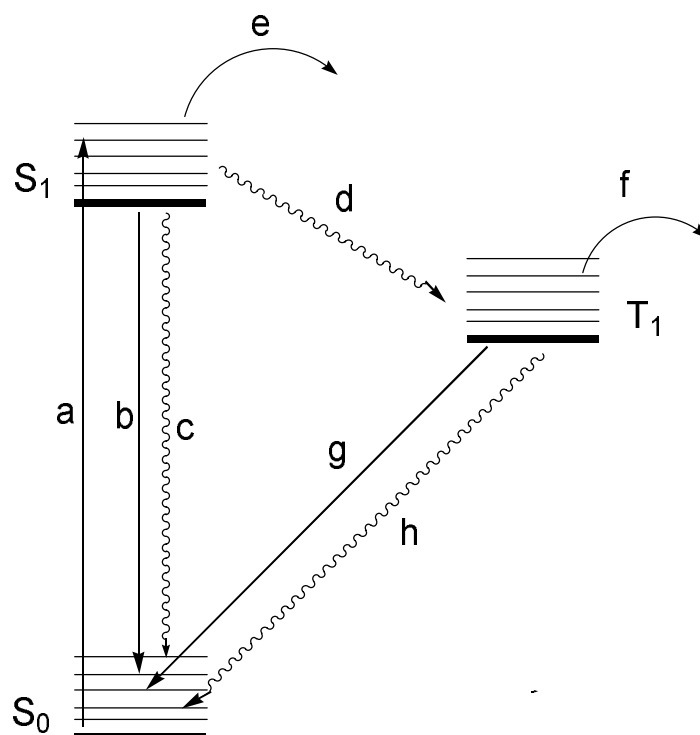
Figure 1.5. Energy level diagram showing modes of deactivation.
(a – absorbance; b – fluorescence; c – nonradiative decay; d – intersystem crossing; e – singlet energy transfer; f – triplet energy transfer; g – phosphorescence; h – internal crossing.)

The conversion between same spin states are termed internal conversion, where as the conversion between different spin are termed intersystem crossing (ISC). A chromophore excited to a higher energy level would immediately relax to the lowest energy state via internal conversion (IC). Intersystem crossing (ISC) is spin forbidden, but made possible by spin-orbit coupling. Heavy atoms such as platinum, iridium and lanthanides increase the intersystem crossing by exerting the "heavy atom effect".[23] The singlet state formed on optical excitation could intersystem cross to produce a triplet state. The excited state (singlet or triplet) could decay radiatively or nonradiatively. In radiationless decay, the electronic energy converts to rotational

or vibrational motions of the polymer or the solvent surrounding the polymer. To be considered as a potential emitter materials for PLEDs, polymers must emit light, thus radiative decay becomes important in this discussion. Radiative decay can be termed; fluorescence, phosphorescence or delayed fluorescence, depending on the origin of the transition. Fluorescence (FL) is the emissive transition between states of same spin multiplicity. Due to favorable spin considerations, fluorescence has shorter lifetimes. Conversely, emission from a triplet excited state to the singlet ground state is phosphorescence (PH). Phosphorescence, therefore, is spin forbidden, and as a result has longer lifetimes with low efficiencies. Delayed fluorescence (DF) occurs from the singlet excited state, which is populated via the triplet state, either by thermal repopulation or by triplet-triplet annihilation, which is represented by Scheme 1.1.

$$S_0 \xrightarrow{h\nu} S_1 \xrightarrow{\text{ISC}} T_1 \xrightarrow[\text{ISC}]{\Delta} S_1 \downarrow DF$$

$$T_1 + T_1 \longrightarrow S_1 + S_0 \downarrow DF$$
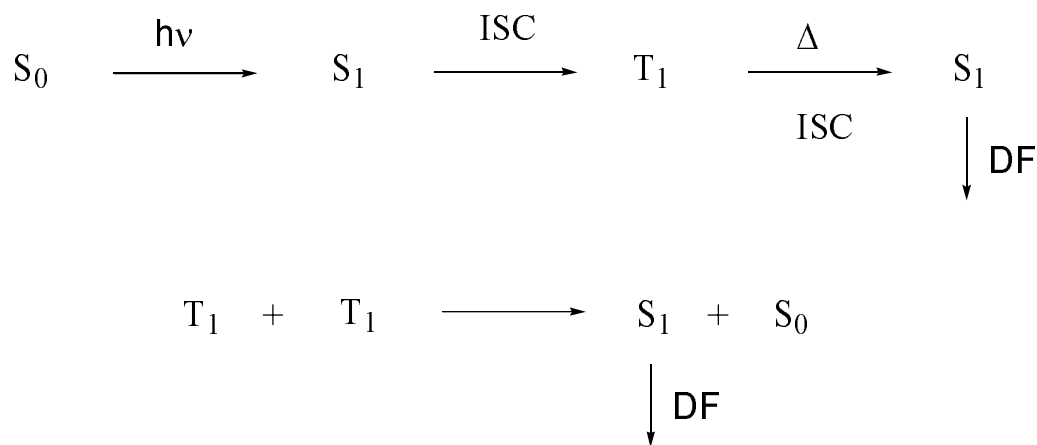
Scheme 1.1. Schematic representation of origin of delayed fluorescence.

Energy transfer donates the transfer of energy from an excited molecule to a molecule in its ground state. Important photophysical processes take place on polymers that are due to interchain interactions, i.e. excimers and aggregates. An excimer is the complex formation between an excited polymeric molecule and another polymer molecule in its ground state. When the π orbitals of the polymeric chains interact to form excimers, the two polymer chains must be separated by about 0.3 nm to form stable excimers. Aggregates, on the other hand, have a new absorption band in the low energy region, which is due to delocalization of the electronic wave function over two or more polymer molecules in the ground state as well as the excited state. Both these interactions have emission in longer wavelengths and have longer lifetimes than the polymer alone.

1.4 Doped Systems

Self-quenching is an important drawback of an Alq_3 device. A method to overcome this problem is to add an emissive dopant into the Alq_3, as illustrated in Figure 1.6.[24] Energy is transferred from the host to the guest dye resulting in efficient emission from the dopant, along with an increased performance from the device. Doping is also used to tune the color of a device by using dyes of different energy.[25] Conventionally, fluorescent laser dyes are used as dopants, however triplet dyes can be used in devices. Since the dopant is used in low concentrations (~1%) triplet-triplet annihilation of the guest dye is not a concern.
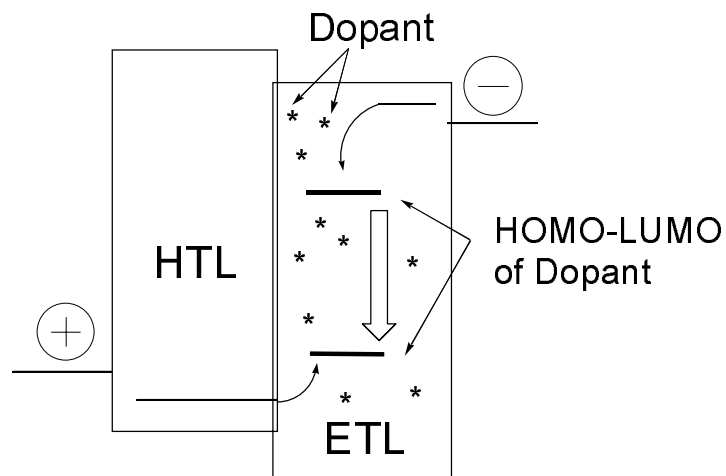
Figure 1.6. A representation of the operation of OLED with a dopant dye.

An organic light-emitting device (OLED) with improved efficiency was fabricated by doping bathocuproine (BCP) into aluminum *tris*(8-hydroxyquinoline) (Alq$_3$) as an electron-transporting and hole-blocking layer. The devices with a 5% BCP doping had an improved luminous efficiency.[26] Device optimization with red dye doped Alq$_3$ emitters in OLEDs were reported to have efficiencies of 3.24 cd/A.[27] Several new 1H-pyrazolo[3,4-b]quinoxaline derivatives with N,N-dialkylamine electron donating groups were used as dopants for Alq$_3$ devices to achieve bright green emission with efficiencies of 7.5-9.7 cdA^{-1}.[28] The use of diphenylamine-substituted Coumarin, (dicyanomethylene)pyran, and benzophenoxazone dyes as potential red and green dopants for OLEDs were reported by IBM.[29] Conjugated polymers doped with singlet dyes such as Coumarin 6 and Nile Red dyes which were diffused selectively into a poly (9-vinylcarbazole)-based emitting layer using a novel method to fabricate dye diffused PLEDs.[30] Since polymers are not able to be used as efficient

electrophosphorescent devices, triplet emitters are used. Efficient single-layer polymer light-emitting diodes that employed a green phosphorescent-sensitizer, bis(2-Ph-pyridinato-N,C2')iridium(acetylacetonate) doped in a PVK/PBD were reported.[31] Also electrophosphorescent devices were fabricated by doping Ir(DPF)$_3$ into a host polymer matrix of poly(N-vinylcarbazole) to achieve a external quantum efficiency of 10% photon/electron.[32] Polymeric light emitting devices with cyclometalated irridium complexes[33] and bis[2-(2'-benzothienyl)-pyridinato-N,C3']iridium(acetylacetonate)[34] as the phosphorescent dopants were reported. Near-infrared-emitting polymer light-emitting diodes were fabricated using blends of conjugated polymers and lanthanide *meso*-tetraphenylporphyrinate complexes, where emission was observed at 1560 nm from a device fabricated using erbium as the lanthanide.[35]

The host, a small molecule or a polymer, has to transfer its energy to the dopant dye molecule. The method of energy transfer for singlet laser dyes was different than that for triplet dyes. The external efficiency of the device depends on the energy transfer efficiency and the emission efficiency of the dopant. The latter can be optimized by selecting laser dyes with near unity efficiency. The energy transfer efficiency is a function of both the donor and the acceptor along with other physical parameters such as donor-acceptor separation. To better understand and design efficient polymer/dye systems, energy transfer of polymers needs to be studied.

1.5 Energy transfer

Energy transfer is of two types, energy transfer between two different molecules (intermolecular) or energy transfer between different sites within the same molecule (intramolecular). To achieve higher energy transfer efficiencies all factors affecting energy transfer processes has to be considered. Initial discussion of energy transfer will focus on intermolecular energy transfer and the importance of intramolecular energy transfer will be discussed later. Energy transfer takes place in two distinctive pathways, radiative mechanism and nonradiative mechanism. The latter is subdivided into long range (resonance) transfer and shorter range (exchange) transfer mechanism.

The radiative (trivial) energy transfer takes place when the acceptor absorbs a photon emitted by the donor. The mechanism of the process is as,

$$D \quad + \quad h\nu \quad \rightarrow \quad D^* \tag{1.1}$$

$$D^* \quad \rightarrow \quad D \quad + \quad h\nu' \tag{1.2}$$

$$A \quad + \quad h\nu' \quad \rightarrow \quad A^* \tag{1.3}$$

The efficiency of the process depends on the spectral overlap (J) between the donor emission and the acceptor absorbance.

$$J = \int_0^\infty F_D(\bar{\nu})\varepsilon_A(\bar{\nu})d\bar{\nu} \tag{1.4}$$

It is obvious that the energy transfer efficiency does not depend on the distance separating the donor and the acceptor, but only on the spectral overlap.

Nonradiative energy transfer takes place when the electronic excitation energy of acceptor is less than that of the donor. The energy transfer process is fast enough so that it takes place during the lifetime of the excited state. The resonance energy transfer (**RET**) is the predominant mechanism that dominates when the donor-acceptor separation is larger than the sum of their collusional radii. This mechanism can be visualized in Scheme 1.2.
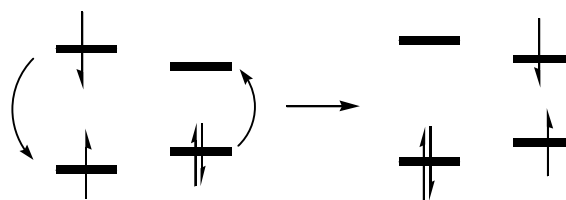
Scheme 1.2. Schematic representation of the energy transfer by Förster mechanism.

This process is also known as the Förster mechanism, due to the major contribution by himself.[36] The rate of energy transfer (k_{et}) is defined as,

$$k_{et} = \frac{C}{\tau_D^0 R^6} \int F_D(\overline{v}) \varepsilon_A(\overline{v}) \frac{d\overline{v}}{\overline{v}^4} \qquad (1.5)$$

where F_D is the spectral distribution of donor emission, ε_A is the molar extinction of the acceptor, τ_D is the intrinsic lifetime of the donor, R is the distance between the donor (D) and the acceptor (A). The validity of the equation 1.5 depends on: the interaction between D* and A being mainly between the electrical dipole transitions moments, thermal equilibrium is complete before energy transfer, and neither D nor

A undergoes significant interaction with the solvent. If $D^* \rightarrow D$ is forbidden (less efficient, longer lifetime) but $A \rightarrow A^*$ is allowed, the energy transfer still takes place with higher efficiency. Conversely, if $D^* \rightarrow D$ is allowed, but $A \rightarrow A^*$ is forbidden, energy transfer is less likely to take place due to rapid deactivation of D^*. The distance between D and A where the energy transfer efficiency is 0.50 is defined as the Föster radii (R_o). Based on the assumption that emission profile of D is similar to the absorbance profile, R_o is calculated theoretically as,

$$R_o^6 = \frac{k_{et}\tau_D}{\bar{v}_0^2} \int \varepsilon_A(\bar{v})\varepsilon_D(2v_0 - \bar{v})d\bar{v} \qquad (1.6)$$

The rate of energy transfer is redefined as,

$$k_{et} = \frac{1}{\tau_D}\left(\frac{R_o}{R}\right)^6 \qquad (1.7)$$

Both processes discussed have common properties and are dependent on the spectral overlap (J). However, for trivial energy transfer the donor has to emit a photon, where as RET takes place before the photon is emitted. The rate of RET depends largely on the distance R, whereas the trivial mechanism is independent of the distance. If the lifetime of the donor emission is dependant of the concentration of the acceptor, then the trivial mechanism is excluded experimentally.

Another method of energy transfer is known as Dexter energy transfer, which is also called the exchange mechanism. The process of Dexter energy transfer is visualized as a double electron shift, although an electron transfer does not take place. The

Dexter mechanism takes place between donor and acceptor that are extremely close, and in most cases they are connected, thus the mechanism is also called the through bond mechanism. This mechanism can be visualized in Scheme 1.3.
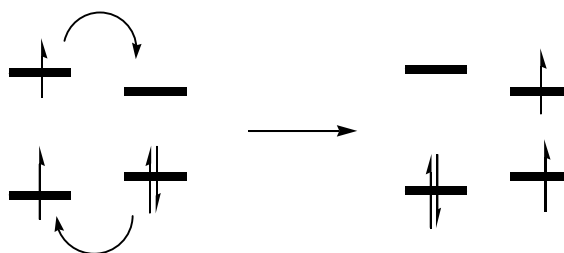
Scheme 1.3. Schematic representation of the energy transfer by Dexter mechanism.

1.6 Scope of this work

The scope of the thesis is the use of luminescent organolanthanide ions as efficient triplet energy acceptors in conjugated polymers. This is a novel method by which both singlet and triplet energy is efficiently harvested. OLEDs and related devices made from these materials are expected to possess efficiencies that exceed the limits imposed by the inability of most conjugated polymers to exhibit triplet luminescence. The lanthanide complexes utilized have the ability to harvest both singlet and triplet excited states from the polymers, which give rise to a higher efficiencies of emission. The removal of long lived polymer triplet states will also reduce excited state chemical reactions, thus slowing down a method of polymer degradation.

Furthermore, these materials are expected to give pure color emission due to narrow linewidths characteristic to the atomic emission of lanthanides. Lanthanide based devices have been reported in literature, the most noteworthy is the europium complexes of β-diketonates prepared and doped into blue-emitting poly[2-(6'-cyano-6'-methyl-heptyloxy)1,4-phenylene] (CN-PPP) by Heeger *et al.*[37] Conjugated polymers with side chains attached with europium complexes have also been reported by Liu *et al.*[38] Two new kinds of complexes, Eu(aspirin)$_3$phen and Tb(aspirin)$_3$phen, were synthesized and doped into the conjugated polymer, PVK.[39] Infrared emitting polymeric devices were made with blends of the conjugated polymers and complexes of Yb, Er, and Ho.[40]

Conjugated polymers were designed to have high energy transfer efficiencies to lanthanides. The *J* states of lanthanides have the proper symmetry to accept energy from triplet states of the organic complexes. The conventional wisdom predicts that the energy transfer from polymer to lanthanides takes place via the exchange mechanism. The separation between the donor and the acceptor has to be extremely small. The polymers designed have the ability to chelate to metals in such a way that the donor-acceptor distance was very small in order to facilitate efficient Dexter energy transfer. The coordination of a heavy atom such as lanthanides served another purpose; the heavy atom effect converts more singlet excited states to triplet excited states. The triplet states were then harvested by the lanthanide giving rise to efficient emission.

The polymers upon optical excitation gave rise to a distribution of excited states. The heavy atom effect, exerted by the lanthanide, created a high concentration of triplet states. This was harvested by the triplet excited states of the ligand system, which in turn was transferred to the lanthanide. Large singlet triplet gaps (ΔE_{ST}) ensured that the triplet state is not transferred back to form singlet states. The energy requirement for polymer $\rightarrow$ ligand energy transfer is that the ligand be lower in energy than the polymer. For this energy to be transferred to europium to obtain efficient emission the ligand has to be higher in energy than the $^5D_1$ level of europium. The energy of the lanthanides remains as a fixed constant troughout the polymer design process. The energy of the ligand should be 2000 cm^{-1} above the $^5D_0$ (17,260 cm^{-1}) level of europium to prevent thermal back energy transfer.[41,42] This meant that the ligands used must have a triplet state energy of 19,000 cm^{-1}. The same reasoning indicates that for efficient energy transfer the triplet energy of the conjugated polymer must be higher than 19,000 cm^{-1}. If the triplet energy of the polymer is lower than the ligand triplet state, only singlet states will be harvested. Since the polymers were designed to give rise to more triplet states, the energy transfer would be less efficient. The triplet states trapped would not relax radiatively, and the long lifetimes will facilitate excited state reactions that enhance polymer degradation. The scope of the dissertation was to understand the structure-property relationship of conjugated polymers, and to utilize that knowledge to develop polymers with the ability to sensitize europium and erbium.

The organization of the remainder of this dissertation continues with a discussion of using *para*-polyphenylene type polymers to sensitize several laser dyes in Chapter 2, with Chapter 3 expanding on this to include a *para*-only and *para-meta* linked polyphenylene type polymers to sensitize a series of singlet emitting Coumarins and several triplet emitting metalloporphines. Chapter 4 concerns the use of *para-meta* polyphenylene type polymers with pendant terpyridine groups which sensitize a variety of europium complexes. Chapter 5 is a study of *para-meta* polyphenylene type polymers with β-diketonate type groups which sensitize a variety of europium complexes. Chapter 6 discusses again *para-meta* polyphenylene type polymers with β-diketonate type groups, but this time they are sensitizing the infrared emitting erbium porphyrinates to which they are bound, and could possibly be used as erbium doped fiber amplifier systems.

1.7 References

[1] Service, R. F. *Science*, **2000**, *290*, 425.

[2] Burroughes, J. H.; Bradley, D. D. C.; Brown, A. R.; Marks, R. N.; Mackay, K.; Friend, R. H.; Burns, P. L.; Holmes, A. B. *Nature*, **1990**, *347*, 539.

[3] Tang, C.W.; vanSlyke S.A. *Appl. Phys. Lett.,* **1987**, *51*, 913.

[4] Tang, C.W.; VanSlyke S.A. *J. Appl. Phys.,* **1989**, *65*, 3610.

[5] Friend, R. H.; Gymer, R. W. ; Holmes, A. B.; Burroughes, J. H.; Marks, R. N.; Taliani, C.; Bradley, D. D. C.; Dos Santos, D. A.; Bredas, J. L.; Logdlund, M.; Salaneck, W. R. *Nature*, **1999**, *397*, 121.

[6] Yan, H.; Huang, Q.; Cui, J.; Veinot, J. G. C.; Kern, M. M.; Marks, T. J.; Yang, R.; Tian, R.; Hou, Q.; Yang, W.; Cao, Y. *Macromolecules*, **2003**, *36*, 7453.

[7] Jin, Y.-D.; Chen, H.-Z.; Heremans, P. L.; Aleksandrzak, K.; Geise, H. J.; Borghs, G.; Van der Auweraer, M. *Synth. Met.,* **2002**, *127*, 155.

[8] Anietz, S.; Wedel, A. *PCT Int. Appl.*, **2002**, 28.

[9]Halls, J. J. M.; Walsh, C. A.; Greenham, N. C.; Marseglia, E. A.; Friend, R. H.; Moratti, S. C.; Holmes, A. B. *Nature*, **1995**, *376*, 498.

[10] Marks, R. N.; Halls, J. J. M.; Bradley, D. D. C.; Friend, R. H.; Holmes, A. B. *J. Phys. Condensed Matter*, **1994**, *6*, 1379.

[11] MacKenzie, J. D.; Stevenson, R.; Halls, J. J. M.; Inbasekaran, M.; Woo, E. P.; Richards, D.; Friend, R. H. *Macromolecules*, **2001**, *34*, 6005.

[12] Koehler, A.; Gruener, J.; Friend, R. H.; Muellen, K.; Scherf, U. *Chem. Phys. Lett.*, **1995**, *243*, 456.

[13] Brown, A. R.; Pichler, K.; Greenham, N. C.; Bradley, D. D.; Friend, R. H.; Holmes, A. B. *Chem. Phys. Lett.*, **1993**, *210*, 61.

[14] Baldo, M. A.; O'Brien, D. F.; Thompson, M. E.; Forrest, S. R. *Phys. Rev. B*, **1999**, *60*, 14422.

[15] Wilson, J. S.; Dhoot, A. S.; Seeley, A. J. A. B.; Khan, M. S.; Kohler, A.; Friend, R. H. *Nature*, **2001**, *413*, 828.

[16] Baldo, M.A.; Lamansky, S.; Burrows, P.E.; Thompson, M.E.; Forrest, S.R. *Appl. Phys. Lett.*, **1999**, *75*, 4.

[17] Kraft, A.; Grimsdale, A. C.; Holmes, A. B. *Agnew. Chem. Int. Ed.*, **1998**, *37*, 402.

[18] Sarnecki, G. J.; Friend, R. H.; Holmes, A. B.; Moratti, S. C. *Synth. Met.*, **1995**, *69*, 545.

[19] Lux, A.; Holmes, A. B.; Cervini, R.; Davies, J. E.; Moratti, S. C.; Grunner, J.; Cacialli, F.; Friend, R. H. *Synth. Met.,* **1997**, *84*, 293.

[20] Tian, J.; Wu, C. C.; Thompson, M. E.; Register, R. A.; Marsella, M. J.; Swager, T. M. *Adv. Mater.*, **1995**, *7*, 395.

[21] Gill, R. E.; Malliaras, G. G.; Wildeman, J.; Hadziioannou, G. *Adv. Mater.,* **1994**, *6*, 132.

[22] Berggren, M.; Inganas, O.; Gustafsson, G.; Rasmusson, J.; Anderson, M. R. Hjertberg, T.; Wennerstrom, O. *Nature*, **1994**, *372*, 444.

[23] Mukherjee, K. K. R. *Fundamentals of Photochemistry*, Wiley Eastern Ltd. India, 1992.

[24] Tang, C.W., VanSlyke, S. A., Chen, C. H., *J. Appl. Phys.*, **1989**, *65*, 3610.

[25] Shoustikov, A. A.; You, Y.; Thompson, M. E. *IEEE J. of Sel. Top. In Quan. Elec.,* **1998**, *4*, 3.

[26] Wu, Z.; Yang, H.; Duan, Y.; Xie, W.; Liu, S.; Zhao, Y. *Semiconductor Science and Technology*, **2003**, *18*, L49.

[27] Liu, T-H.; Iou, C-Y.; Wen, S-W.; Chen, C. H. *Thin Solid Films*, **2003**, *441*, 223.

[28] Wang, P.; Xie, Z.; Hong, Z.; Tang, J.; Wong, O.; Lee, C-S.; Wong, N.; Lee, S. *J. Mat. Chem.,* **2003**, *13*, 1894.

[29] Swanson, S. A.; Wallraff, G. M.; Chen, J. P.; Zhang, W.; Bozano, L.D.; Carter, K. R.; Salem, J. R.; Villa, R.; Scott, J. C. *Chem. Mat.*, **2003**, *15*, 2305.

[30] Nakamura, A.; Tada, T.; Mizukami, M.; Hirose, S.; Yagyu, S. *Appl. Phys. Lett.,* **2002**, *80*, 2189.

[31] He, G.; Chang, S.-C.; Chen, F-C.; Li, Y.; Yang, Y. *Appl. Phys. Lett.,* **2002**, *81*, 1509.

[32] Gong, X.; Robinson, M. R.; Ostrowski, J. C.; Moses, D.; Bazan, G. C.; Heeger, A. J. *Adv. Mater.,* **2002**, *14*, 581.

[33] Chen, X.; Liao, J-L.; Liang, Y.; Ahmed, M. O.; Tseng, H. E.; Chen, S. A. *J. Am. Chem. Soc.*, **2003**, *125*, 636.

[34] Chen, F-C.; Yang, Y.; Pei, Q. *Appl. Phys. Lett.,* **2002**, 81, 4278.

[35] Harrison, B. S.; Foley, T. J.; Bouguettaya, M.; Boncella, J. M.; Reynolds, J. R.; Schanze, K. S.; Shim, J.; Holloway, P. H.; Padmanaban, G.; Ramakrishnan, S. *Appl. Phys. Lett.,* **2001**, *79*, 3770.

[36] Förster T. *Faraday Soc.*, **1959**, *27*,7.

[37] McGehee, M. .; Bergstedt, T.; Zhang, C.; Saab, A. P.; O'Regan, M. B.; Bazan, G. C.; Srdanov, Vojislav I.; Heeger, A. J. *Adv. Mater.,* **1999**, *11*, 1349.

[38] Liu, X.-L.; Pei, J.; Huang, W. *Thin Solid Films*, **2002**, *417*, 85.

[39] Gao, X.; Deng, Z.; Tao, D; Bai, F.; Duan, N.; Xu, Y.; Wu, J. *Zhongguo Xitu Xuebao*, **2001**, *19*, 536.

[40] Boncella, J. M.; Foley, T. J.; Harrison, B.; Schanze, K. S.; Reynolds, J. R.; Bouguettaya, M.; Shim, J.; Holloway, P. H.; Ramakrishnan, S. *Poly. Mater. Sci. Eng.,* **2002**, *86*, 72.

[41] Crosby, G. A.; Whan, R. E.; Alire, R. M. J. *Chem. Phys.,* **1961**, *34*, 743.

[42] Sato, S; Wada, M., *Bull. Chem. Soc. Jpn.,* **1970**, *43*, 1955.

CHAPTER 2

VISIBLE EMISSION RESULTING FROM ENERGY TRANSFER FROM POLYMERS TO SEVERAL ORGANIC DYES

2.1 Introduction

Considerable attention has been focused on conjugated polymers and their use in light-emitting diodes and other devices. Conjugated polymers have the ease of processability and advantageous mechanical properties, as well as optical and electrical properties similar to that of inorganic analogues. Polymers can be made to emit different colors with high photoluminescence efficiencies with relative ease. The electrical and optical properties can be varied by chemical design, as well.

Conjugated polymers can be optically excited to produce singlet excited states. Radiative decay can occur from the singlet state and in absence of nonradiative decay mechanisms, can be very efficient. Designing a polymer to emit in the red region usually leads to less photo and chemically stable materials. It is better to use singlet dyes with high quantum yield of emission as dopants, because red-emitting small molecules are typically more robust.

For Förster energy transfer to occur, the emission spectrum of the donor must overlap the absorption spectrum of the acceptor.[1] The process, known as resonance energy transfer (RET), occurs when the donor and acceptor are coupled by a dipole-dipole interaction, rather than the emission from the donor molecule being absorbed by the acceptor molecule,[2] which is known as trivial energy transfer.

In this study, polyphenylene-type polymers were used as the energy donors. The polymers were an alkoxy-substituted poly(*para*-phenylene) (**P1**) and a poly(4'-methylbenzophenone) (**PB**). The energy acceptors were commercially-available organic dyes, which included: Coumarin 6, Coumarin 343, and Rhodamine 6G. The structures of the polymers are shown in Figure 2.1. The structures of the dyes are shown in Figure 2.2.
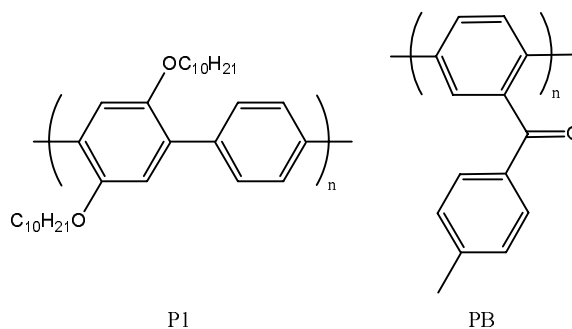
Figure 2.1. Structures of the polymers , P1 and PB.
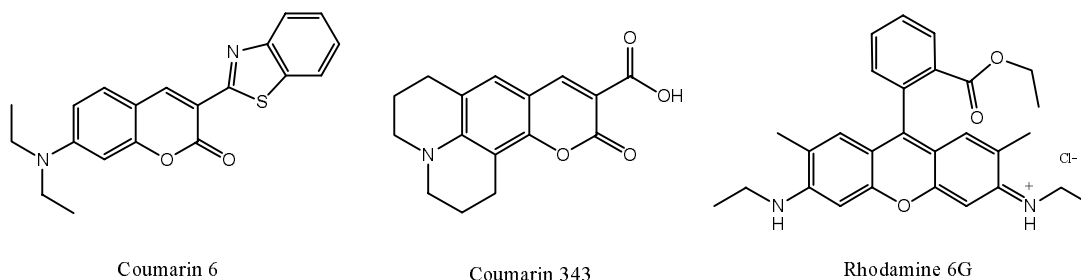
Figure 2.2. Structures of the dyes , Coumarin 6, Coumarin 343, and Rhodamine 6G.

This study is founded upon the concept of using dopants, e.g. organic dyes, to tune the emission color of a polymer.[3, 4, 5]

2.2 Results and discussion

The polymers used had similar photophysical properties in solution; the absorbance maxima of P1 and PB were 350 nm and 370 nm respectively. When exciting at these wavelengths, blue photoluminescence was obtained, which was attributed to fluorescence due to its short lifetime. The quantum yield of emission for P1 was 0.43, while for PB it was 0.115. The position of the emission spectra for the polymers make them ideal candidates to be used in energy transfer studies with selected singlet dyes, as seen in Figure 2.3. The singlet energies of the polymers and dyes are given in Table I, the donors have higher energy and the energy gap between the donor and acceptor is sufficient to prevent thermal depopulation, *i.e.* back energy transfer, of the acceptor-excited states.

a.)
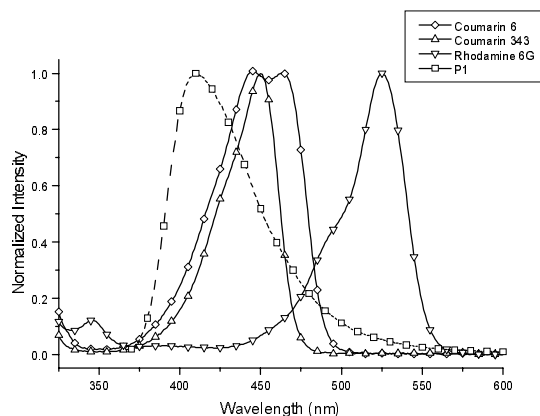
b.)
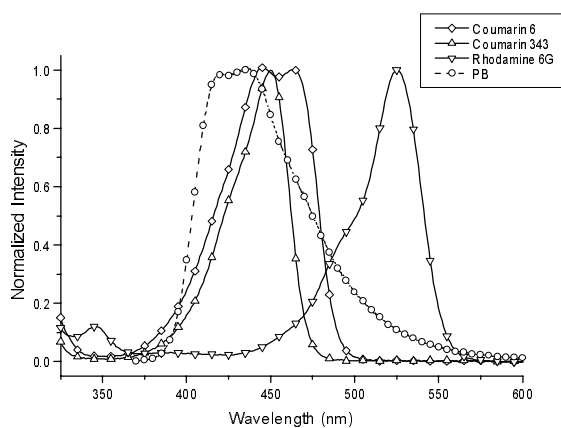
Figure 2.3. Overlaid spectra of the fluorescence of the polymer P1 (a) and PB (b) with the absorbances of the dyes.

The energy transfer efficiencies listed in Table 2.1 are calculated from equation 2.1 below, where ET is the energy transfer efficiency, F_{da} is the fluorescence intensity of the donor in the presence of the acceptor, and F_d is the fluorescence intensity of the donor alone.

$$ET = 1 - \left(\frac{F_{da}}{F_d} \right)$$

(2.1)

This equation does not account for quenching or increase in intensity from the acceptor. It only accounts for the loss of energy from the donor through the polymer emission's loss of intensity. The overlap integrals (J) for the polymers with their respective dyes were calculated with PhotoChemCAD,[6] and these data are summarized in Table 2.1.

Table 2.1. Energy transfer efficiencies and overlap integrals of the polymers with respect to 3% doping of the dyes.

Dye	P1 - J,cm^6/mmol	PB - J,cm^6/mmol	P1 - ET	PB - ET
Coumarin 6	1.1 E-13	1.5 E-13	0.980	0.985
Coumarin 343	1.4 E-13	1.3 E-13	0.935	0.845
Rhodamine 6G	0.35 E-13	1.3 E-13	0.805	0.962

The overlap integrals (J) were calculated in PhotoChemCAD with the following equation 2.2, where: J is the spectral overlap; $f_s(\upsilon)$ is the fluorescence intensity of the donor; $\varepsilon_A(\upsilon)$ is the molar absorption coefficient of the acceptor; and υ is the wave number of the donor emission spectrum and the acceptor absorbance spectrum.

$$J = \int_0^{\infty} \frac{f_s(\upsilon)\varepsilon_A(\upsilon)}{\upsilon} d\upsilon \qquad (2.2)$$

The accuracy of the J values obtained by the program is dependent upon the resolution of the respective absorption and fluorescence spectra, and can not be any more accurate than the extinction coefficient, therefore they are usually restricted to two decimal places. Both the absorbance and fluorescence spectra were recorded at 1.00 nm resolution with a spectral width of interest of 450 nm, and were baseline

corrected.   The program authors stated that the calculated values were consistent with prior calculations in the literature.[7]

It is popular belief that the rate constant of energy transfer depends upon the overlap integral. This may be true for small molecule donors, but in conjugated polymers the spectral overlap should occur at the low energy region of the emission spectra of the polymer.[3] Coumarin 6 and Rhodamine 6G have higher Js with PB than P1, thus the ET are higher for the PB/dye systems. Conversely, Coumarin 343 has a larger J and a higher ET with P1. The polymer P1 has weak overlap with Rhodamine 6G, thus it has a low ET when compared to the other dyes. P1/Coumarin 6 has a lower J than P1/Coumarin 343, but the latter has a lower ET. This can be further explained by the fact that the Coumarin 6 overlap with the polymer P1 extends more towards the low energy region than with Coumarin 343. The systems PB/Coumarin 6 and PB/Coumarin 343 follow the popular belief that ET depends on J. Consider the PB/Rhodamine 6G system, in which the J is the same as the PB/Coumarin 343 system, yet the ETs are significantly different. This can be explained by the fact that Rhodamine 6G overlaps with the lowest excimer emission region of PB. As per studies by Brunner *et al.*,[3] overlap in this region has higher efficiency.

The polymer film of P1 doped with Coumarin 6 (Figure 2.4a) shows residual emission. In the polymer film of PB with Coumarin 6 (Figure 2.4b) though, very little residual emission is seen. The spectra illustrate how a better donor-acceptor

pair, as determined by a larger overlap integral, can have more efficient energy transfer.
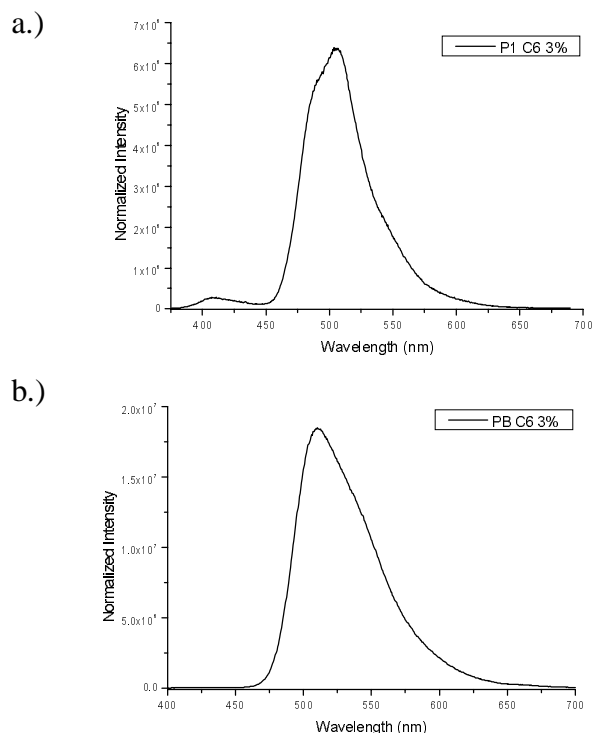
Figure 2.4. Fluorescence spectra of P1 (a) and PB (b) in the presence of Coumarin 6.

In Figure 2.5, the emission spectra of the polymer films doped with Coumarin 343 show PB to be superior to P1. This disagreed with our calculations that stated that P1 should have a better overlap with PB. At higher doping concentrations, the residual emission decreases, but the dye emission also decreases, which is most likely due to aggregate formation and quenching. There is a new peak at higher wavelengths that is due to aggregate formation. The spectra suggest that P1 supports aggregate formation better than PB, which could allow for the discrepancy of the fact that P1 has better overlap.

29
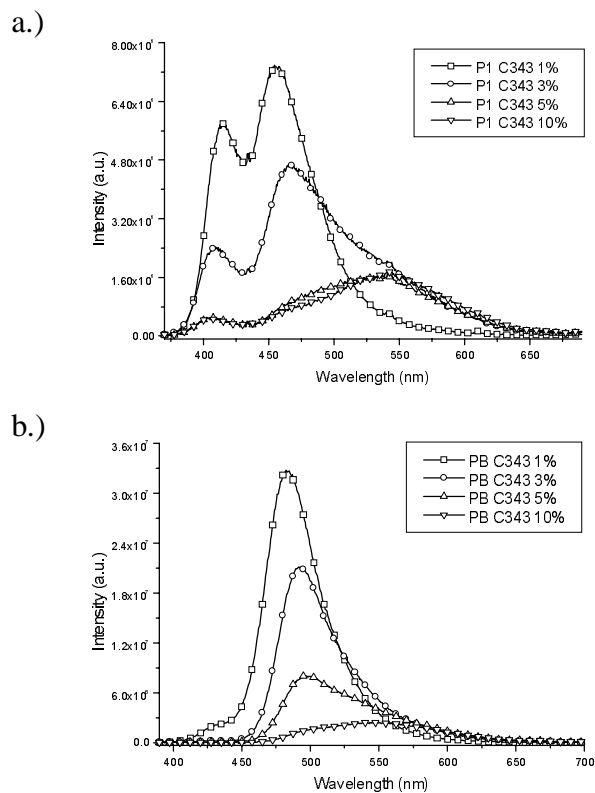
Figure 2.5. Fluorescence spectra of P1 (a) and PB (b) in the presence of Coumarin 343.

In all samples, the dyes overlapped better with PB than with P1. With the Coumarins, energy transfer took place. In the case of Rhodamine 6G though, only the polymer PB was able to transfer energy to it, as illustrated in Figure 2.6. The polymer film of P1 doped with Rhodamine 6G shows no dye emission at all, despite proper spectral overlap. The polymer emission is significantly quenched in the presence of Rhodamine 6G, implying the presence of an efficient non-radiative decay process. The film of PB with Rhodamine 6G shows emission from the dye, as well as residual emission from PB.

a.)

b.)
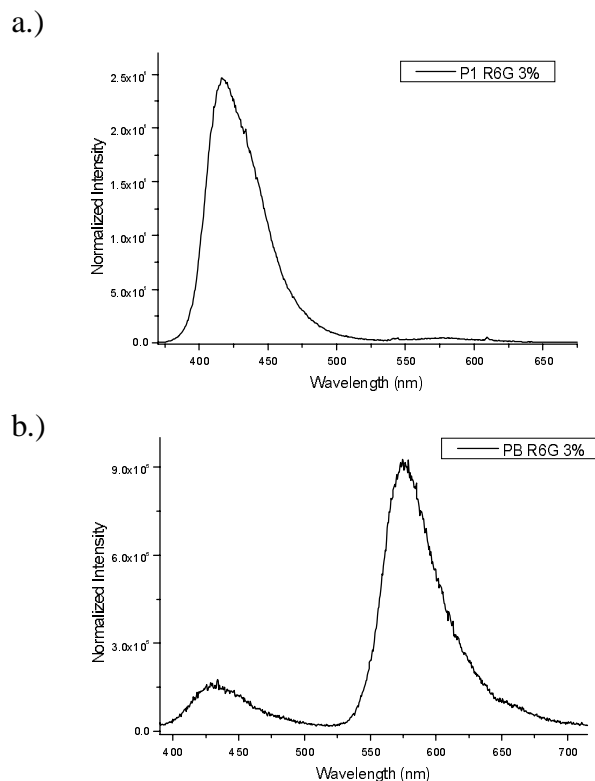
Figure 2.6. Fluorescence spectra of P1 (a) and PB (b) in the presence of Rhodamine 6G.

2.3 Experimental

All starting materials were purchased from Aldrich, TCI, or Lancaster and used with out further purification. The solvents purchased from VWR. The melting transitions of the polymers were obtained using a Shimadzu DSC-50 that performs differential scanning calorimetry (DSC). Samples were run in aluminum crucibles at a heating rate of 5 °C/min under a nitrogen atmosphere. The ^{1}H and ^{13}C NMR solution spectra were recorded on a Bruker AC 250 MHz NMR and a Bruker AM 360 MHz NMR. The abbreviations used are s for singlet, d for doublet, t for triplet, q for quartet, and

m for multiplet. Elemental analysis for C, H, and N was obtained from Atlantic

Microlab, Inc., Norcross Georgia

Materials

Coumarin 6, Coumarin 343, Rhodamine 6G, and 1,4-dibromobenzene were

purchased from Sigma-Aldrich. Reagent grade chloroform was purchased from

Mallinckrodt.

Polymerizations

The polymer poly(4'-methyl-2,5-benzophenone) (**PB**) was synthesized by

polymerizing 2,5-dichloro-4'-methylbenzophenone via nickel-mediated coupling as

per the published procedure.[8] The polymer poly(2,5-didecyloxyphenyl-1,4-

phenylene) (**P1**) was synthesized via Suzuki coupling of 2,5-didecyloxybenzene-1,4-

diboronic acid[9] and 1,4-dibromobenzene, as per the published procedure.[10]
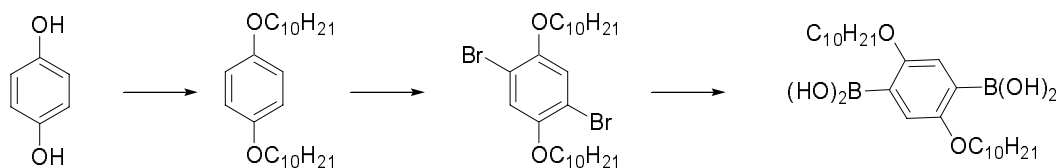
Scheme 2.1. Schematic representation of synthesis of 2,5-bis(decyloxy)-1,4-phenylenebisboronic acid.

1,4-Bis(decyloxy)benzene.[11] 1,4-hydroquinone (25.2 g, 0.50 mol), 1-bromodecane

(320 mL, 1.50 mol), and K_2CO_3 (208.0 g, 1.50 mol) in acetonitrile (500 mL) was

heated at reflux for two days before being poured into water (600 mL). The precipitates were collected by filtration dried, and dissolved in a minimum of hot hexane, poured into methanol (600 mL) to precipitate the product. The precipitates were filtered off dried and dissolved in hot hexane (200 mL) again, reprecipitation of resulting solution in methanol then gave pure product as a white solid. (140.0 g, 72%) ^{1}H NMR (250 MHz, CDCl$_3$): δ 6.77 s, 4H, 3.87 t 4H, 6.65 Hz), 1.72 m, 4H 7 Hz), 1.38 – 1.23 (m, 28H), 0.86 (t, 6H, 6.55 Hz).

2,5-Dibromo-1,4-bis(decyloxy)benzene. 1,4-Bis(decyloxy)benzene (40.0 g, 0.102 mol) was dissolved in 200 mL of chloroform, then bromine (14.0 mL, 0.2 mol) was added drop wise. Stirred overnight 50%w/w sodium hydroxide solution 100 mL was added, organic layer was separated. The excess solvent was removed, recrystallized the crude yellow product using ethyl acetate to give yellow clear crystals (47.49 g, 85%). ^{1}H NMR (250 MHz, CDCl$_3$): δ7.06 (s, 2H), 3.91 (t, 4H, 6.5 Hz), 1.77 (m, 4H, 6.9 Hz), 1.42 – 1.24 (m, 28H), 0.85 (t, 6H, 6.5 Hz).

2,5-bis(decyloxy)-1,4-phenylenebisboronic acid. 2,5-Dibromo-1,4-bis(decyloxy) benzene (25.09 g, 0.046 mol) was placed on a flask, evacuated and put under argon, dissolved in 200 mL of freshly distilled THF. Placed on a dry ice/acetone bath to cool the reaction mixture to -80 ^{o}C, added of *n*-butyl lithium (1.6 M in hexane, 100 mL) dropwise. Stir the reaction mixture at room temperature for 4 hrs. Placed on the

ice bath again to cool to lower temperature, ands added trimethyl borate (30 mL) dropwise, stirred over night at room temperature, quenched with 2N HCl (100 mL) removed excess solvent. The crude solid was boiled in hexanes over night to purify the product. Yield: 9.46 g (43%) ^{1}H NMR (250 MHz, DMSO): δ 7.81 (s, 4H), 7.18 (s, 2H), 3.98 (t, 4H, 6.6 Hz), 1.72 (m, 4H), 1.38 – 1.24 (m, 28H), 0.85 (t, 6H, 6.65 Hz).

Poly(1,4-(2,5-didecyloxy)phenylene-*alt*-1,4-phenylene)   (P1).   2,5-dideceloxyl phenyl-1,3-bisboronic acid (0.5979 g, 1.25 mmol) and 1,4-dibromo-benzene (0.3010 g, 1.25 mmol) was placed in an argon-flushed flask. Toluene (30 mL), methanol (11 mL), and 2M aqueous Na_2CO_3 (13 mL) were added, degassed, and brought to reflux under argon. Palladium catalyst (11 mg) dissolved in toluene (10 mL) was added and the reaction was refluxed for 2 days. The organic phase was added to methanol, producing the polymer as a solid precipitate, which was further purified by reprecipitation in methanol. Yield: 0.578 g: ^{1}H NMR (250 MHz, $CDCl_3$): δ 7.69, 7.07, 3.49, 1.71, 1.37, 1.23, 0.85.

2,5-dichloro-4'-methyl-benzophenone. Thionyl chloride (9.72 mL, 0.13 mol) was added dropwise to a stirred solution of 2,4-dichlorobenzoic acid (20.0 g, 0.1047 mol) in 200 mL of 1,2-dichloroethane and refluxed for 2 hrs. After removal of the solvent the resulting solid was added to $AlCl_3$ (17.4 g, 0.13 mol) in 12 mL of toluene followed by heating the reaction mixture at 75°C for 3 hrs. After cooling to room

temperature reaction was quenched by adding on to 400 mL of ice/water, the organic layer was separated, washed with 3% KOH solution, recrystallized with 90% ethanol. Yield: 17.75 g (64%) (UV Vis 266nm): ^{1}H NMR (360 MHz, CDCl$_3$): δ 7.55 (2H, d, J – 8 Hz), 7.24 (1H. br), 7.19 (1H, t, J – 2 Hz), 7.13 (2H, d, J – 8 Hz), 7.10 (1H, s), 2.28 (3H, s).

Poly(4'-methyl-2,5-benzophenone) (PB). In a three-neck 250 mL flask mixed, Zn (4.16 g, 0.0617 mol), anhydrous nickel(II)chloride (0.258 g, 0.002 mol), triphenyl-phosphine (2.09 g, 0.00796 mol), and bipyridine (0.311 g, 0.002 mol), Added 50 mL of anhydrous DMAc after purging the reaction mixture with argon for 30 min, then added 2,5-dichloro-4'-methyl-benzophenone (5.28 g, 0.0199 mol) heated the mixture for 24 h. Cooled the reaction to room temperature, added to a 500 mL mixture of HCl:methanol (25:75). Collected the solid precipitated out, dissolved in chloroform then precipitated into methanol, reprecipitations was carried out three more times. Yield: 2.321 g: Elemental analysis; Calcd for C$_{14}$H$_{10}$O: C, 86.56: H, 5.19; O, 8.24. Found: C, 85.04; H, 5.41. ^{1}H NMR (360 MHz, CDCl$_3$): δ 7.67, 7.36, 6.98, 6.79, 2.26. (all broad peaks)

Photophysical Measurements

Steady state emission spectra were recorded using a Fluorolog-3 model FL3-21 with a 450 W xenon lamp source, double grating excitation monochromator, single grating emission monochromator, and a room temperature R928 PMT serving as the

detector. Plots were generated using GRAMS/32 and DataMax software. Absorbance spectra were generated using OLIS modernized Cary 14 UV/Vis/NIR spectrophotometer equipped with deuterium and tungsten lamps for UV and Vis/NIR regions. Singlet energies (E_s) of the polymers and the dyes were calculated as described by Turro[12] and summarized in Table 2.2.

Table 2.2. Singlet energy values of donors and acceptors.

	Donors		*Acceptors*		
	P1	*PB*	*Coumarin 6*	*Coumarin 343*	*Rhodamine 6G*
Es (eV)	3.24	3.25	2.59	2.69	2.31

2.4 Conclusions

Energy harvesting from conjugated polymers to light-emitting dopants has been demonstrated. The possible uses for this research includes: organic light emitting diodes (OLEDs) and chemical sensors. Resonance energy transfer is possible from these polymers to common laser dyes. In nearly all samples, PB performed better than P1, although both polymers had similar singlet energies, the greater spectral overlap of PB with the acceptors led to higher transfer efficiencies. We have confirmed that not only the spectral overlap, but the location of overlap is important in energy transfer efficiencies. At high concentrations, dye emission decreases, which is most likely due to dye aggregate formation and quenching.

2.5 References

[1] Förster, T. *Ann. Phys. (Leipzig)* **1948**, *2*, 55. Translated by R. S. Knox.

[2] Lakowicz, J. R. *Principles of Fluorescence Spectroscopy,* 2nd ed., Kluwer Academic / Plenum Publishers, New York, NY, **1999**.

[3] Brunner, K.; van Haare, J. A. E. H.; Langeveld-Voss, B. M. W.; Schoo, H. F. M.; Hofstraat, J. W.; van Dijken, A. *J. Phys. Chem. B* **2002**, *106*, 6834.

[4] Bolivar, P. H.; Wegmann, C.; Kersting, R.; Deussen, M.; Lemmer, U.; Mahrt, R. F.; Bässler, H.; Göbel, E. O.; Kurz, H. *Chem. Phys. Lett.* **1995**, *245*, 534.

[5] Kido, J.; Shionoya, H.; Nagai, K. *Appl. Phys. Lett.* **1995**, *67*, 2281.

[6] Du, H.; Fuh, R. A.; Li, J.; Corkan, A.; Lindsey, J. S. *Photochemistry and Photobiology* **1998**, *68*, 141.

[7] Hsiao, J.-S.; Krueger, B. P.; Wagner, R. W.; Johnson, T. E.; Delaney, J. K.; Mauzerall, D. C.; Fleming, G. R.; Lindsey, J. S.; Bocian, D. F.; Donohoe, R. J. *J. Am. Chem. Soc.* **1996**, *118*, 11181.

[8] Udea, M.; Seino, Y.; Sugiyama, J. *Polym. J.* **1993**, *215*, 12, 1319.

[9] Pasquale, A. J.; Sheares, V. V. *J. Polym. Sci. Pol. Chem.,* **1998**, *36*, 2611.

[10] Q. S. Hu, W. S. Huang, D. Vitharana, X. F. Zheng, L. Pu, *J. Am. Chem. Soc.* **1997**, *119*, 12454.

[11] Wang, B.; Wasielewski, M.R. *J. Am. Chem. Soc.* **1997,** *119,* 12.

[12] Turro, N. J. *Modern Molecular Photochemistry*, University Science Books, Sausalito, CA, **1991**.

CHAPTER 3

VISIBLE EMISSION RESULTING FROM ENERGY TRANSFER FROM POLYMERS TO A SERIES OF COUMARINS AND OTHER ACCEPTORS

3.1 Introduction

Conjugated polymers have received considerable attention in recent years for applications such as light-emitting diodes and other devices. Conjugated polymers have achieved optical and electrical properties similar to that of inorganic analogues, yet retained the ease of processability and mechanical properties of polymers. Polymers can be made to emit different colors with high photoluminescence efficiencies with relative ease. The electrical and optical properties can be varied by chemical design, as well.

Conjugated polymers can be optically excited to produce singlet excited states. Radiative decay can occur from the singlet state and in absence of non-radiative decay mechanisms, can be very efficient. Designing a polymer to emit in the red region usually leads to less photo and chemically stable materials. It is better to use singlet dyes with high quantum yield of emission as dopants, because red-emitting small molecules are typically more robust. This study is founded upon the concept of using dopants, e.g. organic dyes, to tune the emission color of a polymer.[1, 2, 3]

For Förster energy transfer to occur, the emission spectrum of the donor must overlap the absorption spectrum of the acceptor.[4] The process, known as resonance energy transfer (RET), occurs when the donor and acceptor are coupled by a dipole-dipole interaction, rather than the emission from the donor molecule being absorbed by the acceptor molecule,[5] which is known as trivial energy transfer.

In this energy transfer study, polyphenylene-type polymers were used as the donating species. The polymers were an alkoxy-substituted poly(*para*-phenylene) (**P1**) and an alkoxy-substituted poly(*alt-para-meta*-phenylene) (**PM_es**), the structures of which are shown in Figure 3.1.
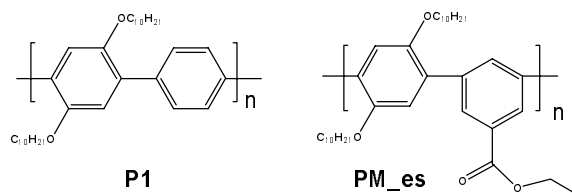
Figure 3.1. Structures of the polymers, P1 and PM_es.

The acceptors were commercially-available organic dyes, which included: Coumarin 6H, Coumarin 7, Coumarin 30, Coumarin 152, Coumarin 153, Coumarin 314¸ Coumarin 500, platinum(II) *meso*-tetra(pentafluorophenyl)porphine (**PtFTPP**), and platinum(II) octaethylporphine (**PtOEP**). The structures of the laser dyes and metalloporphines are found in Figure 3.2.
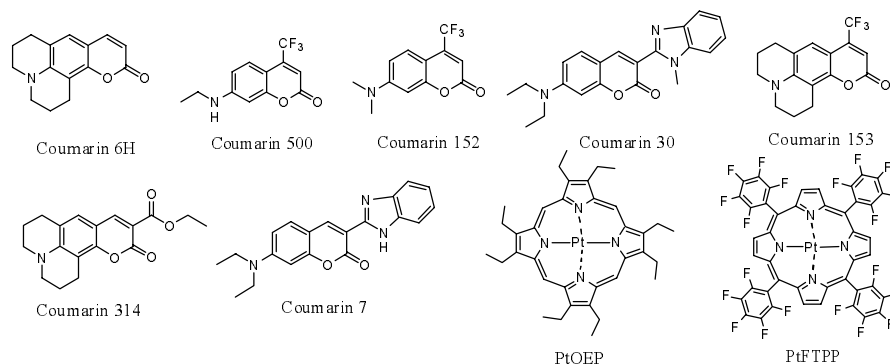
Figure 3.2. Structures of the acceptors.

3.2 Results and Discussion

The polymers P1 and PM_es were synthesized using 2,5-didecyloxyphenyl-1,3-bisboronic acid coupled with 1,4-dibromobenzene and 3,5-dibromoethylbenzoate via Suzuki coupling. The reactions are shown in Scheme 3.1.
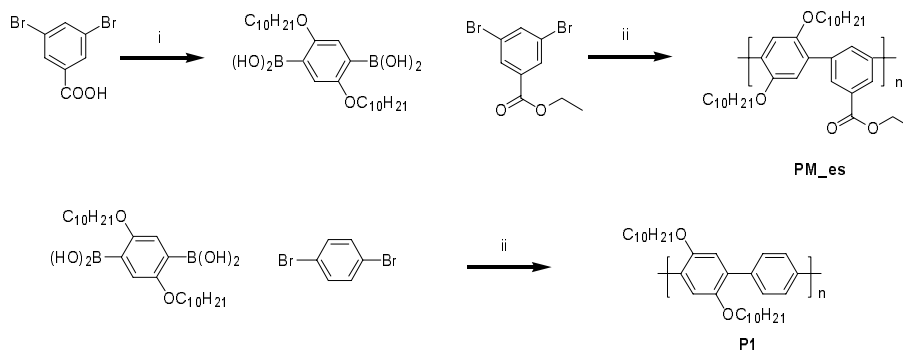
Scheme 3.1. The synthetic route to PM_es and P1 (i.) Ethanol/ PTSA reflux for 24 hrs; (ii.) Pd(PPh$_3$)$_4$, 2 M Na$_2$CO$_3$, Toluene, refluxed 72 hrs).

The photophysical properties of the energy donating polymers are shown in Table 3.1. These properties were determined in solution studies. Small changes in emission maxima were noted in both polymers in the solid state while dispersed in polystyrene. The polymer P1's emission maximum shifted to 408 nm and PM_es' went to 404 nm. PM_es' absorption maximum also shifted to 334 nm, while P1 did not change.

Table 3.1. Photophysical properties of the polymers in THF solution.

Polymers	Abs. Max (nm)	Emission		ϕ_{FL}	τ (ns)	Singlet energy (eV)	Triplet energy (eV)
		Max (nm)	FWHM (nm)				
P1	350	411	61.5	0.386	0.690	3.24	2.31
PM_es	330	392	61.5	0.662	1.665	3.41	2.47

The spectral overlap of the polymer emissions and the dyes absorbances are illustrated in Figures 3.3 and 3.4. In Figure 3.3, the emission of polymer P1 is surrounded by absorbances of the dyes. The same is shown in Figure 3.4 for polymer PM_es. All of these spectra were determined in polystyrene dispersed films.
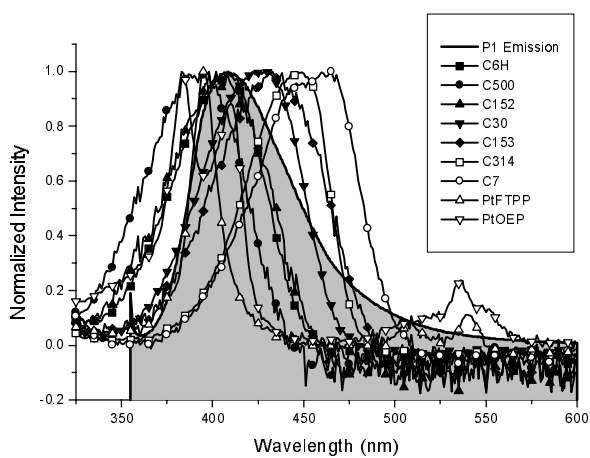
Figure 3.3. Spectral overlay of emission spectra of polymer P1 with absorption spectra of the dyes.
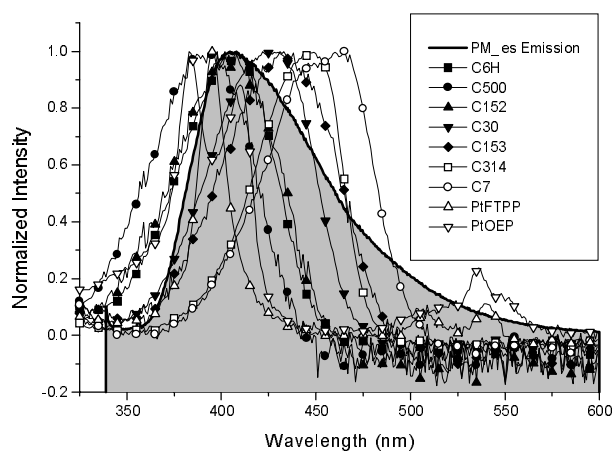
Figure 3.4. Spectral overlay of emission spectra of polymer PM_es with absorption spectra of the dyes.

The dyes were chosen to overlap over the emission spectra of both polymers in specific areas. Some overlap the higher energy portions, as with PtFTPP, PtOEP, Coumarin 6H, Coumarin 500, and Coumarin 152. Some overlap most of the central area, as with Coumarin 30 and Coumarin 153. Others overlap the lower energy areas where the emissions have tails, as with Coumarin 314 and Coumarin 7. The metalloporphines have minor absorption bands in the tail regions of the polymer emissions.

The rationale behind the position of overlap was inspired by the work of Brunner and coworkers,[1] where acceptors with overlap in the lowest excimer region of polymer resulted in higher energy transfer efficiencies. Our findings will be discussed later.

In Figure 3.5, the emission spectra of the polymer P1 alone and when doped are shown. In all of these Coumarin doped systems, negligible to no residual emission was seen from the polymers at 408 nm.
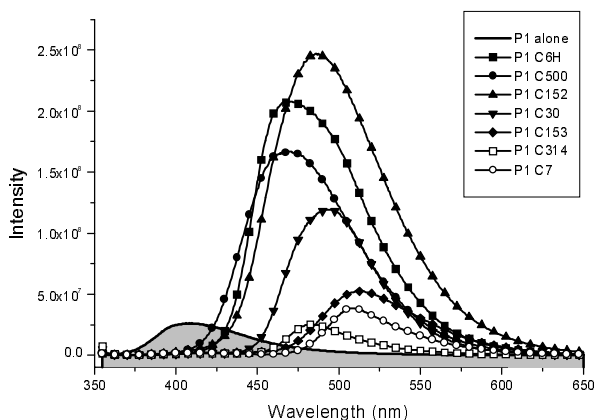
Figure 3.5. Emission spectra of the P1 doped systems, excited at 350 nm.

In Figure 3.6, the emission spectra of the polymer PM_es alone and when doped are shown. Again, residual emission from the polymer at 404 nm is negligible.
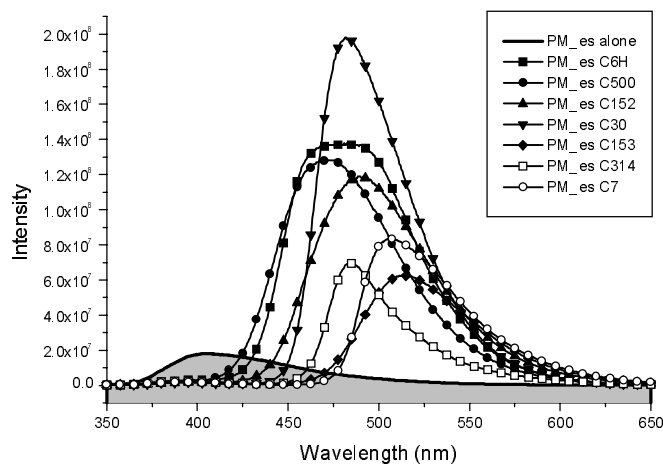
Figure 3.6. Emission spectra of the PM_es doped systems, excited at 334 nm.

The energy transfer efficiencies listed in Table 3.2 are calculated from the equation 3.1 below, where ET is the energy transfer efficiency, F_{da} is the fluorescence intensity of the donor in the presence of the acceptor, and F_d is the fluorescence intensity of the donor alone.

$$ET = 1 - \left(\frac{F_{da}}{F_d} \right)$$

(3.1)

This equation does not account for quenching or increase in intensity from the acceptor. It only accounts for the loss of energy from the donor through the polymer emission's loss of intensity. The overlap integrals (*J*) for the polymers with their

respective dyes were calculated with PhotoChemCAD,[6] and these data are summarized in Table 3.2.

Table 3.2. Energy transfer efficiencies and overlap integrals and the Coumarin doped polymer systems.

Dye	*Abs. Max. (nm)*	*P1 – E(-14) J,cm⁶/mmol*	*PM_es – E(-14) J,cm⁶/mmol*	*P1 - ET*	*PM_es – ET*
Coumarin 6H	381	6.2	5.6	0.925	0.830
Coumarin 500	*383*	*2.6*	*2.4*	*0.819*	*0.841*
Coumarin 152	388	*4.0*	3.6	*0.854*	*0.916*
Coumarin 30	406	9.6	8.7	0.943	0.919
Coumarin 153	413	3.6	3.4	0.924	0.904
Coumarin 314	427	5.9	5.6	0.942	0.885
Coumarin 7	431	6.7	6.7	0.926	0.912

PhotoChemCAD calculated the overlap integrals (*J*) with the following equation 3.2, where: *J* is the spectral overlap; $f_s(\upsilon)$ is the fluorescence intensity of the donor; $\varepsilon_A(\upsilon)$ is the molar absorption coefficient of the acceptor; and υ is the wave number of the donor emission spectrum and the acceptor absorbance spectrum.

$$J = \int\limits_{0}^{\infty} \frac{f_s(\upsilon)\varepsilon_A(\upsilon)}{\upsilon} d\upsilon \tag{3.2}$$

The accuracy of the *J* values obtained by the program is dependent upon the resolution of the respective absorption and fluorescence spectra, and can not be any more accurate than the extinction coefficient, therefore they are usually restricted to two significant figures. Both the absorbance and fluorescence spectra were recorded at 1.00 nm resolution with a spectral width of interest of 300 – 450 nm, and were

baseline corrected. The program authors stated that the calculated values were consistent with prior calculations seen in the literature. [7]

The rate constant of energy transfer typically depends upon the overlap integral, which is the case for small molecule donors. However, conjugated polymers should have spectral overlap in the low energy region of the emission spectra of the polymer.[1] From the data listed in Table 3.2, only Coumarin 500 and Coumarin 152 had higher energy transfer efficiencies in PM_es than in P1, when their overlap integrals suggested the opposite would occur. According to Brunner's findings, Coumarin 337 and Coumarin 7 should have greater energy transfer efficiencies than those that absorb at lower wavelengths. One reason the data would not agree with Brunner's findings was that these polymers did not form aggregates. Therefore, the low energy region of these polymers' emissions would not have as many long lived excited states as it would if aggregation did occur.

Figure 3.7 shows a depiction of the degree of overlap between the polymers and the acceptors in terms of the acceptor's absorption maxima. What is observed is that when a dopant has a large overlap with one polymer, it has a large overlap with the other. The same is true when there is less overlap.
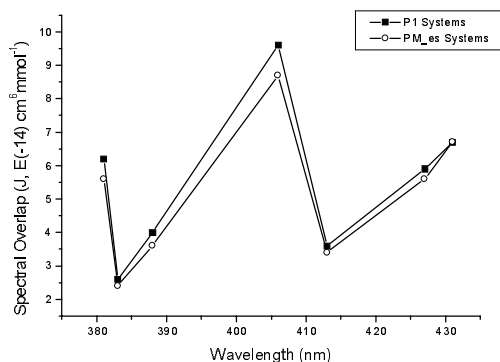
Figure 3.7. Spectral overlap with polymer versus absorption maxima of the Coumarin dopants.

Figure 3.8 shows the energy transfer efficiencies of the Coumarin doped systems in terms of the acceptor's absorption maxima. There is a very general trend of increasing energy transfer as the dopant's absorption maxima increases, at least for polymer P1.
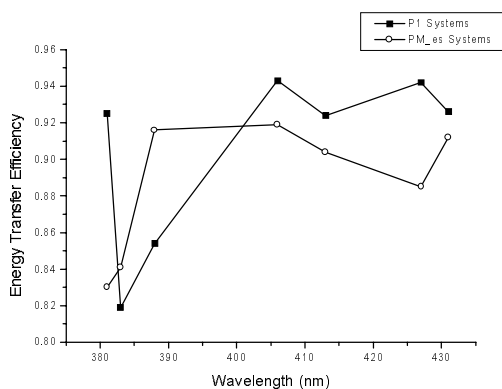
Figure 3.8. Energy transfer efficiency versus absorption maxima of the Coumarin dopants.

In Figure 3.9, energy transfer is shown to occur from both P1 and PM_es to PtFTPP and PtOEP. The sharp spikes located at 668 nm in Figure 3.9(b) are due to the second order Raleigh bands, resulting from exciting the polymer at 334 nm. Residual emission from the polymers was seen in all cases, though less in the systems where PtOEP was the dopant. The PM_es doped systems also had unusual peak shapes in its residual emission, more so with PtFTPP as the dopant, as seen in Figure 3.9(b).
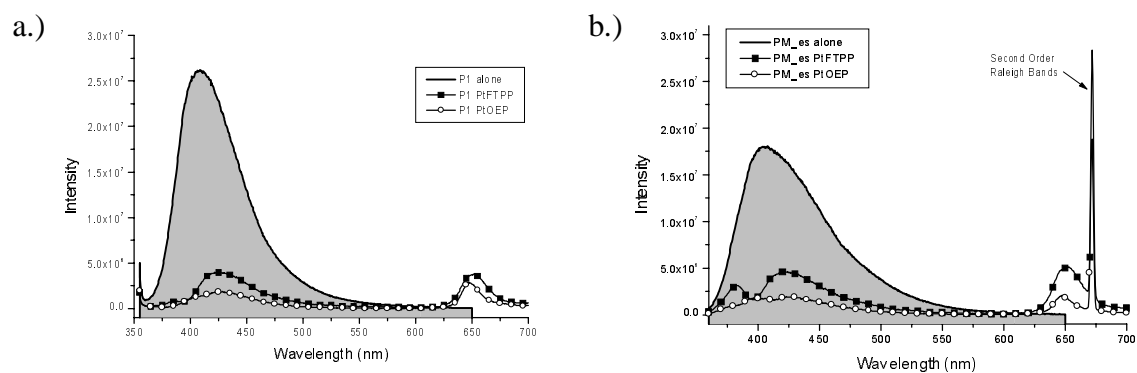
Figure 3.9.(a). Emission spectra of P1 excited at 350 nm, and **(b.)** PM_es excited at 334 nm when doped with platinum porphines.

Significant emission from the dyes was not observed, though the intensities from the porphines were much less than that of the Coumarins. Figure 3.10 illustrates this point by comparing the intensity of emission from a polystyrene film of Coumarin 30 with a polystyrene film of PtFTPP. Back in Figure 3.9, although the acceptor emission was not as intense as the Coumarin doped systems, significant reduction in polymer emission occurred.
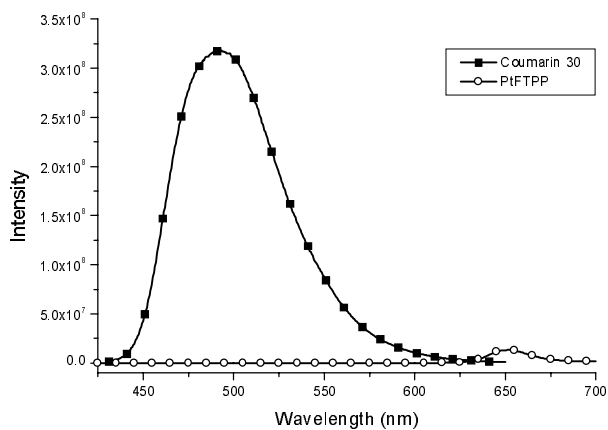
Figure 3.10. Emission spectra of Coumarin 30 and PtFTPP.

In these metalloporphine doped systems, The PtFTPP and PtOEP doped systems exhibited energy transfer as noted by the donor emission's reduction, and the efficiencies of these systems are listed in Table 3.3. Both dopants preferred P1 over PM_es by nearly five percent in each instance.

Table 3.3. Energy transfer efficiencies of the metalloporphine doped polymer systems.

Dye	*P1 – ET*	*PM_es – ET*
PtFTPP	0.904	0.855
PtOEP	0.949	0.902

3.3 Experimental

<u>Materials</u>

1,4-Dibromobenzene, 3,5-dibromobenzoic acid, and all reagents were purchased from Aldrich.   2,5-didecyloxyphenyl-1,3-bisboronic acid[8] were synthesized according to published procedures. 3,5-dibromobenzoic acid was esterified using ethanol prior to polymerization. Polystyrene, Coumarin 102, Coumarin 480D, Coumarin 6H, Coumarin 152, Coumarin 30, Coumarin 153, Coumarin 314, Coumarin 7, Coumarin 337, and Coumarin 6 were purchased from Sigma-Aldrich. Coumarin 500 was purchased from Lambda Physik.   Platinum(II) meso-tetra(pentafluorophenyl)porphine and platinum(II) octaethylporphine were purchased from Frontier Scientific.   2,2,2-Trichloroethanol was purchased from Lancaster Synthesis. Quartz slides were purchased from ChemGlass.

<u>General Procedure for Polymerizations</u>[9]

2,5-Didecyloxyphenyl-1,3-bisboronic   acid   (0.001   mol)   and   corresponding dihaloarene (0.001 mol) were placed in an argon-flushed flask. THF (15 mL) and 1M aqueous Na_2CO_3 (15 mL) were added, degassed, and brought to reflux under argon. Palladium catalyst (35 mg) dissolved in THF (5 mL) was added and the reaction mixture was refluxed for two days. The organic phase was added to methanol, producing the polymer as a solid precipitate, which was further purified by reprecipitation in methanol.

Photophysical Measurements

Steady state emission spectra were recorded using a Fluorolog-3 model FL3-21 with a 450W xenon lamp source, double grating excitation monochromator, single grating emission monochromator, and a room temperature R928 PMT serving as the detector. Phosphorescence studies were carried out using the 1934D3 phosphorimeter in conjunction with the Fluorolog-3 system with a xenon flash lamp. Plots were generated using GRAMS/32 and DataMax software. Absorbance spectra were generated using OLIS (Modernized Cary 14) UV/Vis/NIR spectrophotometer equipped with deuterium and tungsten lamps for UV and Vis/NIR regions. The quantum yield for emission in solution, determined according to the method described by Demas and Crosby[10] relative to quinine sulfate in 1.0M H_2SO_4 (0.546).[11] The singlet and triplet energies of the polymers were calculated according to published methods.[12]

Sample Preparation

A 25 w/v % solution of polystyrene in 2,2,2-trichloroethanol was made in which the polymers P1 and PM_es were each dispersed in a 2.5 w/v % concentration. The acceptors were each dispersed in a 2.5 w/v % concentration as well. The solutions were then spin cast onto quartz slides.

3.4 Conclusions

Energy transfer has been shown to occur from polyphenylenes as the energy donors to singlet energy accepting Coumarins and the triplet energy accepting metalloporphines. Our studies did not follow Brunner's observations mostly due to the fact that the polymers used in this study did not aggregate. By dispersing the donor polymers and acceptor dyes in polystyrene, aggregation was prevented. For the most part, the efficiencies of energy transfer did correlate with the overlap integrals of the doped systems. The disparity noticed with Coumarin 500 and Coumarin 152 is undergoing further study.

3.5 References

[1] Brunner, K.; van Haare, J. A. E. H.; Langeveld-Voss, B. M. W.; Schoo, H. F. M.; Hofstraat, J. W.; van Dijken, A. *J. Phys. Chem. B*, **2002**, *106*, 6834.

[2] Bolivar, P. H.; Wegmann, C.; Kersting, R.; Deussen, M.; Lemmer, U.; Mahrt, R. F.; Bässler, H.; Göbel, E. O.; Kurz, H. *Chem. Phys. Lett.*, **1995**, *245*, 534.

[3] Kido, J.; Shionoya, H.; Nagai, K. *Appl. Phys. Lett.*, **1995**, *67*, 2281.

[4] Förster, T. *Ann. Phys. (Leipzig)*, **1948**, *2*, 55. Translated by R. S. Knox.

[5] Lakowicz, J. R. *Principles of Fluorescence Spectroscopy,* 2nd ed., Kluwer Academic / Plenum Publishers, New York, NY, **1999**.

[6] Du, H.; Fuh, R. A.; Li, J.; Corkan, A.; Lindsey, J. S. *Photochemistry and Photobiology* **1998**, *68*, 141.

[7] Hsiao, J.-S.; Krueger, B. P.; Wagner, R. W.; Johnson, T. E.; Delaney, J. K.; Mauzerall, D. C.; Fleming, G. R.; Lindsey, J. S.; Bocian, D. F.; Donohoe, R. J. *J. Am. Chem. Soc.* **1996**, *118*, 11181.

[8] Frank, M.; Wasgindt, M.; Pautzsch, T.; Klemm, E. *Macromol. Chem. Phys.*, **2001**, *202*, 980.

[9] Hu, Q. S.; Huang, W. S.; Vitharana, D.; Zheng, X. F.; Pu, L. *J. Am. Chem. Soc.*, **1997**, *119*, 12454,.

[10] Demas, N. J.; Crosby, G. A. *J. Phys. Chem.,* **1971**, *75*, 991.

[11] Klink, S. I.; Hebbink, G. A.; Grave, L.; Oude Alink, P. G. B.; Van Veggel, F. C. J. M.; Werts, M. H. V. *J. Phys. Chem. A.*, **2002**, *106*, 3681.

[12] Turro, N. J. *Modern Molecular Photochemistry*, University Science Books, Sausalito, California, **1991**.

CHAPTER 4

VISIBLE EMISSION RESULTING FROM ENERGY TRANSFER FROM A POLYMER WITH PENDANT TERPYRIDINES TO EUROPIUM(III) COMPLEXES

4.1 Introduction

Triplet-Triplet Energy Transfer (**TTET**) is the process by which a triplet excited state of the donor creates a triplet excited state in the acceptor. This process is forbidden by the dipole-dipole mechanism due to the low extinction coefficients (ε) of the S_0 to T_1 transition of the acceptor, but it is spin-allowed by the exchange mechanism. The general form of exchange mechanism is represented as:

$$D^*(T_1) + A(S_0) \quad \rightarrow \quad D(S_0) + A^*(T_1).$$
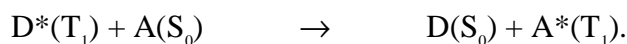
The physical distance separating the donor and acceptor has to be low for efficient energy transfer (in the range of 10–15 Å). The direct excitation of emissive ^5D states of europium is hard due to the low extinction coefficients (ε) of the said transitions.[1] Complexes of europium β-diketonates give rise to efficient europium emission from $^5D_0$ state.[2,3] The β-diketonate ligand produces an excited singlet state upon optical excitation, which intersystem crosses to produce ligand triplet state. The europium J states have the appropriate symmetry to accept energy from the ligand triplet states. The sensitization of europium is represented as:

$$L(S_0) + h\nu \quad \rightarrow \quad L^*(S_1) \quad \rightarrow \quad L^*(T_1) + Eu(J_0) \quad \rightarrow \quad L(S_0) + Eu^*(J_n).$$

Thus, a nearby polymer can be used to donate energy to a ligand, where the ligand triplet state is able to sensitize the ^5D_n states of europium via the electron exchange mechanism, as illustrated in Figure 4.1.
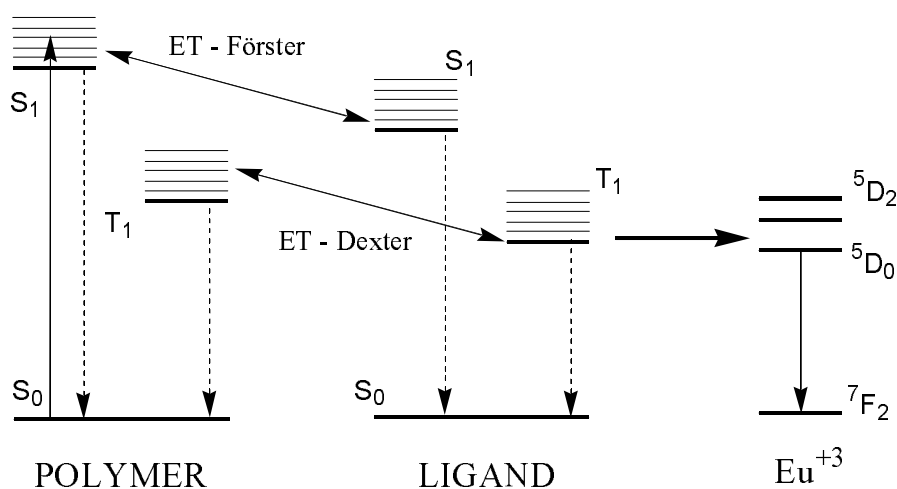
Figure 4.1. The energy transfer pathway from polymer to europium.

If the lowest lying ligand triplet state is lower in energy than the lowest lying polymer triplet state, efficient TTET will take place between the polymer and ligand, provided that the polymer and the complex are in collusion distance,

$$P^*(T_1) + L (S_0) \quad \rightarrow \quad P(S_0) + L^*(T_1).$$
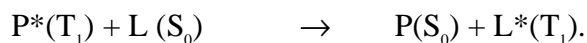
The polymer triplet states are used to sensitize ligand triplets, the direct sensitization of ligand triplet states shut the residual emission from the ligand, resulting in pure color emission from europium. For efficient energy transfer, the first requirement is that the triplet energy of the ligand is above the ^5D_n (n~0-3; $^5D_0$–17,264 cm^{-1}) state of europium.[4] The second and most challenging concern is that the polymer should

have higher energy than the ligand. As discussed before, high energy conjugated polymers are rare.

A novel polymer, poly(1,4-(2,5-didecyloxy) phenylene-*alt*-3,5-[4'-(2,2':6',2"-terpyridine)]phenylene) (PM_trp) with a terpyridine pendant group was designed and synthesized to be used as practical europium sensitizers. As shown in Scheme 4.1, the target polymer PM_trp was synthesized via palladium catalyzed Suzuki coupling of monomers 2,5-didecyloxyphenyl-1,3-bisboronic acid and 4'-(3,5-dibromophenyl)-2,2':6',2"-terpyridine.
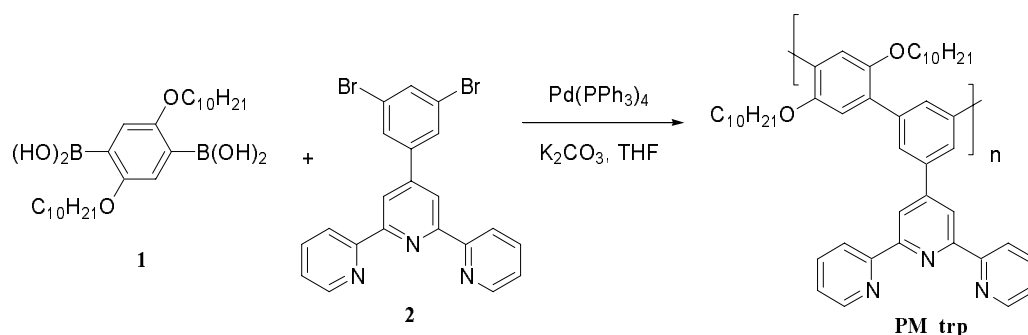
Scheme 4.1. Synthesis of the polymer, PM_trp.

Energy transfer from the polymer to the lanthanide occurred via the Förster or Dexter mechanism, both of which necessitated close proximity of the donor and acceptor. For this reason, a terpyridine pendant group was attached directly to one of the backbone phenyl rings. For efficient energy transfer, the polymer should have higher triplet energies than the europium complex. To achieve polymers of requisitely high energy, we studied the effect of alternating *para* and *meta* linkages in the polymer

backbones. Cross-conjugation of the *meta* linkages raised the singlet and triplet energies of the polymers, relative to traditional all *para*-linked polyphenylenes. The high triplet energies of these polymers, coupled with the chelating ability of the terpyridine group made the polymer PM_trp a suitable candidate for energy transfer to europium. The polymer's photophysical properties were studied by absorption and emission spectroscopy, the spectra of which are shown in Figure 4.2, and are summarized in Table 4.1.

Table 4.1. Photophysical properties of polymers PM_trp in THF.

	PM_trp
Absorption maximum	320 nm
Fluorescence maximum	416 nm
FWHM	85 nm
Stokes' shift	7,212 cm^{-1}
Φ_{FL}	0.062
Lifetime (weighting coefficient)	0.27 ns (0.60) 1.49 ns (0.40)
Singlet energy level (E_S)	3.32 eV
Triplet energy level (E_T)	2.47 eV
Singlet-triplet gap (ΔE_{ST})	0.85 eV

The polymer PM_trp had two strong absorption transitions, an intense $S_2 \leftarrow S_0$ transition centered at 274 nm (36,496 cm^{-1}, 4.52 eV) and a weaker $S_1 \leftarrow S_0$ transition centered at 320 nm (31,250 cm^{-1}, 3.87 eV). Upon exciting the polymer PM_trp at 320 nm, the polymer gave rise to emission centered at 416 nm (24,038 cm^{-1}, 2.98 eV) with a full width at half maximum of 85 nm. The quantum yield of the polymer

PM_trp was measured to be 0.062. The Stokes' shift for the polymers PM_trp was calculated to be 7,212 cm^{-1}.
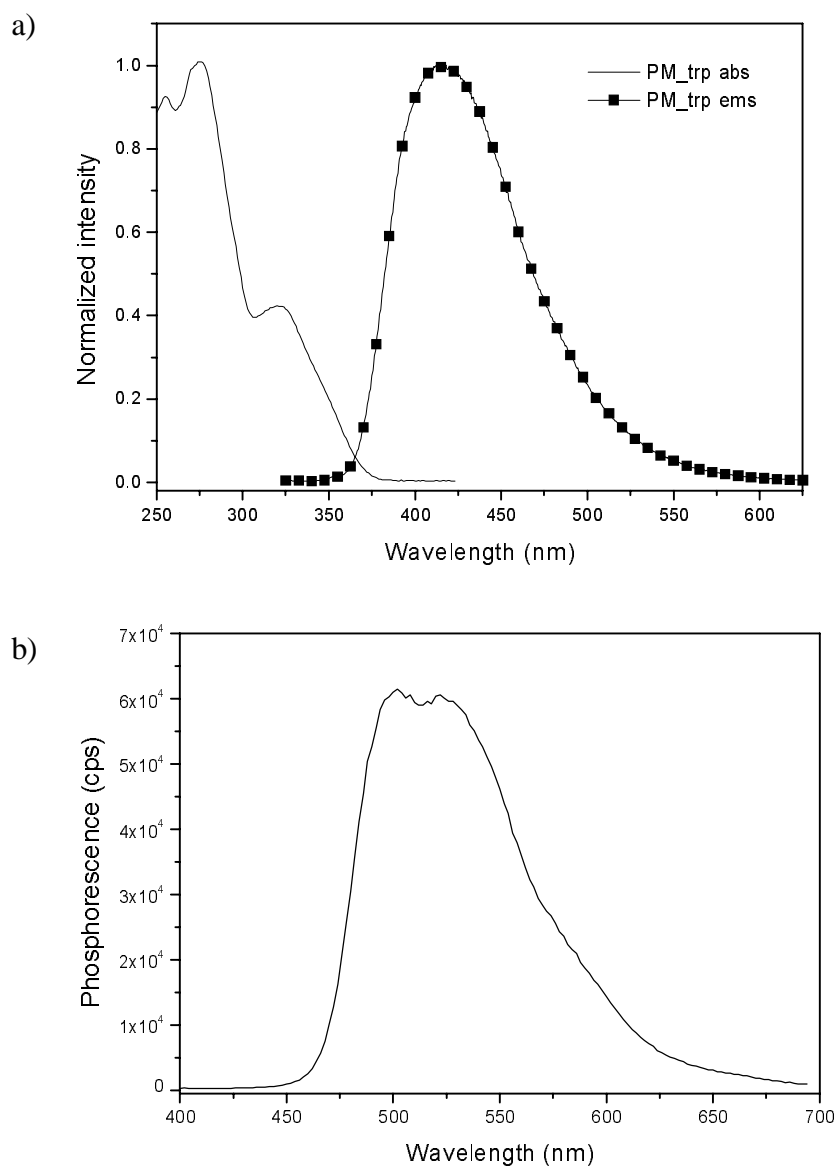
Figure 4.2(a). The absorbance emission spectra of polymer PM_trp in THF (ex = 320 nm). **(b).** Low temperature phosphorescence spectra of PM_trp at 77 K in 2-methyl THF (ex = 320 nm).

Energy transfer studies were performed with the polymer, PM_trp, serving as the primary energy donor, coordinated to a lanthanide tris(β-diketonate). The structure is shown in Figure 4.3.
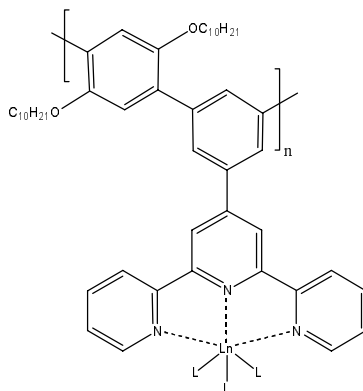
Figure 4.3. Structure of PM_trp:Ln(L)$_3$, where Ln = Eu and Gd, and L = HFA, BTM, DTM, 3-PTM, and 9-PTM.

The other ligands which were bound to the lanthanide included five different β-diketonates: 1,1,1,5,5,5-heaxfluoro-2,4-pentanedione (HFA), benzoyl-2-thenoylmethane (BTM), di-2-thenoylmethane (DTM), 3-phenanthroyl-2-thenoylmethane (3-PTM), and 9-phenanthroyl-2-thenoylmethane (9-PTM). The structures of the ligands are shown in Figure 4.4. HFA was used in order to obtain the triplet state energies of the polymer complex. Substitution of aryl groups in the aroylthenoylmethanes was performed, according to modified Claisen condensation methods, in an attempt to vary the energies of the complexes. The two lanthanides in this study were the non-emitting gadolinium and the red-emitting europium.
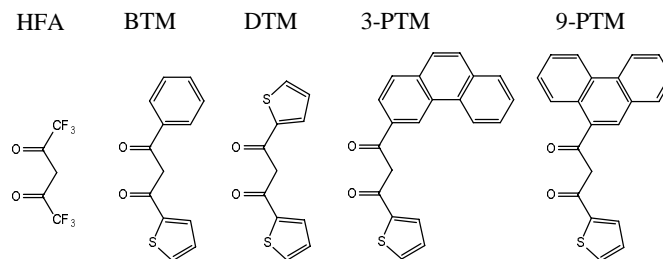
Figure 4.4. Structures of ligands: HFA, BTM, DTM, 3-PTM, and 9-PTM.

The triplet energies of the polymer was determined by studying the PM_trp:Gd(HFA)$_3$ system. In this system, any triplets that were formed were trapped on the polymer since energy transfer cannot take place from the polymer to higher energy levels of the Gd(HFA)$_3$ complex.

The triplet energies of the polymer-lanthanide-aromatic ligand systems were determined by studying the polymer-ligand emission from the gadolinium species. In these systems, energy transfer from polymer to ligand system was able to take place, but then the process was halted, since gadolinium's energy level is higher than any organic ligand can donate. PM_trp:Gd(L)$_3$ solutions were made, where L = BTM, DTM, 3-PTM, and 9-PTM.

Step three of this process was studied by replacing the gadolinium with europium in each of the systems. Europium's energy level is able to accept energy from the ligand systems, thus allowing the process to complete. PM_trp:Eu(L)$_3$ solutions were made, where L = BTM, DTM, 3-PTM, and 9-PTM.

4.2 Results and discussion

The energy transfer studies were all performed in the solution state at a concentration of $1x10^{-5}$ M in anhydrous tetrahydrofuran (THF), except for the low temperature phosphorescence studies on the gadolinium complexes which used 2-methyltetrahydrofuran (2-MeTHF) as the solvent. The solutions were made from $1x10^{-3}$ M stock solutions of polymer, ligand, sodium ethoxide, gadolinium(III) chloride, and europium(III) chloride. The polymer and ligand solutions used anhydrous THF as the solvent, while the base and lanthanide solutions used anhydrous ethanol as solvent. The polymer, appropriate lanthanide, ligand, and base were added together in a 1:1:3:3 ratio in more anhydrous THF until they were finally $1x10^{-5}$ M. The normalized absorbance spectra of the polymer, PM_trp, and the polymer-lanthanide complexes is shown in Figure 4.5.
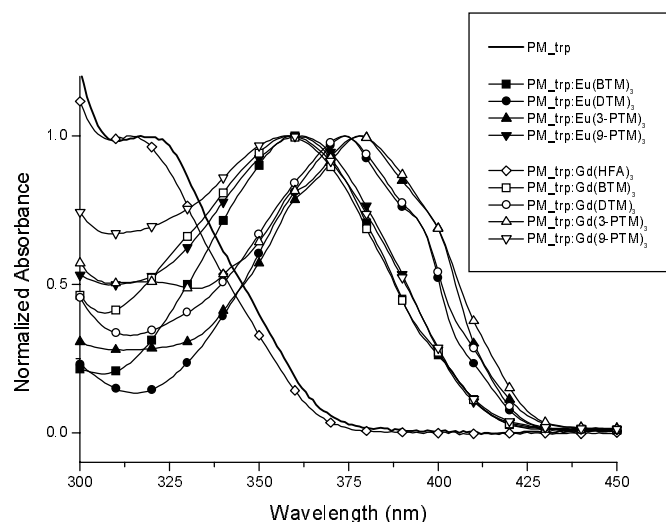
Figure 4.5. Absorbance spectra of PM_trp:Ln(L)$_3$ complexes relative to PM_trp and each other.

The solutions were made from 1×10^{-3} M stock solutions of polymer, ligand, sodium ethoxide, gadolinium(III) chloride, and europium(III) chloride. The polymer and ligand solutions used anhydrous THF as the solvent, while the base and lanthanide solutions used anhydrous ethanol as solvent. The polymer, appropriate lanthanide, ligand, and base were added together in a 1:1:3:3 ratio in more anhydrous THF until they were finally 1×10^{-5} M.

The lanthanide complexes coordinated to PM_trp in this study were: gadolinium *tris*(1,1,1,5,5,5-hexafluoro-2,4-pentanedione) [Gd(HFA)$_3$], gadolinium *tris*(benzoyl-2-thenoylmethane) [Gd(BTM)$_3$], gadolinium *tris*(di-2-thenoylmethane) [Gd(DTM)$_3$], gadolinium *tris*(3-phenanthroyl-2-thenoylmethane) [Gd(3-PTM)$_3$], and gadolinium *tris*(9-phenanthroyl-2-thenoylmethane) [Gd(9-PTM)$_3$]; europium *tris*(benzoyl-2-thenoylmethane) [Eu(BTM)$_3$], europium *tris*(di-2-thenoylmethane) [Eu(DTM)$_3$], europium *tris*(3-phenanthroyl-2-thenoylmethane) [Eu(3-PTM)$_3$], and europium *tris*(9-phenanthroyl-2-thenoylmethane) [Eu(9-PTM)$_3$].

As mentioned previously, PM_trp:Gd(HFA)$_3$ was studied to determine the triplet energy of the polymer, since the HFA ligands are unable to accept energy from the polymer, triplet states are trapped on the polymer. The other gadolinium species were made to determine the triplet energies of the polymer complexes since gadolinium's accepting *J* state is much higher than any organic ligand would be able to donate energy. Therefore, triplet states can be donated from polymer to polymer-

ligand complex, but are trapped at this step since gadolinium is at a higher energy.

The photophysical properties of these complexes are reported in Table 4.2.

Table 4.2. Photophysical properties of PM_trp gadolinium complexes.

	PM_trp: Gd(HFA)$_3$	PM_trp: Gd(BTM)$_3$	PM_trp: Gd(DTM)$_3$	PM_trp: Gd(3-PTM)$_3$	PM_trp: Gd(9-PTM)$_3$
Abs. Max (nm) (cm^{-1})	317 31,546	358 27,933	374 26,738	376 26,596	358 27,933
Em. Max (nm) (cm^{-1})	400 25,000	410 24,390	423 23,641	429 23,310	410 24,390
Δ (cm^{-1})	6,546	3,543	3,097	3,286	3,543
E_S (eV) (cm^{-1})	3.40 27,397	3.21 25,907	3.09 24,938	3.07 24,722	3.20 25,773
E_T (eV) (cm^{-1})	2.76 22,297	2.46 19,841	2.43 19,608	2.48 20,000	2.45 19,763
ΔE_{ST} (eV)	0.64	0.75	0.66	0.59	0.75

The complexes with BTM and 9-PTM had larger singlet to triplet energy gaps (ΔE_{ST}) than those complexes with other ligands. This indicated that it would be less likely for these triplet states on BTM and 9-PTM to convert back to singlet states. If there was competition for energy that was donated to the lanthanide and back energy transfer from the ligand triplet energy to the ligand singlet energy, then residual emission would be seen in the emission spectra. In order for the energy transfer process to europium lead to efficient emission, the ligand had to be higher in energy than the $^5D_1$ (19,030 cm^{-1}) level of europium. In all four instances of the aroyl-2-thenoylmethanes, the triplet energies met the requirements that they be at least 2000 cm^{-1} above the $^5D_0$ (17,260 cm^{-1}) level of europium to prevent thermal back energy transfer.[5,6]

With the information available in Table 4.2, energy transfer pathways of the PM_trp systems were postulated and the one for PM_trp:Eu(BTM)$_3$ is shown in Scheme 4.2. Polymer PM_trp upon interacting with 317 nm light produced a singlet excited state with energy of 3.40 eV. This state would under go three processes; radiative decay (fluorescence), non-radiative decay, and intersystem crossing to produce a triplet state with energy of 2.76 eV. As the gadolinium complex had a singlet energy of 3.21 eV and a triplet energy of 2.46 eV, Förster type energy transfer was possible in this system, as well as Dexter type energy transfer.
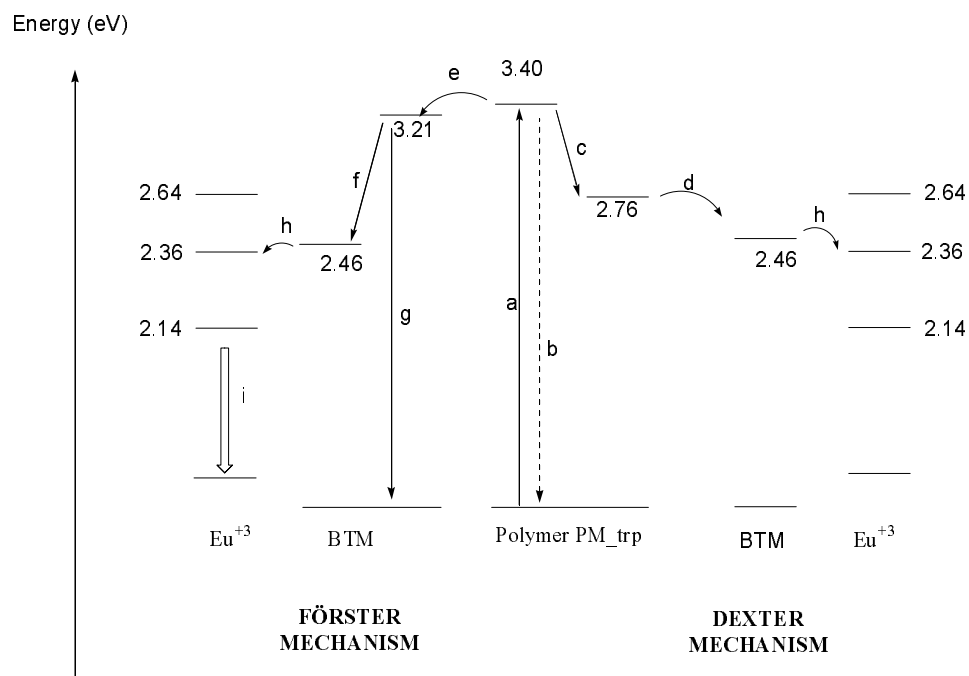
Scheme 4.2. The energy transfer mechanism for the PM_trp:Eu(BTM)$_3$ system.

In the emission spectra shown in Figure 4.6, the polymer complexes were excited at the polymer's absorbance maximum. In both instances, when the polymer was excited singlet excited states were converted to triplet excited states *via* the heavy atom effect of the lanthanide ion. The polymer-centered triplet energy was then transferred to the *β*-diketonate ligand *via* the exchange mechanism, and then again *via* the exchange mechanism to the emitting *J* state of europium, from which emission occurred. When Eu(L)$_3$ complexes were coordinated to the polymer, europium emission was observed, with some residual emission from the polymer or polymer-ligand complex. The residual emission was most likely due to incomplete energy transfer from polymer to the complex.
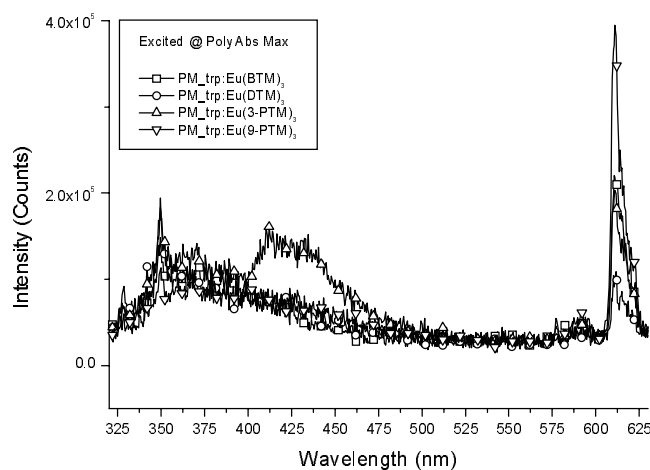
Figure 4.6. Emission from PM_trp:Eu(BTM)$_3$, PM_trp:Eu(DTM)$_3$, PM_trp:Eu(3-PTM)$_3$, and PM_trp:Eu(9-PTM)$_3$, excited at the polymer absorbance maximum.

Another way to visualize the differences in intensities of the residual emission and europium emission is illustrated by Figure 4.7. The residual emission from the

polymer complexes was relatively the same throughout the series, showing that the energy levels between the polymers and the ligands were matched well. The differences in europium emission showed that the ligand's singlet to triplet energy gap (ΔE_{ST}) did play an important role in the energy transfer process. For the ligands with the smaller ΔE_{ST}'s, DTM and 3-PTM, less energy was available to be donated to europium, therefore europium would have a smaller relative emission intensity. Those ligands which had larger ΔE_{ST}'s, BTM and 9-PTM, would have a larger relative emission intensity.
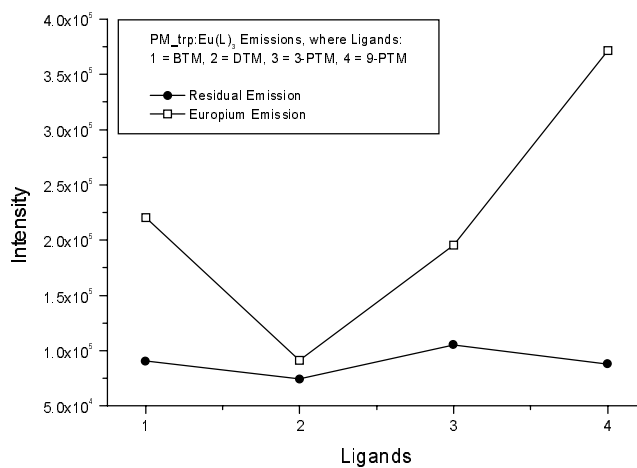
Figure 4.7. Comparison of intensities of emission from europium and PM_trp complex residual emission, relative to the ligands, when the systems were excited at the PM_trp absorbance maximum.

For all ligand systems, the residual polymer complex emission was less than 1% of

PM_trp's emission. Energy transfer efficiencies were calculated using the equation,

$$ET = 1 - \left(\frac{F_{da}}{F_d} \right)$$

where F_{da} is the fluorescence intensity of the donor in the presence of the acceptor,

and F_d is the fluorescence intensity of the donor alone. The results are summarized

in Table 4.3.

Table 4.3. Energy transfer efficiencies from PM_trp to L in PM_trp:Eu(L)₃ systems, where L = BTM, DTM, 3-PTM, and 9-PTM.

	BTM	DTM	3-PTM	9-PTM
PM_trp:Eu(L)₃	0.993	0.994	0.991	0.993

4.3 Experimental

2-acetylthiophene, 2-acetylfuran, 2-acetylpyridine, 2-acetylpyrazine, 2,5-dibromobenzoic acid, 1,1,1,5,5,5-hexafluoro-2,4-pentanedione (HFA), and all reagents were purchased from Aldrich, TCI or Lancaster and used with out further purification. The solvents purchased from VWR. 2,5-didecyloxyphenyl-1,3-bisboronic acid[7] was synthesized according to published procedures. The melting transitions of the polymers were obtained using a Shimadzu DSC-50 that performs differential scanning calorimetry (DSC). Samples were run in aluminum crucibles at a heating rate of 5 °C/min under a nitrogen atmosphere. The ^{1}H and ^{13}C NMR solution spectra were recorded on a Bruker AC 250 MHz NMR and a Bruker AM

360 MHz NMR. The abbreviations used are s for singlet, d for doublet, t for triplet, q for quartet, and m for multiplet. Elemental analysis for C, H, and N was obtained from Atlantic Microlab, Inc., Norcross Georgia

1-Phenyl-3-(2-thienyl)-1,3-propanedione or (BTM). In a r.b. flask under argon, sodium hydride (1.76 g, 73.44 mmol) in 100 mL anhydrous THF and stirred magnetically. Methyl benzoate (4.58 mL, 36.72 mmol) was added and following dissolution, 2-acetylthiophene (3.96 mL, 36.72 mmol) was added, forming a milky white mixture. A reflux condenser was added to the flask and the reaction was heated to 60 °C for 24 h. The reaction was acidified with concentrated hydrochloric acid, poured into a separatory funnel, and extracted with diethyl ether. The ether layer was dried over sodium sulfate, and evaporated. The residue was recrystallized from ethanol, yielding the product which was olive green in color.

1,3-Di-2-thienyl-1,3-propanedione or di-2-thenoylmethane (DTM). Folowing the procedure for BTM, ethyl 2-thiophene carboxylate (4.30 mL, 32.01 mmol), 2-acetylthiopphene (3.45 mL, 32.01 mmol), and sodium hydride 1.54 g, 64.17 mmol) in 100 mL THF, gave, after recrystallization from ethanol, a yellow solid in 33 % yield.

1-(3-Phenanthryl)-3-(2-thienyl)-1,3-propanedione   or   3-phenanthroyl-2-thenoylmethane (3-PTM).   In a r.b. flask under argon, a suspension of sodium hydride (0.635 g, 24.92 mmol), and ethyl thiophene-2-carboxylate (1.68 mL, 12.46 mmol), in anhydrous THF was prepared.   To this suspension, a solution of 3-acetylphenanthrene (2.75 g, 12.46 mmol) and a catalytic amount of 18-C-6 in anhydrous THF was added. The reaction was stirred at room temperature for 30 min an hour and refluxed for 4 h. Once cooled down, 50 mL of (10 % w/v) H_2SO_4 was added and the crude product was extracted three times with ether. The organic layer was washed with saturated brine solution until neutralized, dried over Na_2SO_4, filtered and evaporated to dryness under reduced pressure. Purification of the crude product by recrystallization from ethanol yielded a yellow solid in 64 % yield; ^{1}H NMR (CDCl$_3$) δ 6.84 (s, 1H), 7.16 (dd, 1H, J = 2.25 and   8.25 Hz), 7.58 - 7.92 (m, 9H), 8.03 (d, 1H), 8.77 (d, 1H), 9.28 (s, 1H), 15.10 (br. s, 1H); Melting point: 127.41 °C; HRSM (DEI) Calc for $C_{21}H_{14}SO_2$: m/z 330.40; Found: 330.40 m/z; Elemental Anal Calc for $C_{21}H_{14}SO_2$: C, 76.34; H, 4.27; S, 9.71. Found: C, 76.33; H, 4.41; S, 9.50.

1-(9-Phenanthryl)-3-(2-thienyl)-1,3-propanedione   or   9-phenanthroyl-2-thenoylmethane (9-PTM). Following the procedure for the preparation of 3-PTM, 9-acetylphenanthrene (3.00 g, 13.62 mmol), sodium amide (1.06 g, 27.24 mmol), ethyl thiophene-2-carboxylate (1.83 mL, 13.62 mmol), and   18-C-6 in anhydrous THF, gave, after recrystallization from isopropanol, a yellow solid in 60 % yield; [1]H

NMR (CDCl$_3$) δ 6.60 (s, 1H), 7.14 (dd, 1H, J = 2.25 and 8.25 Hz), 7.60 - 7.80 (m, 7H), 7.95 (d, 1H), 8.04 (s, 1H), 8.48 (d, 1H), 8.68 (d, 1H), 8.73 (d, 1H), 15.60 (br. s, 1H); Melting point: 135.66 °C; HRMS (DEI) Calc for C$_{21}$H$_{14}$SO$_2$: m/z 330.40;Found: 330.40 m/z; Elemental Anal Calc for C$_{21}$H$_{14}$SO$_2$: C, 76.34; H, 4.27; S, 9.71. Found: C, 76.33; H, 4.41; S, 9.50.
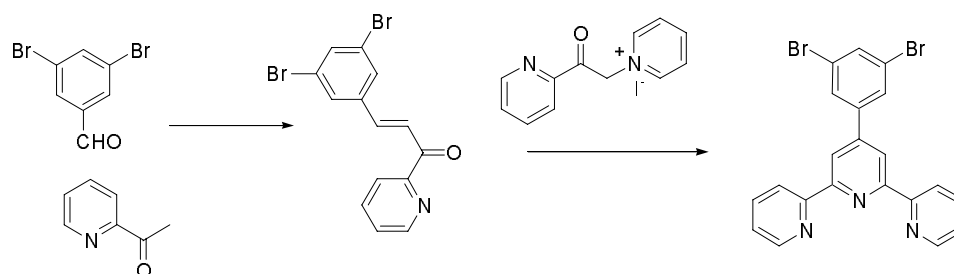
Scheme 4.3. Schematic representation of the synthesis of 4'-(3,5-dibromophenyl)-2,2':6',2''-terpyridine.

2-Pyridyl-3,5-dibromostyrylketone. Dissolved 3,5-dibromobenzaldehyde in 3% wt potassium hydroxide in methanol at 0°C. Added 2-acetylpyridine (2.15 mL) drop wise while stirring. Continued stirring overnight, the mixture was concentrated to a third by volume, followed by cooling. Collected the pale yellow crystals, filtered washed with cold methanol, dried in vacuum oven to collect the pre product.

Pyridacyl pyridinium iodide.[8] Added 2-acetylpyridine (5.61 mL, 50 mmol) drop wise to a stirred mixture of iodine (12.69 g, 50 mmol) in dry pyridine (60 mL). The reaction was refluxed for one hour, cooled to room temperature slowly then placed on ice to complete precipitation of a thick black solid. The solid was collected washed with ether-ethanol solution (9:1, 50 mL), dried and redissolved in boiling

methanol, added activated charcoal filtered hot through celite. Upon cooling the clear yellow solution the product, precipitated as golden yellow crystals.

4'-(3,5-dibromophenyl)-2,2':6',2''-terpyridine.[9] To a mixture of pyridacyl pyridinium iodide (4.80 g, 0.0147 mol), 2-pyridyl-3,5-dibromostyrylketone (5.411 g, 0.0147 mol) and ammonium acetate (12.0 g) in 100mL of methanol was refluxed overnight. The reaction mixture of concentrated and cooled collected the white crude product, which was purified by recrystallized from acetone to yield the pure product. Yield: 3.35 g (49%) ^{1}H NMR (250 MHz, CDCl$_3$): δ 8.73 (d, 2H, 4.5 Hz), 8.66 (d, 2H, 8 Hz), 8.63 (s, 2H), 7.95 (d, 2H, 2 Hz), 7.88 (td, 2H 2 Hz, 8 HZ), 7.74 (t, 1H, 2 Hz), 7.37 (qd, 2H, 2 Hz, 7 Hz).

Poly(1,4-(2,5-didecyloxy)phenylene-*alt*-3,5-[4'-(2,2':6',2''-terpyridine)] phenylene) (PM_trp) 2,5-bis(decyloxy)-1,4-phenylenebisboronic acid (0.5979 g 1.25 mmol) 4'-(3,5-dibromophenyl)-2,2':6',2''-terpyridine (0.584 g 1.25 mmol) was placed on a flask, degassed by evacuating the flask and filling with argon three times. Added degassed toluene (25 mL), methanol (12 mL) and sodiumcarbonate (2M, 13 mL), added Pd(PPh$_3$)$_4$ (11 mg) in toluene (5 mL) at reflux, and continued to reflux for 48 hours. Cooled to room temperature, separated the organic phase, washed the organic phase with water and added to methanol. Collected the polymer, dissolved in chloroform and reprecipitated in methanol, collected the product, washed with cold methanol, air dried and dried further in a vacuum over overnight.

Yield: 0.639 g: ^{1}H NMR (360 MHz, CDCl$_3$): δ 8.97, 8.70, 8.68, 8.26, 7.94, 7.86, 7.32, 7.23, 4.04, 1.77, 1.34, 1.13, 1.02, 0.73. ^{13}C NMR (360 MHz, CDCl$_3$): δ 156.69, 156.24, 150.68, 149.32, 139.15, 137.84, 136.89, 130.88, 127.68, 123.81, 121.43, 119.38, 116.35, 69.87, 32.074, 29.620, 26.496, 22.789, 14.27.

Steady state emission spectra were recorded using a Fluorolog-3 model FL3-21 with a 450 W xenon lamp source, double grating excitation monochromator, single grating emission monochromator, and a room temperature R928 PMT serving as the detector. Phosphorescence studies were carried out using the 1934D3 phosphorimeter in conjunction with the Fluorolog-3 system with a xenon flash lamp. Plots were generated using GRAMS/32 and DataMax software. Absorbance spectra were generated using OLIS (Modernized Cary 14) UV/Vis/NIR spectrophotometer equipped with deuterium and tungsten lamps for UV and Vis/NIR regions. The quantum yield for emission in solution, determined according to the method described by Demas and Crosby[10] relative to quinine sulfate in 1.0M H$_2$SO$_4$ (0.546).[11] The singlet and triplet energies of the polymers were calculated according to published methods.[12] Solution concentrations were kept below 10^{-5} M, to prevent inner filter effects, reabsorption of emission, and concentration quenching. The triplet energies of the polymers were calculated from low temperature phosphorescence spectra (2-methyltetrahydrofuran solutions at 77 K).

Polymer molecular weights were determined by gel permeation chromatography (GPC) and multiple angle laser light scattering (MALLS) using a Waters gel permeation chromatography system coupled with a Wyatt miniDAWN (690nm laser) light scattering detector, and are shown in Table 4.3.

Table 4.4. Polymer molecular weights were determined by gel permeation chromatography (GPC) and multiple angle laser light scattering (MALLS).

Polymer	dn/dc (mL/g)	M_n (g/mol)	M_w (g/mol)	PDI
PM_trp	0.1608	8.669×10^6	1.117×10^7	1.29

4.4 Conclusions

Energy transfer was shown to occur from the polymer, PM_trp, to a variety of ligands on europium *tris*(chelates), and finally to europium. Besides matching the energy levels between polymer and ligand, the ligand's singlet to triplet energy gap was shown to be important in obtaining intense emission from europium.

4.5 References

[1] Weissman, S. I. *J. Chem. Phys.*, **1942**, *10*, 214.

[2] Melby, L. R.; Rose, N. J.; Abramson, E.; Caris, J. C. *J. Am. Chem. Soc.*, **1964**, *86*, 5117.

[3] Sato, S.; Wada, M.; Seki. T. *Jpn. J. Appl. Phys.*, **1968**, *7*,7.

[4] Carnall, W. T.; P. R. Fields, and K. Rajnak, *J. Chem. Phys.*, **1968**, *49***,** 4443.

[5] Crosby, G. A.; Whan, R. E.; Alire, R. M. J. *Chem. Phys.,* **1961**, *34*, 743.

[6] Sato, S; Wada, M., *Bull. Chem. Soc. Jpn.,* **1970**, *43*, 1955.

[7] Frank, M.; Wasgindt, M.; Pautzsch, T.; Klemm, E. *Macromol. Chem. Phys.*, **2001**, *202*, 980.

[8] Priimov, G. U.; Moore, P.; Maritim P. K.; Butlanyi, P. K. Alcock N. W. *J. Chem. Soc., Dalton Trans.*, **2000**, 445.

[9] Hanabusa, K.; Nakamura, A.; Koyama, T.; Shirai, H. *Makromol. Chem*., **1992**, *193*, 1309.

[10] Demas, N. J.; Crosby, G. A. *J. Phys. Chem.,* **1971**, *75*, 991.

[11] Klink, S. I.; Hebbink, G. A. ; Grave, L. ; Oude Alink, P. G. B. ; Van Veggel, F.C.J.M.; Werts, M.H.V. *J. Phys. Chem. A*., **2002**, *106*, 3681.

[12] Turro, N. J. *Modern Molecular Photochemistry*, University Science Books, 1991.

CHAPTER 5

VISIBLE EMISSION RESULTING FROM ENERGY TRANSFER FROM POLYMERS WITH PENDANT β-DIKETONATES TO BOUND EUROPIUM(III) COMPLEXES

5.1 Introduction

Triplet-Triplet Energy Transfer (TTET) was analyzed again with polymers that could bind to the europium complexes. In these energy transfer studies though, the polymers used had bidentate ligating pendant groups, β-diketonates. The structure of these polymers are shown in Figure 5.1. This meant that the polymers bound to the lanthanide ions *via* a formal dative bond as one of the ligands of a *tris*(chelate), rather than a *tris*(chelate) coordinating to a polymer bound ancillary ligand, such as the terpyridine used in PM_trp.
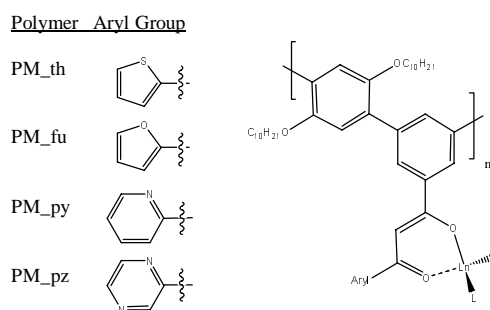
Figure 5.1. Structures of PM_aryl:Ln(L)$_2$, where Ln = Eu or Gd, and L = HFA, BTM, DTM, 3-PTM, or 9-PTM.

The other ligands which were bound to the lanthanide included five different β-diketonates: 1,1,1,5,5,5-heaxfluoro-2,4-pentanedione (HFA), benzoyl-2-thenoylmethane (BTM), di-2-thenoylmethane (DTM), 3-phenanthroyl-2-thenoylmethane (3-PTM), and 9-phenanthroyl-2-thenoylmethane (9-PTM). The structures of the ligands are shown in Figure 5.2. HFA was used in order to obtain the triplet state energies of the polymer complex. Substitution of aryl groups in the aroylthenoylmethanes was performed, according to modified Claisen condensation methods, in an attempt to vary the energies of the complexes. The two lanthanides in this study were the non-emitting gadolinium and the red-emitting europium.
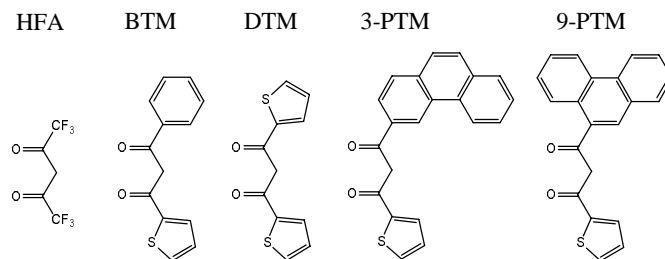
Figure 5.2. Structures of ligands: HFA, BTM, DTM, 3-PTM, and 9-PTM.

The triplet energies of the polymers was determined by studying the PM_fu:Gd(HFA)$_2$, PM_py:Gd(HFA)$_2$, PM_pz:Gd(HFA)$_2$, and PM_th:Gd(HFA)$_2$ systems. In these systems, any triplets that were formed were trapped on the polymer since energy transfer cannot take place from the polymer to higher energy levels of the Gd(HFA)$_2$ complex.

The triplet energies of the polymer-lanthanide-aromatic ligand systems were determined by studying the polymer-ligand emission from the gadolinium species. In these systems, energy transfer from polymer to ligand system was able to take place, but then the process was halted, since gadolinium's energy level is higher than any organic ligand can donate. PM_fu:Gd(L)$_2$, PM_py:Gd(L)$_2$, PM_pz:Gd(L)$_2$, PM_th:Gd(L)$_2$, and PM_trp:Gd(L)$_3$ solutions were made, where L = BTM, DTM, 3-PTM, and 9-PTM.

Step three of this process was studied by replacing the gadolinium with europium in each of the systems. Europium's energy level is able to accept energy from the ligand systems, thus allowing the process to complete. PM_fu:Eu(L)$_2$, PM_py:Eu(L)$_2$, PM_pz:Eu(L)$_2$, and PM_th:Eu(L)$_2$ solutions were made, where L = BTM, DTM, 3-PTM, and 9-PTM.

5.2 Results and discussion

The precursor polymer, PM_es, for polymers with *β*-diketonate-type pendant groups was synthesized by coupling 2,5-didecyloxyphenyl-1,3-bisboronic acid and 1,3-dibromoethylbenzoate via Suzuki coupling, as shown in Scheme 5.1. PM_es was further reacted with the corresponding aromatic ketone to get the final polymer .
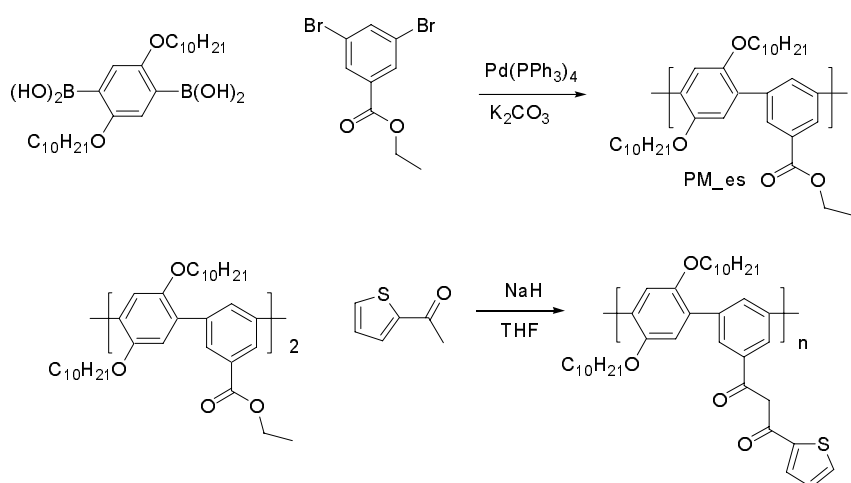
Scheme 5.1. Synthetic route to prepare the polymer PM_th.

The molecular weight of polymer PM_es (M_n – 1.27 x 10^4 g/mol) was determined using gel permeation chromatography and multiple angle laser light scattering, and the molecular weights of polymers PM_th (M_n – 14,850 g/mol), PM_fu (M_n – 14,420 g/mol), PM_py (M_n – 14,685 g/mol), and PM_pz (M_n – 14,750 g/mol) were calculated from the degree of polymerization (DP) of PM_es and molecular weights of the repeat units of the polymers. The polymer photophysical properties were studied in THF and shown in Table 5.1.

Table 5.1. Photophysical properties polymers with β-diketonate pendant groups.

	PM_th	PM_fu	PM_py	PM_pz
Abs. Max (nm)	330	332	330	330
(cm^{-1})	30,300	30,120	30,300	30,300
Em. Max (nm)	396.5	391	391	396
(cm^{-1})	25,220	25,575	25,575	25,250
FWHM (nm)	59	54	54.5	58.4
Δ (cm^{-1})	5,082	4,545	4,728	5,051
QE	0.2121	0.2154	0.1915	0.2134
Life Times (ns)	1.65	1.66	1.52	1.68
k_f (s^{-1})	1.32 x 10^8	1.32 x 10^8	1.26 x 10^8	1.27 x 10^8
k_{ST} (s^{-1})	4.74 x 10^8	4.72 x 10^8	5.31 x 10^8	4.68 x 10^8
E_S (eV)	3.40	3.40	3.42	3.40
(cm^{-1})	27,425	27,425	27,585	27,425
E_T (eV)	2.50	2.50	2.50	2.47
(cm^{-1})	20,165	20,165	20,165	19,920
ΔE_{ST} (eV)	0.90	0.90	0.92	0.93

The photophysical properties of the polymers did not change appreciably upon changing the substitution of the *β*-diketonate pendant groups. The rate constant of fluorescence for the polymers PM_th, PM_fu, PM_py, and PM_pz were calculated to be 1.32 x 10^8 s^{-1}, 1.30 x 10^8 s^{-1}, 1.26 x 10^8 s^{-1}, and 1.27 x 10^8 s^{-1}, respectively. For molecules with a band gap greater than 24,000 cm^{-1}, non-radiative decay can be neglected. Hence, the radiative decay and the intersystem crossing are the only important pathways available to the singlet state.[1] The rate constant of intersystem crossing for the polymers PM_th, PM_fu, PM_py, and PM_pz were calculated to be 4.74 x 10^8 s^{-1}, 4.72 x 10^8 s^{-1}, 5.31 x 10^8 s^{-1}, and 4.68 x 10^8 s^{-1}, respectively. The rate of intersystem crossing was greater than radiative decay for all polymers; therefore, most singlet excited states produced were converted to triplets. These polymers were inefficient as emitting layers in organic light emitting devices. However, these polymers were used efficiently as sensitizers for europium.

To understand and explain the photophysical properties of polymers, PM_th was studied in detail. The low energy absorbance transition at 330 nm was attributed to the $S_1 \leftarrow S_0$ transition of the polymer. Upon exciting at the absorbance maximum of the polymer, emission centered at 396.5 nm, with a corresponding Stokes' shift of 5,082 cm^{-1} was obtained. The fluorescence quantum yield of emission was low, and the rate of intersystem crossing was 3.6 times greater than the rate fluorescence. However, there was no room temperature phosphorescence of the polymers, thus the polymer was a great candidate for triplet energy transfer to lanthanides. The *para-meta* linkage of the polymer backbone gave rise to a high energy polymer with a triplet energy of 2.50 eV.

The energy transfer studies were all performed in the solution state at a concentration of 1×10^{-5} M in anhydrous tetrahydrofuran (THF), except for the low temperature phosphorescence studies on the gadolinium complexes which used 2-methyltetrahydrofuran (2-MeTHF) as the solvent. The solutions were made from 1×10^{-3} M stock solutions of polymer, ligand, sodium ethoxide, gadolinium(III) chloride, and europium(III) chloride. The polymer and ligand solutions used anhydrous THF as the solvent, while the base and lanthanide solutions used anhydrous ethanol as solvent. The polymer, appropriate lanthanide, ligand, and base were added together in a 1:1:2:3 ratio in more anhydrous THF until they were finally 1×10^{-5} M. The normalized absorbance spectra of the polymers and the polymer-lanthanide complexes are shown in Figures 5.3 to 5.6.
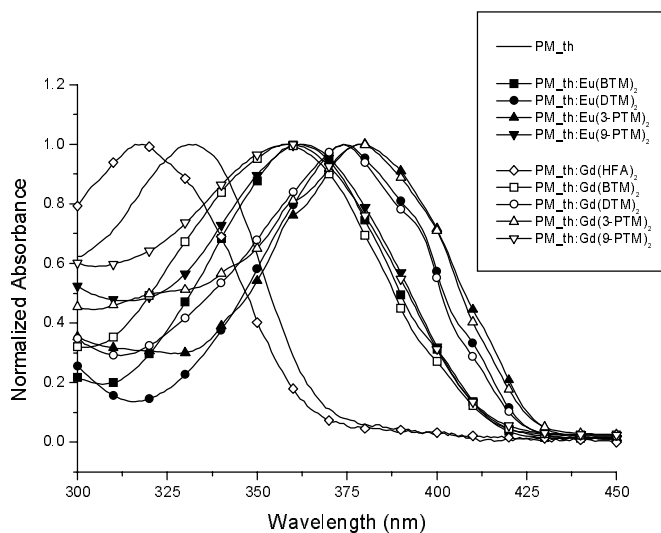
Figure 5.3. Absorbance spectra of PM_th:Ln(L)$_2$ complexes relative to PM_th and each other.
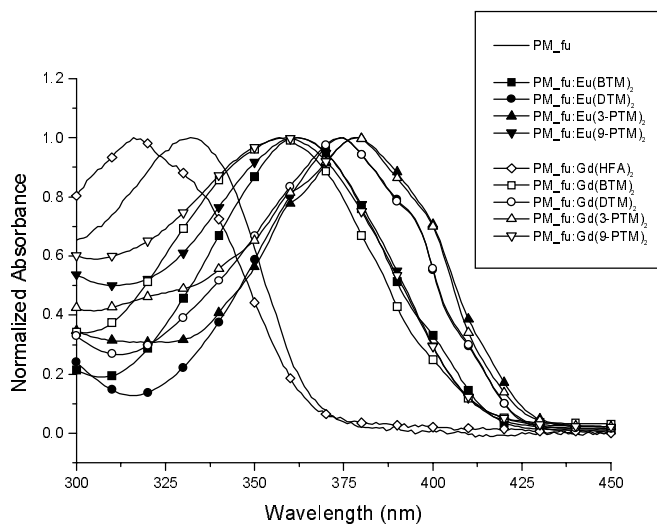
Figure 5.4. Absorbance spectra of PM_fu:Ln(L)$_2$ complexes relative to PM_fu and each other.
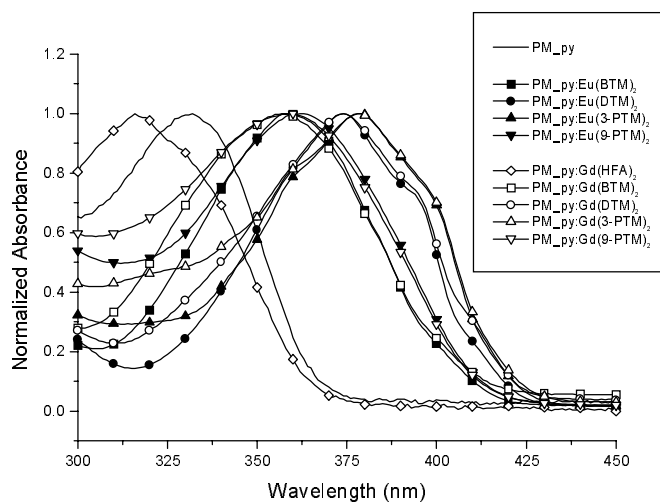
Figure 5.5. Absorbance spectra of PM_py:Ln(L)$_2$ complexes relative to PM_py and each other.
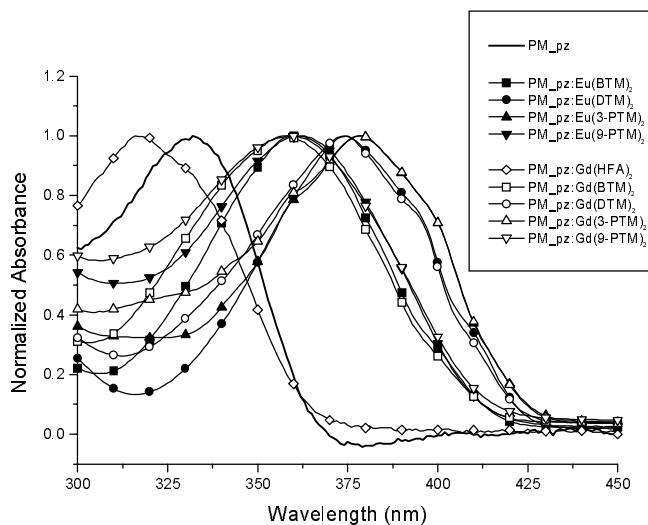
Figure 5.6. Absorbance spectra of PM_pz:Ln(L)$_2$ complexes relative to PM_pz and each other.

The lanthanide complexes coordinated to PM_th, PM_fu, PM_py, and PM_pz in this study were: gadolinium bis(1,1,1,5,5,5-hexafluoro-2,4-pentanedione) [Gd(HFA)$_2$], gadolinium *bis*(benzoyl-2-thenoylmethane) [Gd(BTM)$_2$], gadolinium *bis*(di-2-thenoylmethane) [Gd(DTM)$_2$], gadolinium *bis*(3-phenanthroyl-2-thenoylmethane) [Gd(3-PTM)$_2$], and gadolinium *bis*(9-phenanthroyl-2-thenoylmethane) [Gd(9-PTM)$_2$]; europium *bis*(benzoyl-2-thenoylmethane) [Eu(BTM)$_2$], europium *bis*(di-2-thenoylmethane) [Eu(DTM)$_2$], europium *bis*(3-phenanthroyl-2-thenoylmethane) [Eu(3-PTM)$_2$], and europium *bis*(9-phenanthroyl-2-thenoylmethane) [Eu(9-PTM)$_2$].

As mentioned previously, the PM_aryl:Gd(HFA)$_2$ complexes were studied to determine the triplet energies of the polymers, since the HFA ligands are unable to accept energy from the polymer, triplet states are trapped on the polymer. The other gadolinium species were made to determine the triplet energies of the polymer complexes since gadolinium's accepting *J* state is much higher than any organic ligand would be able to donate energy. Therefore, triplet states can be donated from polymer to polymer-ligand complex, but are trapped at this step since gadolinium is at a higher energy. The photophysical properties of these complexes are reported in Tables 5.2 to 5.5.

Table 5.2. Photophysical properties of PM_th gadolinium complexes.

	PM_th: Gd(HFA)$_2$	PM_th: Gd(BTM)$_2$	PM_th: Gd(DTM)$_2$	PM_th: Gd(3-PTM)$_2$	PM_th: Gd(9-PTM)$_2$
Abs. Max (nm) (cm^{-1})	331 30,211	358 27,933	374 26,738	378 26,455	358 27,933
Em. Max (nm) (cm^{-1})	391 25,575	416 24,038	421 23,753	427 23,419	405 24,691
Δ (cm^{-1})	4,636	3,895	2,985	3,036	3,242
E_S (eV) (cm^{-1})	3.42 27,548	3.23 26,042	3.09 24,876	3.06 24,691	3.21 25,907
E_T (eV) (cm^{-1})	2.75 22,148	2.42 19,531	2.38 19,231	2.40 19,380	2.39 19,305
ΔE_{ST} (eV)	0.67	0.81	0.71	0.66	0.82

Table 5.3. Photophysical properties of PM_fu gadolinium complexes.

	PM_fu: Gd(HFA)$_2$	PM_fu: Gd(BTM)$_2$	PM_fu: Gd(DTM)$_2$	PM_fu: Gd(3-PTM)$_2$	PM_fu: Gd(9-PTM)$_2$
Abs. Max (nm) (cm^{-1})	332 30,120	356 28,090	374 26,738	379 26,385	359 27,855
Em. Max (nm) (cm^{-1})	393 25,445	399 25,063	430 23,256	427 23,419	402 24,876
Δ (cm^{-1})	4,675	3,027	3,482	2,966	2,979
E_S (eV) (cm^{-1})	3.40 27,397	3.25 26,178	3.09 24,938	3.06 24,691	3.22 25,974
E_T (eV) (cm^{-1})	2.76 22,297	2.45 19,763	2.38 19,231	2.47 19,920	2.40 19,380
ΔE_{ST} (eV)	0.64	0.80	0.71	0.59	0.82

Table 5.4. Photophysical properties of PM_py gadolinium complexes.

	PM_py: Gd(HFA)$_2$	PM_py: Gd(BTM)$_2$	PM_py: Gd(DTM)$_2$	PM_py: Gd(3-PTM)$_2$	PM_py: Gd(9-PTM)$_2$
Abs. Max (nm) (cm^{-1})	332 30,120	356 28,090	374 26,738	379 26,385	359 27,855
Em. Max (nm) (cm^{-1})	391 25,575	416 24,038	425 23,529	431 23,202	402 24,876
Δ (cm^{-1})	4,545	4,052	3,209	3,183	2,979
E$_S$ (eV) (cm^{-1})	3.40 27,397	3.25 26,178	3.09 24,876	3.07 24,753	3.23 26,042
E$_T$ (eV) (cm^{-1})	2.76 22,247	2.42 19,531	2.39 19,305	2.45 19,763	2.44 19,685
ΔE$_{ST}$ (eV)	0.64	0.83	0.70	0.62	0.79

Table 5.5. Photophysical properties of PM_pz gadolinium complexes.

	PM_pz: Gd(HFA)$_2$	PM_pz: Gd(BTM)$_2$	PM_pz: Gd(DTM)$_2$	PM_pz: Gd(3-PTM)$_2$	PM_pz: Gd(9-PTM)$_2$
Abs. Max (nm) (cm^{-1})	332 30,120	357 28,011	374 26,738	378 26,455	358 27,933
Em. Max (nm) (cm^{-1})	393 25,445	399 25,063	422 23,697	430 23,256	401 24,938
Δ (cm^{-1})	4,675	2,948	3,041	3,199	2,995
E$_S$ (eV) (cm^{-1})	3.39 27,322	3.24 26,110	3.09 24,876	3.06 24,691	3.23 26,042
E$_T$ (eV) (cm^{-1})	2.76 22,247	2.44 19,685	2.39 19,305	2.45 19,763	2.44 19,685
ΔE$_{ST}$ (eV)	0.63	0.80	0.70	0.61	0.79

In all four polymer systems, the complexes with BTM and 9-PTM had larger singlet to triplet energy gaps (ΔE$_{ST}$) than those complexes with other ligands. This indicated that it would be less likely for these triplet states on BTM and 9-PTM to convert back to singlet states. If there was competition for energy that was donated to the lanthanide and back energy transfer from the ligand triplet energy to the ligand singlet energy, then residual emission would be seen in the emission spectra. In

order for the energy transfer process to lead to efficient emission from europium, the ligand had to be higher in energy than the $^5D_1$ (19,030 cm^{-1}) level of europium. In all four instances of the aroyl-2-thenoylmethanes, the triplet energies met the requirements that they be at least 2000 cm^{-1} above the $^5D_0$ (17,260 cm^{-1}) level of europium to prevent thermal back energy transfer.[2,3]

All four systems had similar energies, regardless of the identity of the aryl group on the pendant β-diketonates. With the information available in Table 5.2, energy transfer pathways of the PM_th systems were postulated and the one for PM_th:Eu(BTM)$_2$ is shown in Scheme 5.2. Polymer PM_th upon interacting with 332 nm light produced a singlet excited state with energy of 3.40 eV. This state would under go three processes; radiative decay (fluorescence), non-radiative decay, and intersystem crossing to produce a triplet state with energy of 2.50 eV. As the gadolinium complex had a singlet energy of 3.23 eV and a triplet energy of 2.42 eV, Förster type and Dexter type energy transfer was possible in this system.
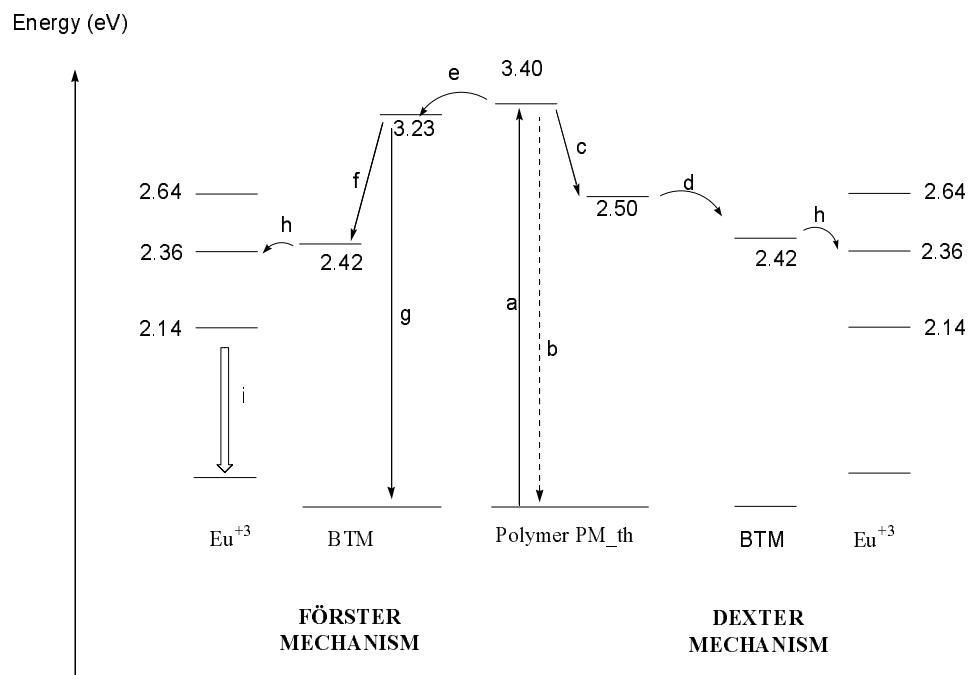
Energy (eV)

Scheme 5.2. The energy transfer mechanism for the PM_trp:Eu(BTM)$_3$ system.

In the emission spectra shown in Figure 5.7 to 5.10, the polymer complexes were excited at the polymer absorbance maxima. In all instances, when the polymer was excited, singlet excited states were converted to triplet excited states *via* the heavy atom effect of the lanthanide ion. The polymer-centered triplet energy was then transferred to the *β*-diketonate ligand *via* the exchange mechanism, and then again *via* the exchange mechanism to the emitting *J* state of europium, from which emission occurred. When Eu(L)$_2$ complexes were coordinated to the polymer, europium emission was observed, with some residual emission from the polymer or polymer-ligand complex. The residual emission was most likely due to incomplete energy transfer from polymer to the complex.
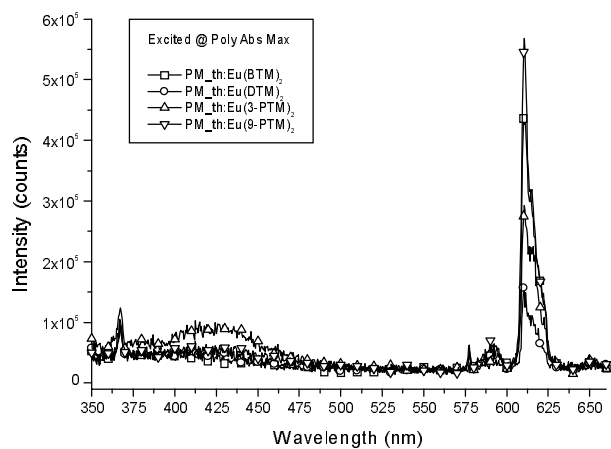
Figure 5.7. Emission from PM_th:Eu(BTM)₂, PM_th:Eu(DTM)₂, PM_th:Eu(3-PTM)₂, and PM_th:Eu(9-PTM)₂, excited at the polymer absorbance maximum.
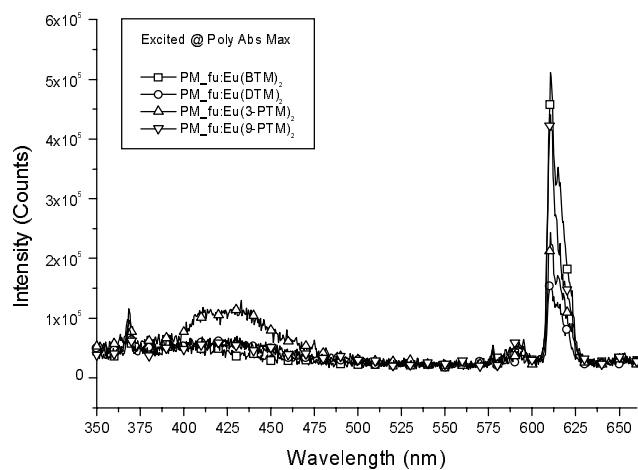
Figure 5.8. Emission from PM_fu:Eu(BTM)₂, PM_fu:Eu(DTM)₂, PM_fu:Eu(3-PTM)₂, and PM_fu:Eu(9-PTM)₂, excited at the polymer absorbance maximum.
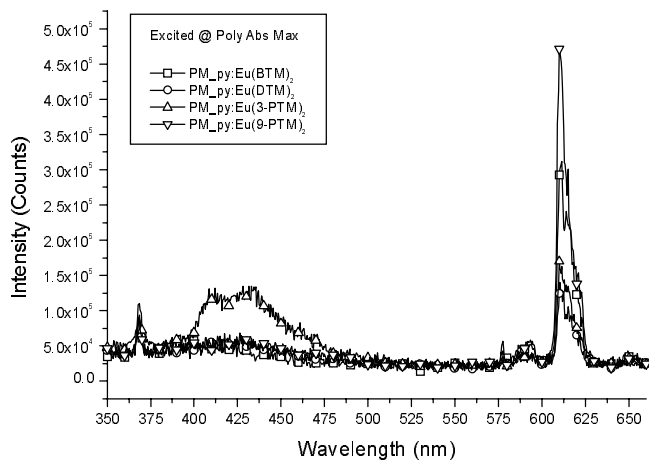
Figure 5.9. Emission from PM_py:Eu(BTM)$_2$, PM_py:Eu(DTM)$_2$, PM_py:Eu(3-PTM)$_2$, and PM_py:Eu(9-PTM)$_2$, excited at the polymer absorbance maximum.
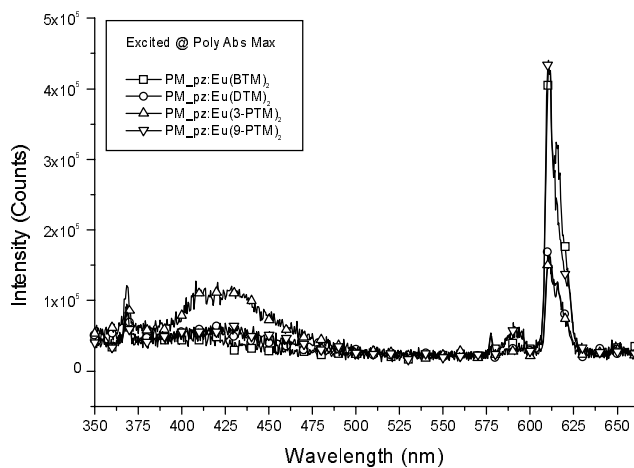
Figure 5.10. Emission from PM_pz:Eu(BTM)$_2$, PM_pz:Eu(DTM)$_2$, PM_pz:Eu(3-PTM)$_2$, and PM_pz:Eu(9-PTM)$_2$, excited at the polymer absorbance maximum.

Another way to visualize the differences in intensities of the residual emission and europium emission is illustrated by Figures 5.11 to 5.14. The residual emission from the polymer complexes was relatively the same throughout the series, showing that the energy levels between the polymers and the ligands were matched well. The differences in europium emission showed that the ligand's singlet to triplet energy gap (ΔE_{ST}) did play an important role in the energy transfer process. For the ligands with the smaller ΔE_{ST}'s, DTM and 3-PTM, less energy was available to be donated to europium, therefore europium would have a smaller relative emission intensity. Those ligands which had larger ΔE_{ST}'s, BTM and 9-PTM, would have a larger relative emission intensity.
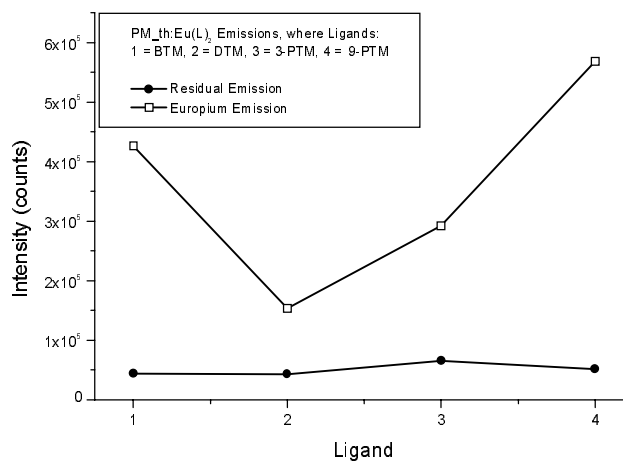
Figure 5.11. Comparison of intensities of emission from europium and PM_th complex residual emission, relative to the ligands.
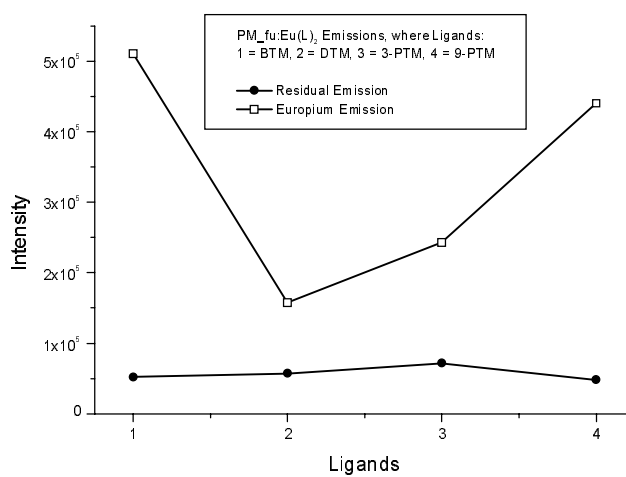
Figure 5.12. Comparison of intensities of emission from europium and PM_fu complex residual emission, relative to the ligands.
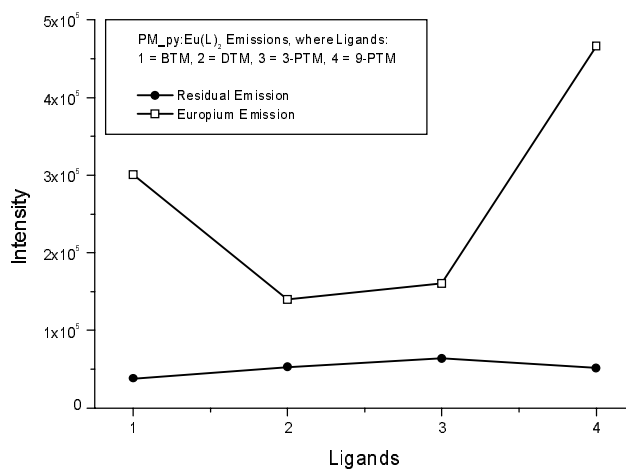
Figure 5.13. Comparison of intensities of emission from europium and PM_py complex residual emission, relative to the ligands.
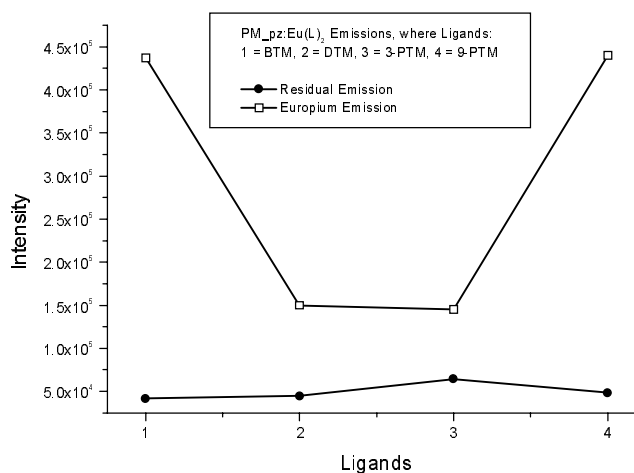
Figure 5.14. Comparison of intensities of emission from europium and PM_pz complex residual emission, relative to the ligands.

For all ligand systems, the residual polymer complex emission was less than 1% of PM_trp's emission. Energy transfer efficiencies were calculated using the equation,

$$ET = 1 - \left(\frac{F_{da}}{F_d} \right)$$

where F_{da} is the fluorescence intensity of the donor in the presence of the acceptor, and F_d is the fluorescence intensity of the donor alone. The results are summarized in Table 5.6.

Table 5.6. Energy Transfer Efficiencies from Polymer to Ligand to PM_aryl:Eu(L)$_2$ Systems, where L = HFA, BTM, DTM, 3-PTM, or 9-PTM.

	BTM	DTM	3-PTM	9-PTM
PM_fu:Eu(L)₂	0.998	0.998	0.998	0.998
PM_py:Eu(L)₂	0.999	0.998	0.998	0.998
PM_pz:Eu(L)₂	0.998	0.998	0.997	0.998
PM_th:Eu(L)₂	0.998	0.998	0.998	0.998

5.3 Experimental

2-acetylthiophene, 2-acetylfuran, 2-acetylpyridine, 2-acetylpyrazine, 2,5-dibromobenzoic acid, 1,1,1,5,5,5-hexafluoro-2,4-pentanedione (HFA), and all reagents were purchased from Aldrich. 2,5-didecoylxyphenyl-1,3-bisboronic acid[4] was synthesized according to published procedures. The melting transitions of the polymers were obtained using a Shimadzu DSC-50 that performs differential scanning calorimetry (DSC). Samples were run in aluminum crucibles at a heating rate of 5 °C/min under a nitrogen atmosphere. The ^{1}H and ^{13}C NMR solution spectra were recorded on a Bruker AC 250 MHz NMR and a Bruker AM 360 MHz NMR. The abbreviations used are s for singlet, d for doublet, t for triplet, q for quartet, and m for multiplet.

Ethyl-3,5-dibromobenzoate. 3,5-dibromobenzoic acid was refluxed in excess ethanol (200 mL) with catalytic amount of PTSA for 48 hours. The product was purified by purified by column chromatography (SiO$_2$) using 10% ethyl acetate and hexanes. (92% yield) ^{1}H NMR (CDCl$_3$) δ 8.079 (2H, d, J – 1.7 Hz), 7.820 (1H, t, J – 1.7 Hz), 4.361 (2H, q, J – 7 Hz), 1.376 (3H, t, J – 7 Hz)

Poly(2,5-didecyloxyphenyl-3,5-ethylbenzoate) (PM_es). 2,5-didecyloxyphenyl-1,3-bisboronic acid (0.4783 g, 0.001 mol), ethyl-3,5-dibromobenzoate (0.3079 g, 0.001 mol), and the palladium catalyst [Pd(PPh$_3$)$_4$, 30 mg] were placed in an argon-flushed flask. Toluene (6 mL) and 2 M aqueous K$_2$CO$_3$ (3 mL) were added, degassed,

and heated at reflux under argon for 2 days. The organic phase was added to methanol, producing the polymer as a solid precipitate, which was further purified by reprecipitation in methanol. Yield 0.5085 g (94.73%) ^{1}H NMR (CDCl$_3$) δ 8.271, 7.7976, 7.035, 4.374, 3.915, 1.664, 1.365, 1.292, 1.139, 0.776. ^{13}C NMR (CDCl$_3$) δ 165.662, 149.321, 137.065, 129.121, 128.778, 115.049, 68.521, 59.669, 30.785, 28.610, 28.515, 28.435, 38.355, 28.316, 28.219, 25.019, 21.565, 13.333, 12.966.

PM_th. Sodium hydride (0.024 g, 1 mmol) was suspended in anhydrous THF (10 mL). In separate containers, PM_es (0.20 g, 0.373 mmol) and 2-acetylthiophene (0.11 mL,) were dissolved in 2 mL of anhydrous THF. Then each solution was added consecutively to the sodium hydride suspension. After the addition of the two reagents, the reaction was stirred at room temperature for 30 min. Then the mixture was stirred at 60 °C for 24 hrs. After cooling the reaction mixture to room temperature, acidified with HCl solution, and poured onto methanol. The polymer was collected by filetration, and purified by dissolving the polymer in CHCl$_3$ and precipitating in methanol. Yield 0.088 g (38%)

PM_fu. Sodium hydride (0.024 g, 1 mmol) was suspended in anhydrous THF (10 mL). In separate containers, PM_es (0.20 g, 0.373 mmol) and 2-acetylpyrazine (0.0.083 g, 0.68 mmol) were dissolved in 2 mL of anhydrous THF. Then each solution was added consecutively to the sodium hydride suspension. After the addition of the two reagents, the reaction was stirred at room temperature for 30 min.

Then the mixture was stirred at 60 °C for 48 hrs, followed the reaction progress with TLC. After cooling the reaction mixture to room temperature, acidified with HCl solution, and poured onto methanol. The polymer was collected by filetration, and purified by dissolving the polymer in CHCl$_3$ and precipitating in methanol. Yield 0.175 g (77%)

PM_py. Sodium hydride (0.024 g, 1 mmol) was suspended in anhydrous THF (10 mL). In separate containers, PM_es (0.20 g, 0.373 mmol) and 2-acetylpyridine (0.11 mL,) were dissolved in 2 mL of anhydrous THF. Then each solution was added consecutively to the sodium hydride suspension. After the addition of the two reagents, the reaction was stirred at room temperature for 30 min. Then the mixture was stirred at 60 °C for 24 hrs. After cooling the reaction mixture to room temperature, acidified with HCl solution, and poured onto methanol. The polymer was collected by filetration, and purified by dissolving the polymer in CHCl$_3$ and precipitating in methanol. Yield 0.080 g (36%)

PM_pz. Sodium hydride (0.024 g, 1 mmol) was suspended in anhydrous THF (10 mL). In separate containers, PM_es (0.20 g, 0.373 mmol) and 2-acetylfuran (0.075 g, 0.68 mmol) were dissolved in 2 mL of anhydrous THF. Then each solution was added consecutively to the sodium hydride suspension. After the addition of the two reagents, the reaction was stirred at room temperature for 30 min. Then the mixture was stirred at 60 °C for 48 hrs, followed the reaction progress with TLC. After

cooling the reaction mixture to room temperature, acidified with HCl solution, and poured onto methanol. The polymer was collected by filetration, and purified by dissolving the polymer in $CHCl_3$ and precipitating in methanol. Yield 0.174 g (76%)

Polymer molecular weights were determined by gel permeation chromatography (GPC) and multiple angle laser light scattering (MALLS) using a Waters gel permeation chromatography system coupled with a Wyatt miniDAWN (690 nm laser) light scattering detector, and the results are summarized in Table 5.7.

Table 5.7. Polymer molecular weights determined by GPC and MALLS in $CHCl_3$.

Polymer	dn/dc mL/g	Mn g/mol	Mw g/mol	DP	PDI
PM_es	0.0975	1.27×10^4	1.64×10^4	24	1.28

Steady state emission spectra were recorded using a Fluorolog-3 model FL3-21 with a 450 W xenon lamp source, double grating excitation monochromator, single grating emission monochromator, and a room temperature R928 PMT serving as the detector. Phosphorescence studies were carried out using the 1934D3 phosphorimeter in conjunction with the Fluorolog-3 system with a xenon flash lamp. Plots were generated using GRAMS/32 and DataMax software. Absorbance spectra were generated using OLIS (Modernized Cary 14) UV/Vis/NIR spectrophotometer equipped with deuterium and tungsten lamps for UV and Vis/NIR regions. The quantum yield for emission in solution, determined according to the method described by Demas and Crosby[5] relative to quinine sulfate in 1.0 M H_2SO_4 (0.546).[6]

The singlet and triplet energies of the polymers were calculated according to published methods.[7]

5.4 Conclusions

Energy transfer was shown to occur from the polymers: PM_fu, PM_py, PM_pz, and PM_th, to a variety of ligands on europium *bis*(chelates), and finally to europium. Besides matching the energy levels between polymer and ligand, the ligand's singlet to triplet energy gap was shown to be important in obtaining intense emission from europium.

5.5 References

[1] Plotnikov, V. G.; Dolgih, B. A. *Opt. Spectr.*, **1977**, *43*, 882.

[2] Crosby, G. A.; Whan, R. E.; Alire, R. M. J. *Chem. Phys.,* **1961**, *34*, 743.

[3] Sato, S; Wada, M., *Bull. Chem. Soc. Jpn.,* **1970**, *43*, 1955.

[4] Frank, M.; Wasgindt, M.; Pautzsch, T.; Klemm, E. *Macromol. Chem. Phys.*, **2001**, *202*, 980.

[5] Demas, N. J.; Crosby, G. A. *J. Phys. Chem.,* **1971**, *75*, 991.

[6] Klink, S. I.; Hebbink, G. A. ; Grave, L. ; Oude Alink, P. G. B. ; Van Veggel, F.C.J.M.; Werts, M.H.V. *J. Phys. Chem. A.*, **2002**, *106*, 3681.

[7] Turro, N. J. *Modern Molecular Photochemistry*, Univeristy Science Books, 1991.

CHAPTER 6

INFRARED EMISSION RESULTING FROM ENERGY TRANSFER FROM POLYMERS WITH PENDANT β-DIKETONATES TO BOUND ERBIUM(III) COMPLEXES

6.1 Introduction

The traditional electronic communications approaches are being replaced by optical fiber communications. The optical signal transmitted along the optical fiber undergoes attenuation and loss, hence the signal has to be recovered. The distance traveled by a signal and be detected error free is limited by noise to about 100 km. Electrical repeaters are used to regenerate the signal, where the optical signal is converted to an electrical signal, which is then reconverted to an optical signal by a laser diode. This process is expensive and cannot be upgraded to higher bit rates. The optical amplifiers are used to overcome this shortcoming of optical fiber communications.[1] Amplifiers operate by amplifying light in the fiber by simulated emission. Optical amplifiers are divided into two groups according to the signal wavelength ranges; the conventional C-band (1530 nm - 1560 nm) and the latest L-band (1570 nm – 1605 nm) developed by Lucent Technologies.[2]

Erbium is a rare earth metallic element used extensively to amplify light signals sent through fiber optic cables. Erbium-doped fiber amplifiers (EDFA), obtained by doping erbium to a optical fiber, and pumping with light, are used to transmit optical signals over a very long distance without the need for signal regeneration.[3,4] A large gain is obtained when these erbium doped fibers are "pumped" by an external light source, such as a laser at a wavelength shorter than 1.55 µm. The typical setup of an EDFA, as shown in Figure 6.1, contains a pump, coupler, erbium-doped fiber, and an isolator.
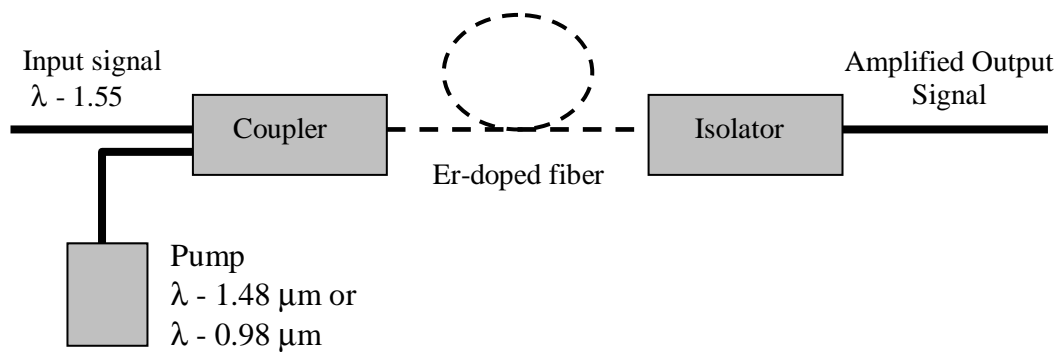
Figure 6.1. A typical setup of erbium-doped fiber amplifier (EDFA).

The Coupler combines the incoming signal (1.55 µm) with the pump laser (1.48 µm or 0.98 µm). The coupled signal then passes through an erbium-doped fiber and finally, decouples the amplified original input signal. The EDFAs placed along the telecommunication lines are used to amplify the input signal, thereby receiving an error free message over thousands of miles. The EDFA units are economical enough to be placed along the fiber optic lines, but the pump lasers required to excite the

erbium to a higher excited state are expensive. Optical excitation of erbium using common excitation sources would be cheaper, therefore beneficial to the industry.

The operation of an EDFA is explained by a 3-level lasing model, as illustrated in Figure 6.2. The pump photon promotes electrons to a higher energy state, which then relaxes to a long lived metastable state. The transition $^4I_{13/2} \rightarrow {}^4I_{15/2}$ leads to emission around 1.55 μm, with a long radiative lifetime of 10 ms. Coincidently, the emission of erbium corresponds to the spectral region where the optical fiber has the smallest loss. The metastable excited state of erbium is stimulated to emit another photon, which is coherent with the stimulating photons. This process occurred along the erbium-doped fiber repeatedly to amplify the input signal.
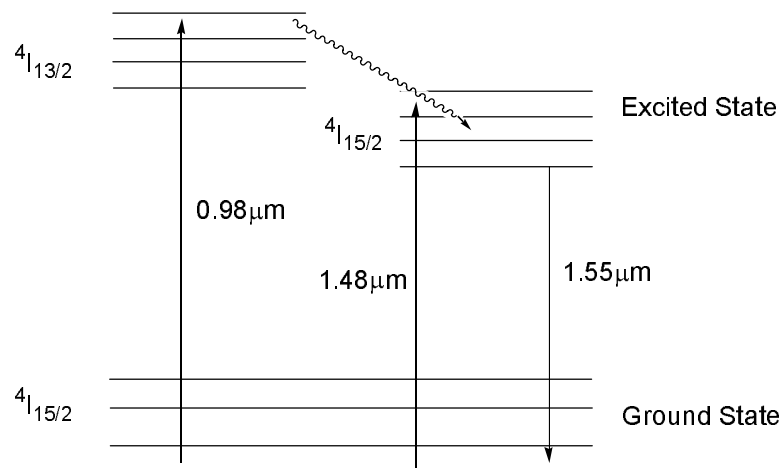
Figure 6.2. The optical amplifying occurs in a 3-level lasing model. Optical pumping at 0.98 μm would excite to $^4I_{11/2}$, which would then relax to $^4I_{13/2}$, pumping at 1.48 μm would excite direct to $^4I_{13/2}$. Stimulated emission from the $^4I_{13/2}$ is obtained at 1.55 μm.

Erbium containing nanoparticles are used as EDFAs,[5] but these materials need to be pumped by a laser. A realistic goal will be to develop materials that can be pumped using inexpensive excitations sources. Triphenylene-functionalized erbium complexes and erbium porphyrin complexes doped onto polymers are used to obtain emission from erbium as an alternate route.[6,7] Organic materials such as β-diketonates are used to sensitize lanthanides that emit visible light such as europium and samarium.[8]

This chapter discusses the use of erbium-bound porphyrinates bound to β-diketonate containing polymers which are able to sensitize erbium at both the polymer's and porphyrinate's absorbance maxima, leading to stimulated emission centered at 1.55 µm. The structures of these materials are shown in Figure 6.3.
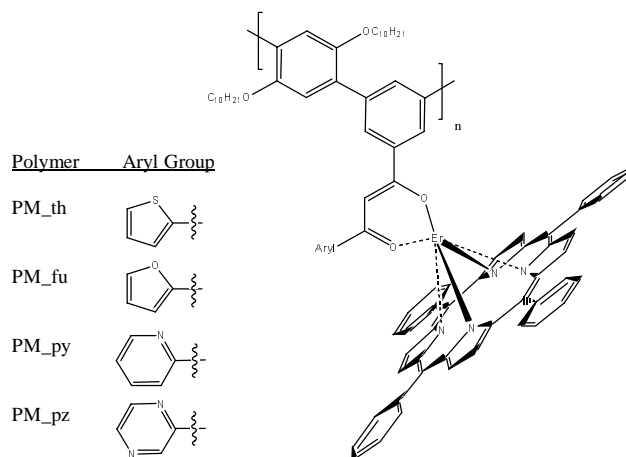
Figure 6.3. Structures of PM_aryl:ErTPP.

Energy transfer studies were performed on a series of polymers with β-diketonate pendant groups. The other ligand which was bound to the erbium was tetradentate *meso*-tetraphenylporhphine, (TPP). The lanthanides in this study was the infrared-emitting erbium and the non-emitting gadolinium *bis*(HFA) for polymer triplet energies determination.

The triplet energies of the polymers was determined by studying the Poly:Gd(HFA)$_2$ systems. In these systems, any triplets that were formed were trapped on the polymer since energy transfer cannot take place from the polymer to higher energy levels of the Gd(HFA)$_2$ complex. PM_fu:Gd(HFA)$_2$, PM_py:Gd(HFA)$_2$, PM_pz:Gd(HFA)$_2$, and PM_th:Gd(HFA)$_2$.

Ideally, the triplet energies of the polymer-lanthanide-TPP systems would have been determined by studying the polymer-ligand emission from the gadolinium species. In these systems, energy transfer from polymer to ligand system would be able to take place, but then the process would be halted, since gadolinium's energy level is higher than any organic ligand can donate. PM_fu:GdTPP, PM_py:GdTPP, PM_pz:GdTPP, and PM_th:GdTPP solutions would have been made. These materials were difficult to synthesize because of gadolinium's tendency to form sandwich complexes with TPP, therefore the synthesis of a useful gadolinium-TPP complex has yet to be fully realized.

Step three of this process was studied by replacing the gadolinium with erbium in each of the systems. Erbium's energy level is able to accept energy from the ligand systems, thus allowing the process to complete. PM_fu:ErTPP, PM_py:ErTPP, PM_pz:ErTPP, and PM_th:ErTPP solutions were made.

6.2 Results and discussion

The synthesis and photophysical properties of the polymers, PM_fu, PM_py, PM_pz, and PM_th were reported in the previous chapter. The erbium porphyrinate synthesis is shown in Scheme 6.1. The *meso*-tetraphenylporphyrin (H$_2$TPP) was dilithiated using lithium bis(trimethylsilyl)amide in dry 1,2-dimethoxyethane to yield Li$_2$TPP. The subsequent addition of erbium(III) chloride in anhydrous toluene produced Cl(DME)ErTPP.
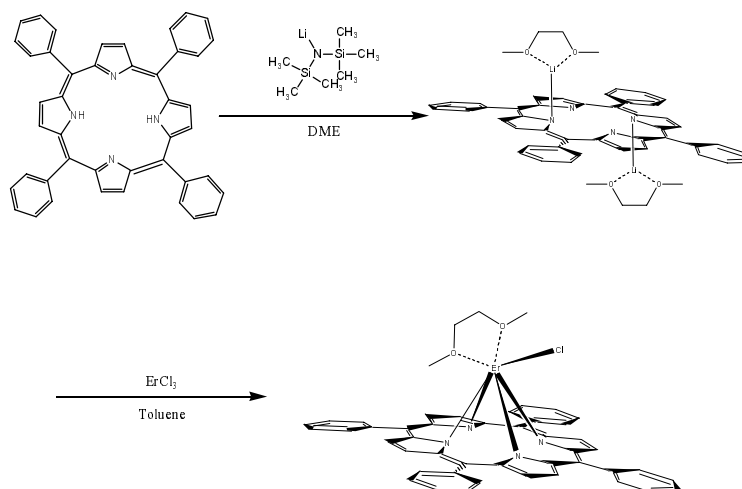
Scheme 6.1. Synthesis of Cl(DME)ErTPP.

The polymer and the porphyrinate were combined by deprotonating the β-diketonate, with sodium ethoxide as base, which then displaced the chloride on the Cl(DME)ErTPP, as shown in Scheme 6.2.
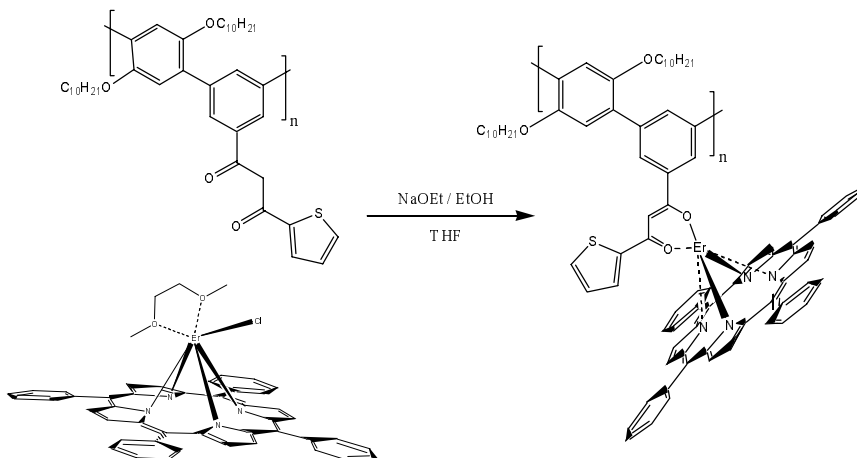
Scheme 6.2. Synthesis of PM_th:ErTPP .

The energy transfer studies were all performed in the solution state at a concentration of 1×10^{-5} M in anhydrous tetrahydrofuran (THF). The solutions were made from 1×10^{-3} M stock solutions of polymer, sodium ethoxide, and Cl(DME)ErTPP. The polymer and Cl(DME)ErTPP solutions used anhydrous THF as the solvent, while the base solution used anhydrous ethanol as solvent. The polymer, Cl(DME)ErTPP, and base were added together in a 1:1:1 ratio in more anhydrous THF until they were finally 1×10^{-5} M. The normalized absorbance spectra of the polymers and the polymer-lanthanide complexes are shown in Figures 6.4. The peaks overlap quite well and show that the porphyrin has a higher molar absorptivity than the polymers.
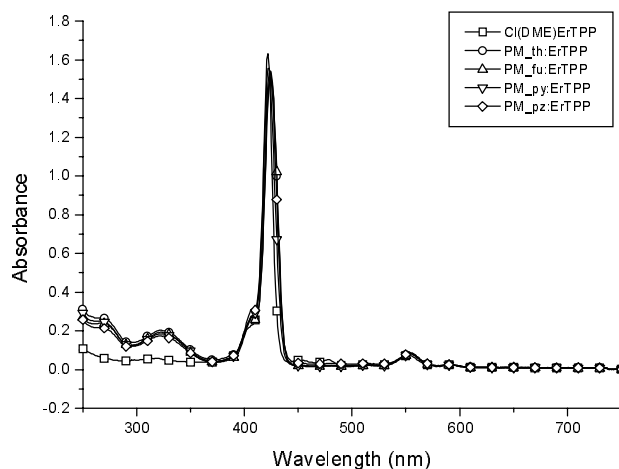
Figure 6.4. Absorption spectra of PM_th:ErTPP, PM_fu:ErTPP, PM_py:ErTPP, and PM_pz:ErTPP, along with Cl(DME)ErTPP for comparison.

Figure 6.5 shows the infrared emission from the PM_aryl:ErTPP systems when they are excited at the porphyrin's absorption maxima. Room temperature infrared emission is produced from these systems, which were in an anhydrous THF solution at 1×10^{-5} M concentration. There seems to be a small signal from the Cl(DME)ErTPP, which is most likely quenched through solvent interactions, since there is no capping ligand above the erbium in the porphyrin system.

Figure 6.6 shows room temperature infrared emission from these systems as well, but in this case the systems were excited at the polymer absorption maxima. The intensity of emission is about two thirds that of the emission shown in Figure 6.5. This is due to the fact that there is a multi-step energy transfer process involved when exciting at the polymer, than when exciting the porphyrin which has fewer processes involved.
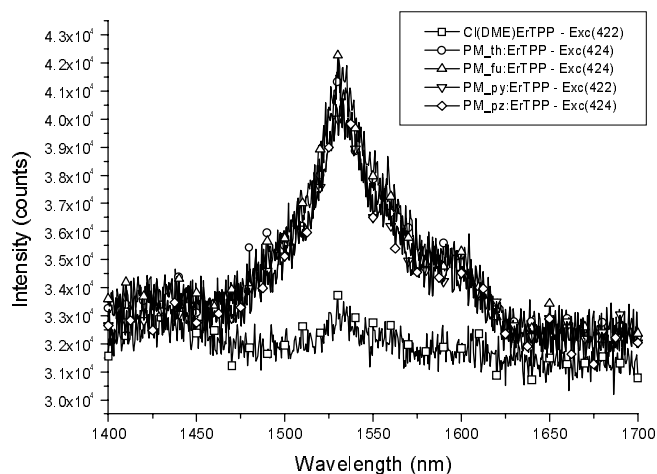
Figure 6.5. Infrared emission from PM_th:ErTPP, PM_fu:ErTPP, PM_py:ErTPP, and PM_pz:ErTPP, as compared to Cl(DME)ErTPP, when exciting at the porphyrin absorbance maxima.
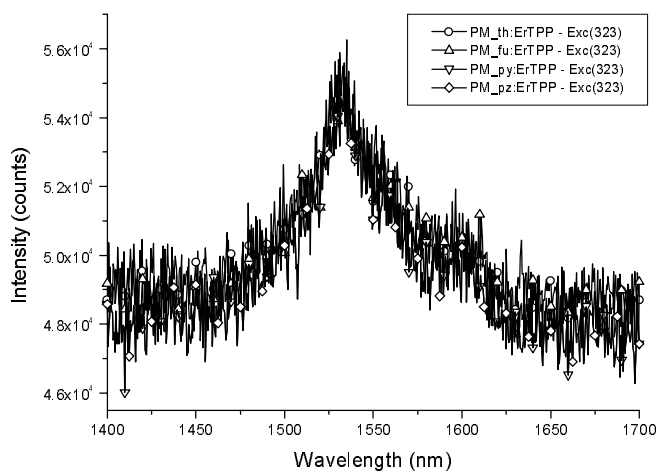
Figure 6.6. Infrared emission from PM_th:ErTPP, PM_fu:ErTPP, PM_py:ErTPP, and PM_pz:ErTPP, when exciting at the polymer absorbance maxima.

In Figure 6.7, the residual emission from the PM_th:ErTPP complex is shown, relative to the emission from PM_th and Cl(DME)ErTPP, when excited at the polymer's absorption maximum. The regular emission from PM_th is shown as reference. The large reduction in emission intensity for PM_th:ErTPP was due to the energy transfer process, with the dip around 424 nm due to the high extinction coefficient of the porphyrin system. Cl(DME)ErTPP did not show emission in this region, which was expected since it does not absorb energy near the polymer's absorption maximum. All four polymer systems behaved in the same manner.
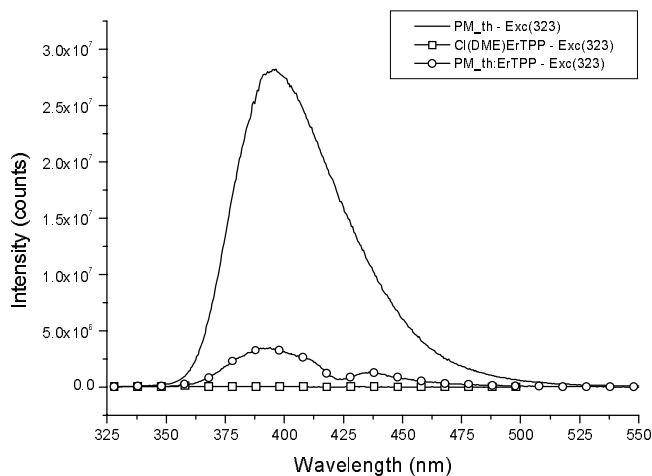
Figure 6.7. Residual emission from PM_th:ErTPP as compared to PM_th and Cl(DME)ErTPP, when exciting at the polymer absorbance maxima.

Figure 6.8 shows the porphyrin emission from the Cl(DME)ErTPP and PM_th:ErTPP systems. The porphyrins had very small Stokes' shifts due to the limited ability for rearrangement in structural geometries between the ground and excited states.
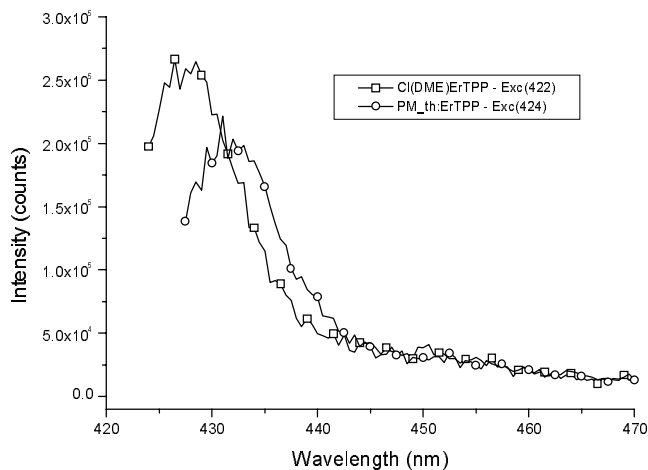
Figure 6.8. Residual emission from PM_th:ErTPP as compared to Cl(DME)ErTPP, when exciting at the porphyrin absorbance maxima.

6.3 Experimental

Erbium(III) chloride, *meso*-tetraphenylporphine, 1,2-dimethoxyethane, tetrahydrofuran, toluene, and all reagents were purchased from Aldrich. (LiDME)2TPP[9] and Cl(DME)ErTPP[10] was synthesized according to published procedures. All reactions involving the formation of Cl(DME)ErTPP were carried out under nitrogen in a glove box or using standard Schlenk techniques with the assistance of C. J. Jones in Roy Periana's group at USC. Crystal structures for the erbium complexes were determined by Muhammed Yousufuddin in Robert Bau's group at USC. Solvents were reagent grade or higher quality and were dried by distillation from sodium benzophenone, degassed, and stored over activated molecular sieves.

(LiDME)$_2$TPP. In the glove box, 1,2-DME (40 mL) was added by pipette to a mixture of H$_2$TPP (1.00 g; 1.60 mmol) and LiN(SiMe$_3$)$_2$ (0.59 g, 3.53 mmol) in a Schlenk flask. The flask was sealed and brought out of the glove box, where it was heated to relux with stirring overnight. The solution was cooled to room temperature and then filtered to obtain 1.27 g (92%) of a bright purple powder that was dried *in vacuo* overnight. The reaction was monitored by UV/Vis.

Cl(DME)ErTPP. In the glove box, ErCl$_3$ and (LiDME)$_2$TPP were combined in a Schlenk flask equipped with a sidearm. Toluene was added, the flask was brought out of the glove box reaction was then heated to reflux in a sealed flask. After 4 hours, a precipitate formed and was separated from the solution by filtration of the hot reaction mixture. The residue in the reaction flask was washed twice with dichloromethane, the combined filtrates were combined with the toluene solution. The solvent mixture was then reduced to one third the original volume *in vacuo* and cooled to 0 °C, where upon a red purple crystalline material precipitated and was isolated by filtration. The mother liquor was then concentrated to by half and cooled to -78 °C affording a second crop of product. The two fractions were combined and dissolved in hot toluene, the solution was then cooled to room temperature, layered with pentane, and cooled to 0 °C yielding the product. X-ray quality crystals were grown from the toluene/pentane solution under an inert atmosphere for several weeks. The reaction was monitored by UV/Vis absorption and the final product was verified by X-ray crystallography, as shown in Figure 6.9. The literature reference

did not list the crystal structure for the erbium complex, but for other lanthanide complexes with similar structural characteristics.
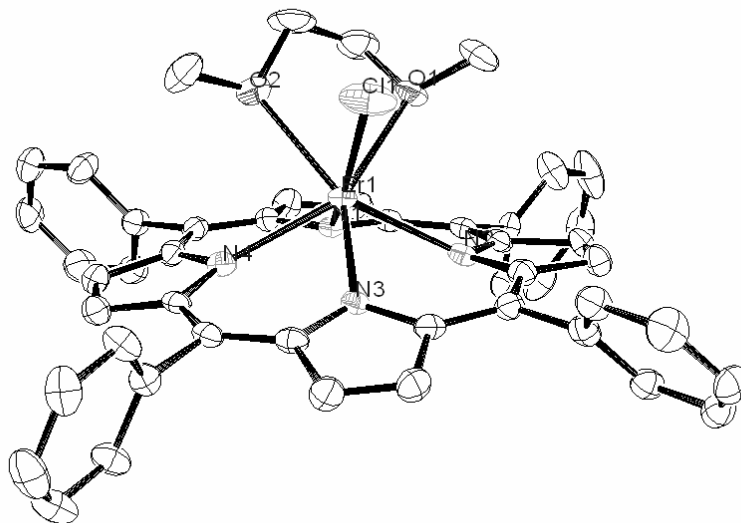
Figure 6.9. ORTEP representation of the thermal ellipsoid plot of the molecular structure of Cl(DME)ErTPP showing selected atom labels. All hydrogen atoms and solvent atoms in the crystal structure have been omitted for clarity. Nonlabeled atoms are carbon.

To verify that the Cl(DME)ErTPP reacted as expected and to also generate another unreported crystal structure, TpErTPP[11] was synthesized.

TpErTPP. In the glove box, Cl(DME)ErTPP, potassium hydridotris(1-pyrazolyl)borate (KTp), and DME were added together in a Schlenk flask. Following addition, the solution was taken out of the glove box, and was allowed to stir at room temperature overnight. The solvent was then removed *in vacu*o, and the

purple residue was extracted with methylene chloride, leaving behind a brown residue. The solution was then filtered, reduced to one third volume, and layered with pentane. Purple crystals formed on standing overnight. The supernatant was filtered, concentrated, and cooled to -78 °C whereupon an additional amount of product precipitated. The isolated solids were then combined, dissolved in methylene chloride, and cooled to -78 °C. Crystals then formed, which were isolated by cannula filtration giving the product. Crystals of X-ray diffraction quality were grown by slow evaporation of a letting the methylene chloride/pentane solution sit without any intervention for at least 1 week. The crystal structure is shown in Figure 6.10.
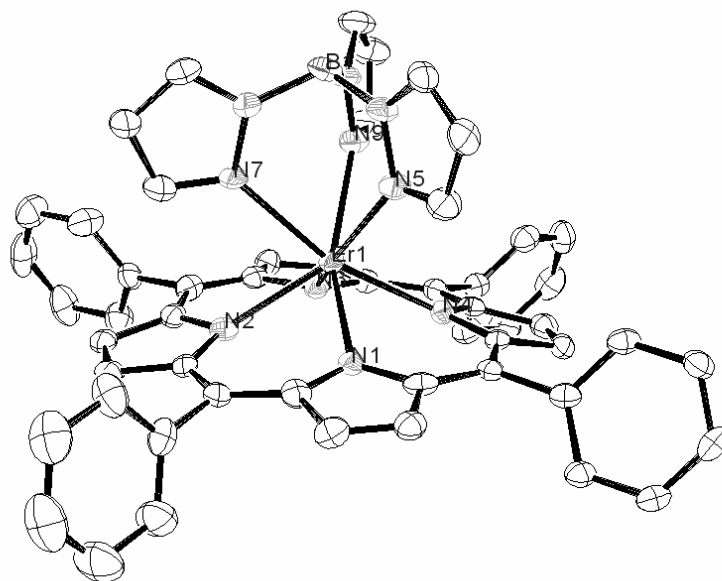
Figure 6.10. ORTEP representation of the thermal ellipsoid plot of the molecular structure of TpErTPP showing selected atom labels. All hydrogen atoms in the crystal structure have been omitted for clarity. Nonlabeled atoms are carbon.

Tables 6.1 and 6.2 list structural information about the erbium porphyrinates obtained by generating the crystal structures.

Table 6.1. Crystal data for the ErTPP complexes.

	Cl(DME)ErTPP	TpErTPP
Empirical formula	$C_{51}H_{41}ClErN_4O_2$	$C_{53}H_{37}BErN_{10}$
Fw	944.59	992.00
T/K	133(2)	133(2)
Wavelength/Å	0.71073	0.71073
cryst syst	monoclinic	orthorhombic
space group	P2(1)/c	P2(1)2(1)2(1)
a/Å	12.191(3)	9.0579(16)
b/Å	26.854(7)	23.340(4)
c/Å	13.699(4)	23.820(4)
α/deg	90	90
β/deg	111.459(4)	90
γ/deg	90	90
V/Å^3	4173.5(19)	5035.8(15)
Z	4	4
D(calcd) Mg/m^3	1.503	1.308

Table 6.2. Selected structural data for the ErTPP complexes; all measurements in Angstroms.

	Cl(DME)ErTPP	TpErTPP
Er-N1	2.368(6)	2.375(5)
Er-N2	2.322(6)	2.337(4)
Er-N3	2.337(5)	2.371(4)
Er-N4	2.342(6)	2.366(4)
Er-Cl	2.602(2)	n/a
Er-O1	2.419(5)	n/a
Er-O2	2.444(5)	n/a
Er-N5	n/a	2.538(5)
Er-N7	n/a	2.500(5)
Er-N9	n/a	2.528(5)

Steady state emission spectra were recorded using a Fluorolog-3 model FL3-21 with a 450 W xenon lamp source, double grating excitation monochromator, single grating emission monochromator, a room temperature R928 PMT serving as the visible range detector, and a liquid nitrogen cooled Hamamatsu R5502-72 NIR PMT serving as the near-infrared range detector. Phosphorescence studies were carried out using the 1934D3 phosphorimeter in conjunction with the Fluorolog-3 system with a xenon flash lamp. Plots were generated using GRAMS/32 and DataMax software. Absorbance spectra were generated using OLIS (Modernized Cary 14) UV/Vis/NIR spectrophotometer equipped with deuterium and tungsten lamps for UV and Vis/NIR regions.

6.4 Conclusions

Energy transfer was shown to occur from the polymers: PM_fu, PM_py, PM_pz, and PM_th, to the erbium porphyrinate, and finally to the erbium, resulting in room temperature erbium emission. The residual emissions from the polymer complex systems were similar to each other regardless of the identity of the aryl group at the end of the pendant β-diketonate. Larger relative emission intensity was observed when exciting the PM_aryl:ErTPP systems at the absorbance maxima for the porphyrinate when compared to exciting at the polymer absorbance maxima.

6.5 References

[1] Poole, S.; Payne, D. N.; Mears, R. J.; Fermann, M. E.; Laming, R. I. *J. Light. Tech.,* **1985**, *21*, 737.

[2] Oshima,I.; Nihiyama, K.; Kurotori, K.; Hayakawa, H. *Furakawa Review*, **2003**, *23*, 71.

[3] Mears, R. J.; Reekie, L.; Jauncie, I. M.; Payne, D. N.; *Elect. Lett.*, **1987**, *23*, 1026.

[4] Desurvire, E.; Simpson, J. R. ; Becker, P. C. *Opt. Lett.,* **1987**, *12*, 888.

[5] Lehmann, O.; Meyssamy, H.; Kompe, K.; Schnablegger, H.; Hasse, M. *J. Phys. Chem. B*., **2003**, *107*, 7449.

[6] Klink, S. I.; Grave, L.; Reinhoudt, D. N.; Van Veggel, F.C.J.M.; Werts, M.H.V.; Geurts, F. A. J.; Hofstraat, J. W. *J. Phys. Chem. A.*, **2000**, *104*, 5457.

[7] Harrison, B. S.; Foley, T. J.; Bouguettaya, M.; Reynolds, J. R.; Schanze, K.; Shim, J.; Holloway, H.; Padmanaban, G.; Ramakrishnana, S. *Appl. Phys. Lett.*, **2001**, *79*, 3770.

[8] Sager, W. F.; Filipescu, N.; Serafin, F. A. *J. Phys. Chem.*, **1965**, *69*, 1092.

[9] Arnold, J.; Dawson, D.Y.; Hoffman, C.G. *J. Am. Chem. Soc.*, **1993,** *115*, 2707

[10] Foley, T. J.; Abboud, K. A.; Boncella, J. M. *Inorg. Chem.*, **2002**, *41*, 1704.

[11] Foley, T. J.; Harrison, B. S.; Knefely, A. S.; Abboud, K. A.; Reynolds, J. R.; Schanze, K. S.; Boncella, J. M. *Inorg. Chem.*, **2003**, *42*, 5023.

CHAPTER 7

CONCLUSIONS

Polymer light-emitting devices have attracted attention because of their potential utility in a wide variety of flat-panel display applications. To be used as such, polymers must emit colors of interest and have high emission intensities. The emission can be tuned by varying the band gap of the polymer, which is related to the extent of conjugation of the π-electrons. In order to design better polymers, a comprehensive understanding of the relationship between structure and the resultant properties of the polymer is required. Electrical excitation of organic molecules produces more triplet excited states than singlet excited states, and the large gap between the two states prevents the back transfer of triplet excited states to singlet excited states. Since electrophosphorescent devices have higher efficiencies conjugated polymers have to be doped with triplet dyes such as organolanthanides. Lanthanides are robust elements with pure color emission due to narrow atomic emission. The emissive states of lanthanides cannot be optically excited due to their low extinction coefficients. Ligands, such as β-diketonates are used to overcome this and to achieve high emission intensities from lanthanides. The excitation of the polymer produces singlet and triplet excited states, which are then harvested by the ligands to sensitize the lanthanide.

The purpose of this dissertation was to conduct systematic studies of conjugated polymers, in terms of the effects of the polymer structure on the photophysical properties and energy transfer efficiencies of the polymer. Efficient energy transfer from polymers to europium depends on the energy matching of the species involved and the physical separation between them. Polymers with triplet energies higher than the triplet energy of the ligands gave rise to efficient energy transfer. Direct coordination of the lanthanide to the polymer backbone enhanced the energy transfer efficiencies, and the intersystem crossing rates. The polymer systems were designed to produce a higher triplet population upon electrical excitation. The dissertation concentrated on four key areas to achieve higher energy transfer efficiencies from polymers to lanthanides:

1. design and synthesis of polymers with higher singlet energies;

2. design and synthesis of polymers with higher triplet energies;

3. design and synthesis of europium complexes with lower triplet energies; and

4. design and synthesis of polymers with the ability to coordinate to lanthanides.

Polymers with higher singlet energies:

The second and third chapters demonstrated energy harvesting from conjugated polymers to light-emitting dopants. Resonance energy transfer was possible from these polymers to common laser dyes. In Chapter 2, for nearly all samples, PB performed better than P1, although both polymers had similar singlet energies, the

greater spectral overlap of PB with the acceptors led to higher transfer efficiencies. We have confirmed that not only the spectral overlap, but the location overlap is important in energy transfer efficiencies. At high concentrations, dye emission decreases, which is most likely due to dye aggregate formation and quenching.

In Chapter 3, energy transfer was shown to occur from polyphenylenes, P1 and PM_es, as the energy donors to singlet energy accepting Coumarins and the triplet energy accepting metalloporphines. Our studies did not follow Brunner's observations mostly due to the fact that the polymers used in this study did not aggregate. By dispersing the donor polymers and acceptor dyes in polystyrene, aggregation was prevented. Some of the dyes were aggregating as well which complicated matters, so dispersion was necessary for both the polymer and acceptors. For the most part, the efficiencies of energy transfer did correlate with the overlap integrals of the doped systems.

The ability of the polymers to transfer singlet energy to laser dyes such as Coumarins was studied. All polymers studied gave rise to efficient energy transfer to Coumarins. As the energy transfer efficiency depend on the spectral overlap, polymer/dye systems with poor overlap could be used to generate white light. Polymers with longer lived excited states such as aggregates enhanced the rates of energy transfer significantly. The effects of the position and the magnitude of spectral overlap on energy transfer efficiency were discussed.

Polymers with higher triplet energies:

The triplet energy of the polymer can be manipulated by changing the structure of the polymer backbone. Simple variations such as, changing the connectivity from *para-para* to *para-meta* would increase the energy of the polymer significantly. This phenomenon was exploited to design and synthesize polymers with high energy that could be used to sensitize lanthanide complexes with the assistance of pendant ligating groups off the polymer backbone.

Polymers with the ability to coordinate to lanthanides:

High energy polymers were designed and synthesized with *para-meta* connectivity of phenyl rings. In Chapters 4 and 5, these polymers had two-types of pendant groups attached to them: (1) polymers with terpyridine type pendant groups and (2) β-diketonate type pendant groups. The terpyridine pendant groups coordinated to the lanthanide as an ancillary ligand, where as the β-diketonate group coordinated as a part of the primary ligand system. More importantly, the triplet energy of the polymers with pendant groups was similar to the parent polymers. The state energies of the polymeric PM_aryl:Gd(L)$_2$ complexes were evaluated in two stages. The complexes had high energy polymeric components and lower energy ligand systems. Excitation of the polymeric complex PM_aryl:Eu(L)$_2$ at the polymer absorption maxima, produced a stepwise energy transfer from polymer to ligand to europium. The energy of the polymeric system was sufficiently high to sensitize the ligand

system. The ability to transfer energy from the polymers to europium was studied and reported.

Europium complexes with lower triplet energies:

A variety of aroyl-2-thenoylmethanes were used as ligands in the studies performed in Chapters 4 and 5. The aryl group substitutions on these molecules changed the singlet and triplet energies of the complexes formed with them, as well as the singlet to triplet energy gaps of the ligand systems. From what was observed, the systems whose ligands had larger singlet to triplet energy gaps also produced europium emissions of greater intensity.

Infrared emissive materials:

The possibility of fabricating erbium-doped fiber amplifiers (EDFA) was discussed using PM_aryl:ErTPP polymeric complexes. The porphyrinate ligand had sufficient energy to sensitize infrared-emitting lanthanide, Er^{+3}. Optical excitation of PM_aryl:ErTPP in THF at 332 nm produced emission centered at 1530 nm, due to the $4f$ ($^4I_{13/2}$) $\rightarrow$ $4f$ ($^4I_{15/2}$) transition of erbium. Similarly, excitation of polymeric complex PM_aryl:ErTPP at 422 nm, produced characteristic erbium emission.

BIBLIOGRAPHY

Anietz, S.; Wedel, A. *PCT Int. Appl.*, **2002**, pp. 28.

Arnold, J.; Dawson, D.Y.; Hoffman, C.G. *J. Am. Chem. Soc.*, **1993,** *115*, 2707

Baldo, M. A.; O'Brien, D. F.; Thompson, M. E.; Forrest, S. R. *Phys. Rev. B*, **1999**, *60*, 14422.

Berggren, M.; Inganas, O.; Gustafsson, G.; Rasmusson, J.; Anderson, M. R. Hjertberg, T.; Wennerstrom, O. *Nature*, **1994**, *372*, 444.

Bolivar, P. H.; Wegmann, C.; Kersting, R.; Deussen, M.; Lemmer, U.; Mahrt, R. F.; Bässler, H.; Göbel, E. O.; Kurz, H. *Chem. Phys. Lett.* **1995**, *245*, 534.

Boncella, J. M.; Foley, T. J.; Harrison, B.; Schanze, K. S.; Reynolds, J. R.; Bouguettaya, M.; Shim, J.; Holloway, P. H.; Ramakrishnan, S. *Poly. Mater. Sci. Eng.,* **2002**, *86*, 72.

Brown, A. R.; Pichler, K.; Greenham, N. C.; Bradley, D. D.; Friend, R. H.; Holmes, A. B. *Chem. Phys. Lett*., **1993**, *210*, 61.

Brunner, K.; van Haare, J. A. E. H.; Langeveld-Voss, B. M. W.; Schoo, H. F. M.; Hofstraat, J. W.; van Dijken, A. *J. Phys. Chem. B*, **2002**, *106*, 6834.

Burroughes, J. H.; Bradley, D. D. C.; Brown, A. R.; Marks, R. N.; Mackay, K.; Friend, R. H.; Burns, P. L.; Holmes, A. B. *Nature*, **1990**, *347*, 539.

Carnall, W. T.; P. R. Fields, and K. Rajnak, *J. Chem. Phys.*, **1968**, *49***,** 4443.

Chen, F-C.; Yang, Y.; Pei, Q. *Appl. Phys. Lett.,* **2002**, 81, 4278.

Chen, X.; Liao, J-L.; Liang, Y.; Ahmed, M. O.; Tseng, H. E.; Chen, S. A. *J. Am. Chem. Soc.*, **2003**, *125*, 636.

Crosby, G. A.; Whan, R. E.; Alire, R. M. J. *Chem. Phys.,* **1961**, *34*, 743.

Demas, N. J.; Crosby, G. A. *J. Phys. Chem.,* **1971**, *75*, 991.

Desurvire, E.; Simpson, J. R. ; Becker, P. C. *Opt. Lett.,* **1987**, *12*, 888.

Du, H.; Fuh, R. A.; Li, J.; Corkan, A.; Lindsey, J. S. *Photochemistry and Photobiology* **1998**, *68*, 141.

Foley, T. J.; Abboud, K. A.; Boncella, J. M. *Inorg. Chem.*, **2002**, *41*, 1704.

Foley, T. J.; Harrison, B. S.; Knefely, A. S.; Abboud, K. A.; Reynolds, J. R.; Schanze, K. S.; Boncella, J. M. *Inorg. Chem.*, **2003**, *42*, 5023.

Förster T. *Faraday Soc.*, **1959**, *27*,7.

Förster, T. *Ann. Phys. (Leipzig)* **1948**, *2*, 55. Translated by R. S. Knox.

Frank, M.; Wasgindt, M.; Pautzsch, T.; Klemm, E. *Macromol. Chem. Phys.*, **2001**, *202*, 980.

Frank, M.; Wasgindt, M.; Pautzsch, T.; Klemm, E. *Macromol. Chem. Phys.*, **2001**, *202*, 980.

Friend, R. H.; Gymer, R. W. ; Holmes, A. B.; Burroughes, J. H.; Marks, R. N.; Taliani, C.; Bradley, D. D. C.; Dos Santos, D. A.; Bredas, J. L.; Logdlund, M.; Salaneck, W. R. *Nature*, **1999**, *397*, 121.

Gao, X.; Deng, Z.; Tao, D; Bai, F.; Duan, N.; Xu, Y.; Wu, J. *Zhongguo Xitu Xuebao*, **2001**, *19*, 536.

Gill, R. E.; Malliaras, G. G.; Wildeman, J.; Hadziioannou, G. *Adv. Mater.,* **1994**, *6*, 132.

Gong, X.; Robinson, M. R.; Ostrowski, J. C.; Moses, D.; Bazan, G. C.; Heeger, A. J. *Adv. Mater.,* **2002**, *14*, 581.

Halls, J. J. M.; Walsh, C. A.; Greenham, N. C.; Marseglia, E. A.; Friend, R. H.; Moratti, S. C.; Holmes, A. B. *Nature*, **1995**, *376*, 498.

Hanabusa, K.; Nakamura, A.; Koyama, T.; Shirai, H. *Makromol. Chem.*, **1992**, *193*, 1309.

Harrison, B. S.; Foley, T. J.; Bouguettaya, M.; Boncella, J. M.; Reynolds, J. R.; Schanze, K. S.; Shim, J.; Holloway, P. H.; Padmanaban, G.; Ramakrishnan, S. *Appl. Phys. Lett.,* **2001**, *79*, 3770.

He, G.; Chang, S.-C.; Chen, F-C.; Li, Y.; Yang, Y. *Appl. Phys. Lett.,* **2002**, *81*, 1509.

Hsiao, J.-S.; Krueger, B. P.; Wagner, R. W.; Johnson, T. E.; Delaney, J. K.; Mauzerall, D. C.; Fleming, G. R.; Lindsey, J. S.; Bocian, D. F.; Donohoe, R. J. *J. Am. Chem. Soc.* **1996**, *118*, 11181.

Hu, Q. S.; Huang, W. S.; Vitharana, D.; Zheng, X. F.; Pu, L. *J. Am. Chem. Soc.*, **1997**, *119*, 12454,.

Jin, Y.-D.; Chen, H.-Z.; Heremans, P. L.; Aleksandrzak, K.; Geise, H. J.; Borghs, G.; Van der Auweraer, M. *Synth. Met.,* **2002**, *127*, 155.

Kido, J.; Shionoya, H.; Nagai, K. *Appl. Phys. Lett.* **1995**, *67*, 2281.

Klink, S. I.; Grave, L.; Reinhoudt, D. N.; Van Veggel, F.C.J.M.; Werts, M.H.V.; Geurts, F. A. J.; Hofstraat, J. W. *J. Phys. Chem. A.*, **2000**, *104*, 5457.

Klink, S. I.; Hebbink, G. A.; Grave, L.; Oude Alink, P. G. B.; Van Veggel, F. C. J. M.; Werts, M. H. V. *J. Phys. Chem. A.*, **2002**, *106*, 3681.

Koehler, A.; Gruener, J.; Friend, R. H.; Muellen, K.; Scherf, U. *Chem. Phys. Lett.*, **1995**, *243*, 456.

Kraft, A.; Grimsdale, A. C.; Holmes, A. B. *Agnew. Chem. Int. Ed.*, **1998**, *37*, 402.

Lakowicz, J. R. *Principles of Fluorescence Spectroscopy,* 2nd ed., Kluwer Academic / Plenum Publishers, New York, NY, **1999**.

Lehmann, O.; Meyssamy, H.; Kompe, K.; Schnablegger, H.; Hasse, M. *J. Phys. Chem. B*., **2003**, *107*, 7449.

Liu, T-H.; Iou, C-Y.; Wen, S-W.; Chen, C. H. *Thin Solid Films*, **2003**, *441*, 223.

Liu, X.-L.; Pei, J.; Huang, W. *Thin Solid Films*, **2002**, *417*, 85.

Lux, A.; Holmes, A. B.; Cervini, R.; Davies, J. E.; Moratti, S. C.; Grunner, J.; Cacialli, F.; Friend, R. H. *Synth. Met.,* **1997**, *84*, 293.

MacKenzie, J. D.; Stevenson, R.; Halls, J. J. M.; Inbasekaran, M.; Woo, E. P.; Richards, D.; Friend, R. H. *Macromolecules*, **2001**, *34*, 6005.

Marks, R. N.; Halls, J. J. M.; Bradley, D. D. C.; Friend, R. H.; Holmes, A. B. *J. Phys. Condensed Matter*, **1994**, *6*, 1379.

McGehee, M. .; Bergstedt, T.; Zhang, C.; Saab, A. P.; O'Regan, M. B.; Bazan, G. C.; Srdanov, Vojislav I.; Heeger, A. J. *Adv. Mater.,* **1999**, *11*, 1349.

Mears, R. J.; Reekie, L.; Jauncie, I. M.; Payne, D. N.; *Elect. Lett.*, **1987**, *23*, 1026.

Melby, L. R.; Rose, N. J.; Abramson, E.; Caris, J. C. *J. Am. Chem. Soc.*, **1964**, *86*, 5117.

Mukherjee, K. K. R. *Fundamentals of Photochemistry*, Wiley Eastern Ltd. India, 1992.

Nakamura, A.; Tada, T.; Mizukami, M.; Hirose, S.; Yagyu, S. *Appl. Phys. Lett.,* **2002**, *80*, 2189.

Oshima,I.; Nihiyama, K.; Kurotori, K.; Hayakawa, H. *Furakawa Review*, **2003**, *23*, 71.

Pasquale, A. J.; Sheares, V. V. *J. Polym. Sci. Pol. Chem.,* **1998**, *36*, 2611.

Plotnikov, V. G.; Dolgih, B. A. *Opt. Spectr.*, **1977**, *43*, 882.

Poole, S.; Payne, D. N.; Mears, R. J.; Fermann, M. E.; Laming, R. I. *J. Light. Tech.,* **1985**, *21*, 737.

Priimov, G. U.; Moore, P.; Maritim P. K.; Butlanyi, P. K. Alcock N. W. *J. Chem. Soc., Dalton Trans.*, **2000**, 445.

Sager, W. F.; Filipescu, N.; Serafin, F. A. *J. Phys. Chem.*, **1965**, *69*, 1092.

Sarnecki, G. J.; Friend, R. H.; Holmes, A. B.; Moratti, S. C. *Synth. Met.*, **1995**, *69*, 545.

Sato, S.; Wada, M.; Seki. T. *Jpn. J. Appl. Phys.*, **1968**, *7*,7.

Sato, S; Wada, M., *Bull. Chem. Soc. Jpn.,* **1970**, *43*, 1955.

Service, R. F. *Science*, **2000**, *290*, 425.

Shoustikov, A. A.; You, Y.; Thompson, M. E. *IEEE J. of Sel. Top. In Quan. Elec.,* **1998**, *4*, 3.

Swanson, S. A.; Wallraff, G. M.; Chen, J. P.; Zhang, W.; Bozano, L.D.; Carter, K. R.; Salem, J. R.; Villa, R.; Scott, J. C. *Chem. Mat.*, **2003**, *15*, 2305.

Tang, C. W., VanSlyke, S. A., Chen, C. H., *J. Appl. Phys.*, **1989**, *65*, 3610.

Tang, C. W.; VanSlyke S. A. *Appl. Phys. Lett.,***1987**, *51*, 913.

Tian, J.; Wu, C. C.; Thompson, M. E.; Register, R. A.; Marsella, M. J.; Swager, T. M. *Adv. Mater.*, **1995**, *7*, 395.

Turro, N. J. *Modern Molecular Photochemistry*, University Science Books, Sausalito, California, **1991**.

Udea, M.; Seino, Y.; Sugiyama, J. *Polym. J.* **1993**, *215*, 12, 1319.

Wang, B.; Wasielewski, M.R. *J. Am. Chem. Soc.* **1997,** *119,* 12.

Wang, P.; Xie, Z.; Hong, Z.; Tang, J.; Wong, O.; Lee, C-S.; Wong, N.; Lee, S. *J. Mat. Chem.,* **2003**, *13*, 1894.

Weissman, S. I. *J. Chem. Phys.*, **1942**, *10*, 214.

Wilson, J. S.; Dhoot, A. S.; Seeley, A. J. A. B.; Khan, M. S.; Kohler, A.; Friend, R. H. *Nature*, **2001**, *413*, 828.

Wu, Z.; Yang, H.; Duan, Y.; Xie, W.; Liu, S.; Zhao, Y. *Semiconductor Science and Technology*, **2003**, *18*, L49.

Yan, H.; Huang, Q.; Cui, J.; Veinot, J. G. C.; Kern, M. M.; Marks, T. J.; Yang, R.; Tian, R.; Hou, Q.; Yang, W.; Cao, Y. *Macromolecules*, **2003**, *36*, 7453.

APPENDIX

PHOTOPHYSICAL SPECTRA

POLYMERS AND POLYMER-LANTHANIDE(LIGAND)$_X$ COMPLEXES
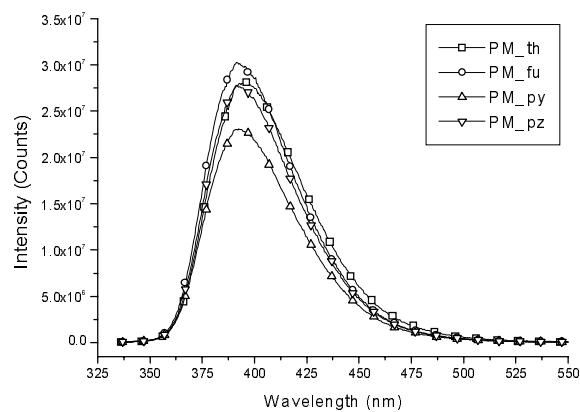
Figure A.1. Emission spectra of PM_th, PM_fu, PM_py, and PM_pz.
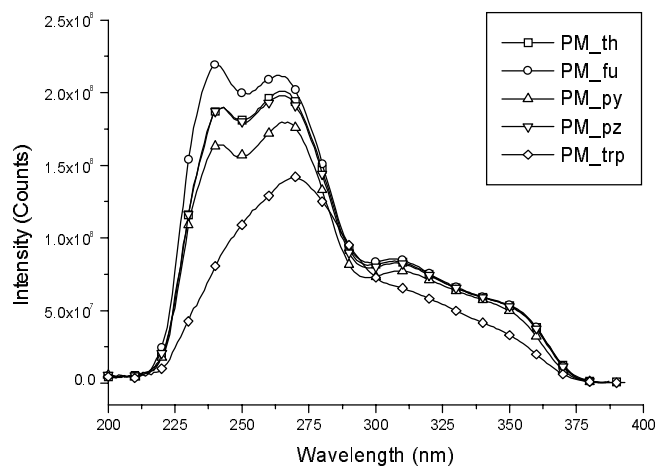
Figure A.2. Excitation spectra of PM_th, PM_fu, PM_py, PM_pz, and PM_trp.
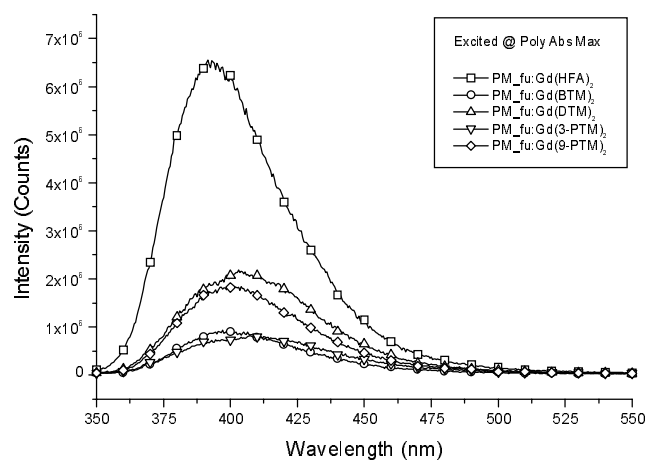
Figure A.3. Emission spectra of PM_fu:Gd(L)$_2$ complexes, excited at the polymer absorbance maximum.
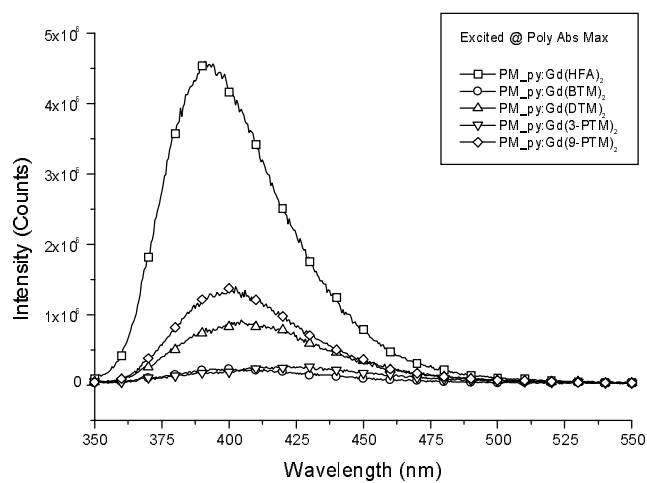
Figure A.4. Emission spectra of PM_py:Gd(L)$_2$ complexes, excited at the polymer absorbance maximum.
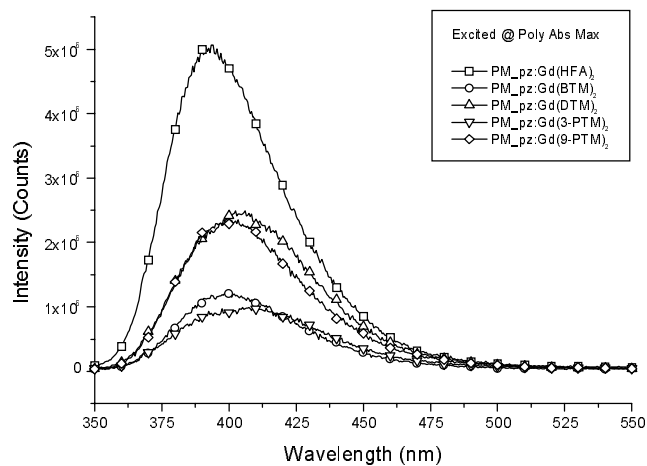
Figure A.5. Emission spectra of PM_pz:Gd(L)$_2$ complexes, excited at the polymer absorbance maximum.
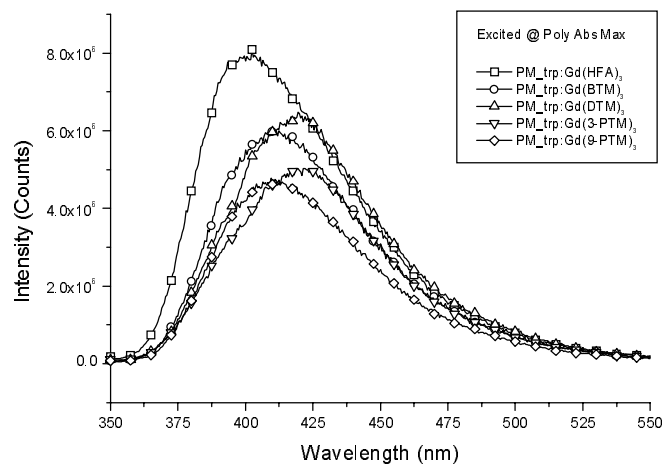
Figure A.6. Emission spectra of PM_trp:Gd(L)$_3$ complexes, excited at the polymer absorbance maximum.
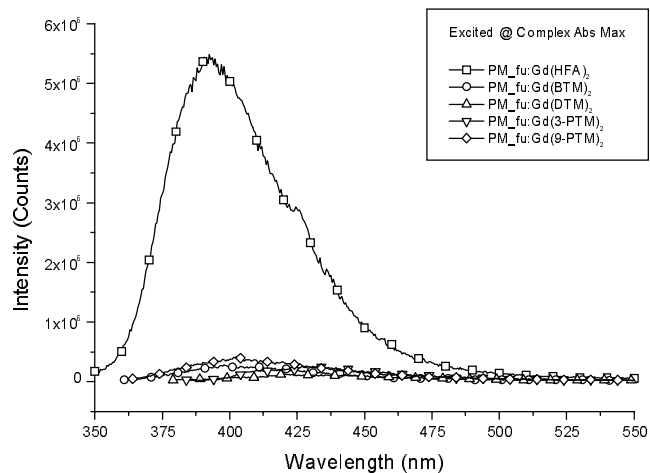
Figure A.7. Emission spectra of PM_fu:Gd(L)$_2$ complexes, excited at the complex absorbance maxima.
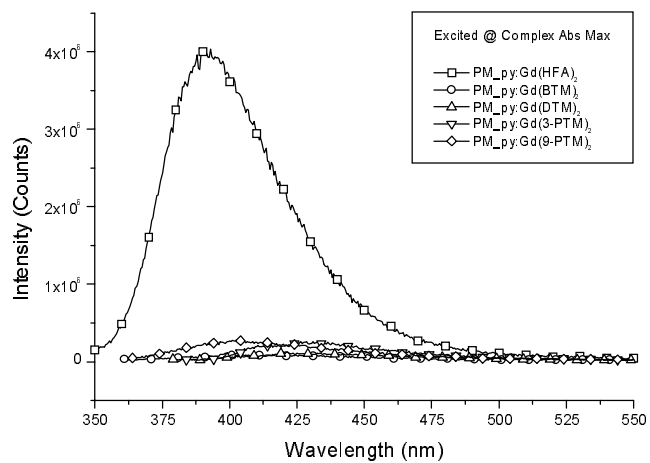
Figure A.8. Emission spectra of PM_py:Gd(L)$_2$ complexes, excited at the complex absorbance maxima.
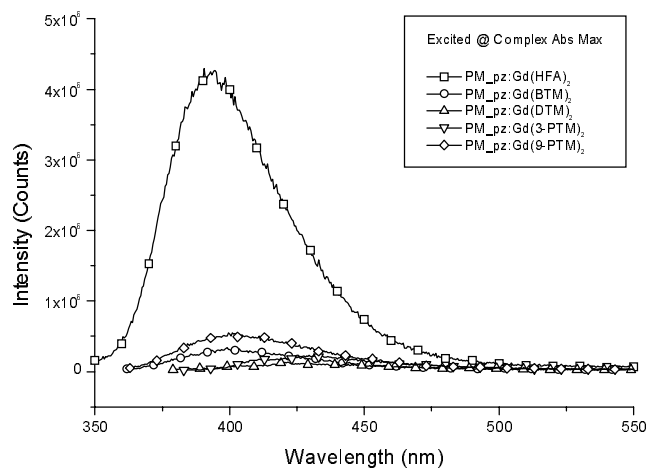
Figure A.9. Emission spectra of PM_pz:Gd(L)$_2$ complexes, excited at the complex absorbance maxima.
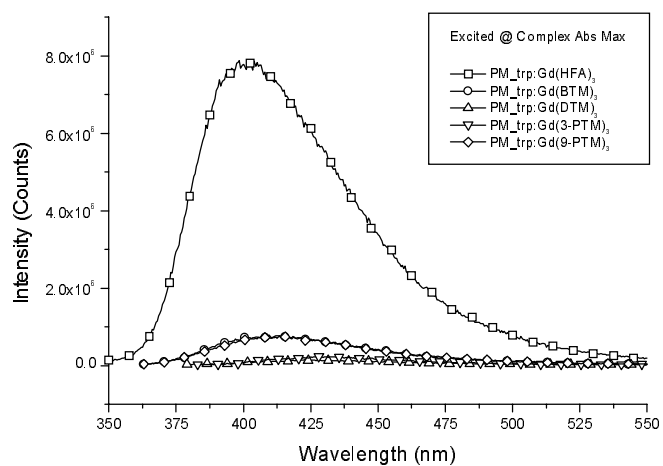
Figure A.10. Emission spectra of PM_trp:Gd(L)$_3$ complexes, excited at the complex absorbance maxima.
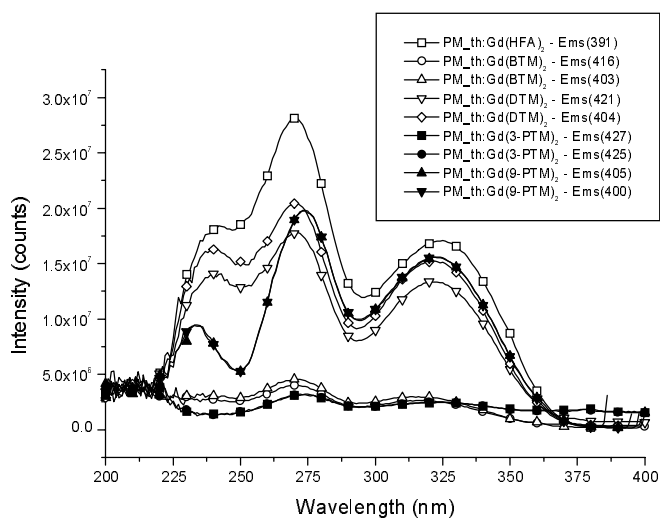
Figure A.11. Excitation spectra of PM_th:Gd(L)$_2$ complexes.
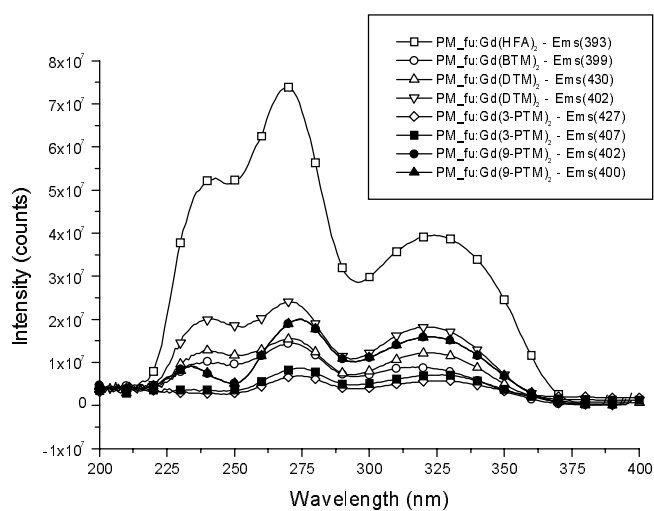
Figure A.12. Excitation spectra of PM_fu:Gd(L)$_2$ complexes.
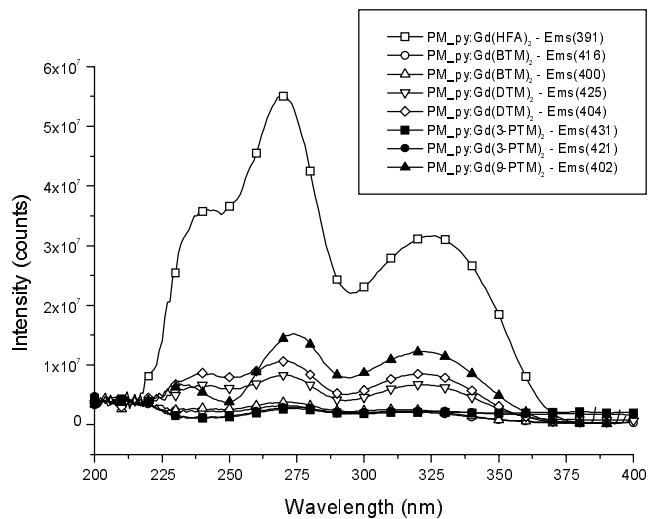
Figure A.13. Excitation spectra of PM_py:Gd(L)$_2$ complexes.
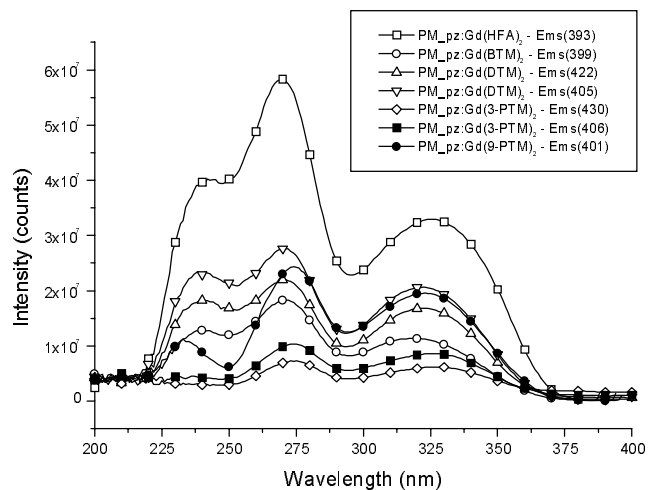
Figure A.14. Excitation spectra of PM_pz:Gd(L)$_2$ complexes.
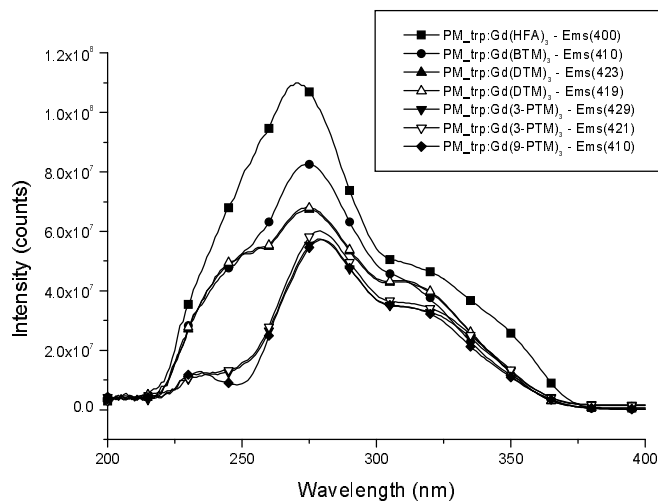
Figure A.15. Excitation spectra of PM_trp:Gd(L)$_3$ complexes.
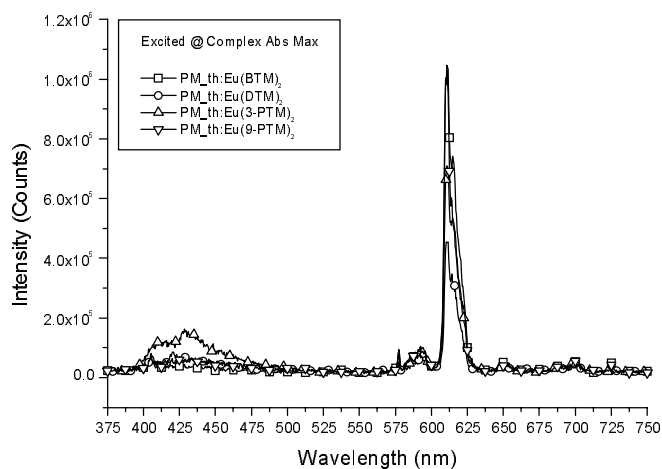
Figure A.16. Emission from PM_th:Eu(BTM)$_2$, PM_th:Eu(DTM)$_2$, PM_th:Eu(3-PTM)$_2$, and PM_th:Eu(9-PTM)$_2$, excited at the complex absorbance maxima.
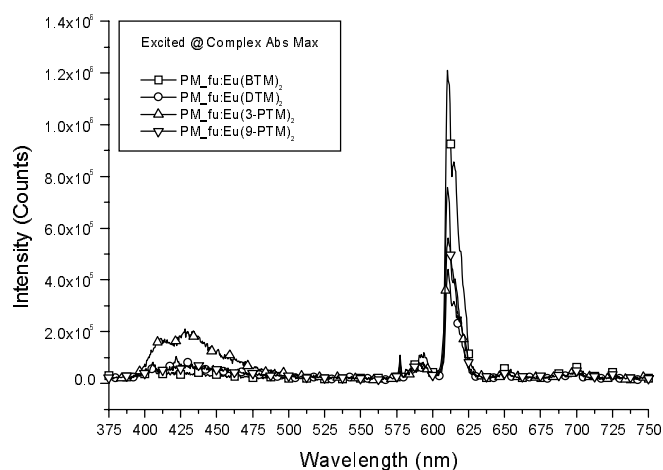
Figure A.17. Emission from PM_fu:Eu(BTM)$_2$, PM_fu:Eu(DTM)$_2$, PM_fu:Eu(3-PTM)$_2$, and PM_fu:Eu(9-PTM)$_2$, excited at the complex absorbance maxima.
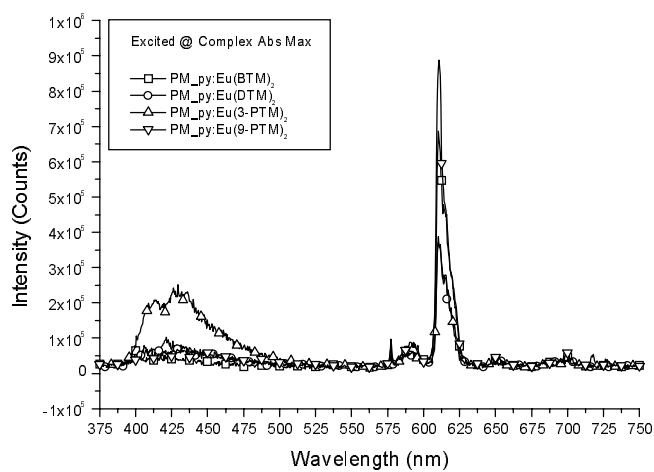
Figure A.18. Emission from PM_py:Eu(BTM)$_2$, PM_py:Eu(DTM)$_2$, PM_py:Eu(3-PTM)$_2$, and PM_py:Eu(9-PTM)$_2$, excited at the complex absorbance maxima.
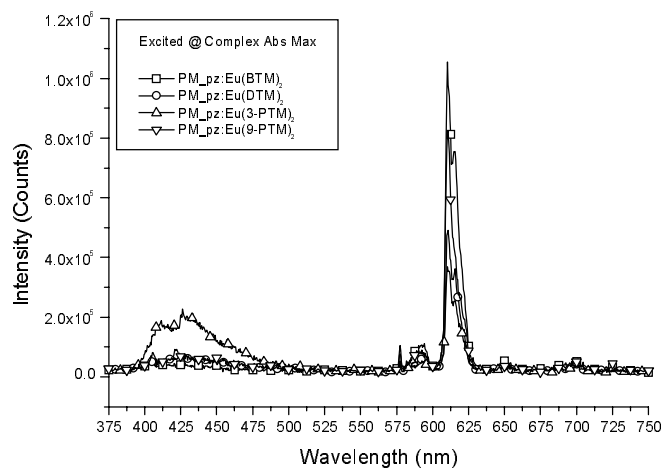
Figure A.19. Emission from PM_pz:Eu(BTM)₂, PM_pz:Eu(DTM)₂, PM_pz:Eu(3-PTM)₂, and PM_pz:Eu(9-PTM)₂, excited at the complex absorbance maxima.
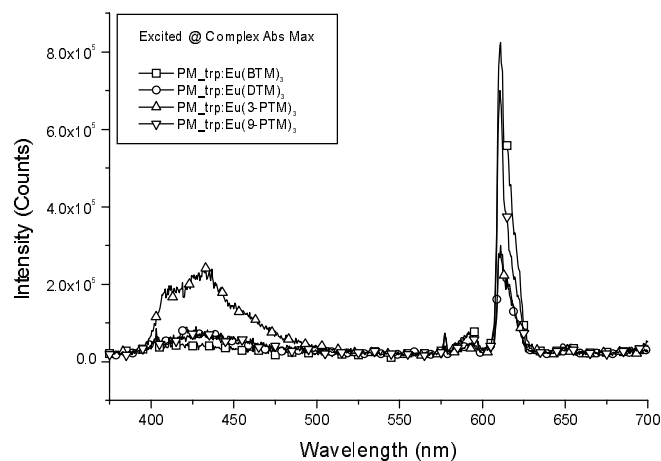
Figure A.20. Emission from PM_trp:Eu(BTM)₃, PM_trp:Eu(DTM)₃, PM_trp:Eu(3-PTM)₃, and PM_trp:Eu(9-PTM)₃, excited at the complex absorbance maxima.
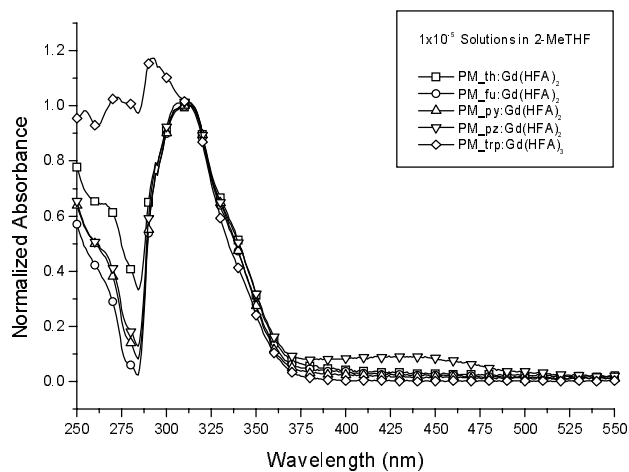
Figure A.21. Absorbance spectra of PM_aryl:Gd(HFA)$_x$ in 2-methyltetrahydrofuran at $1x10^{-5}$ M.
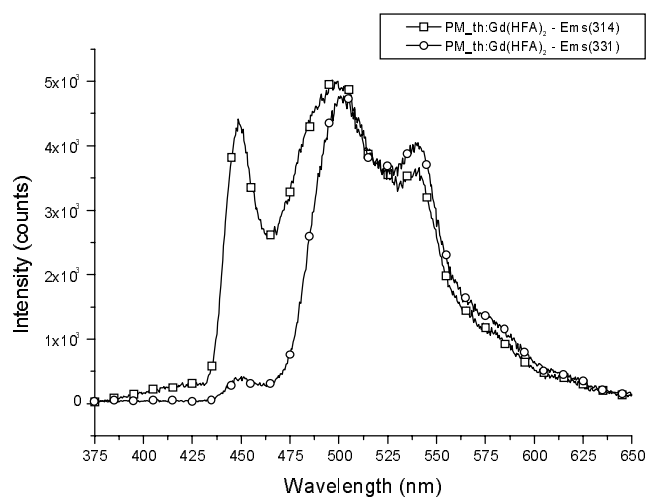
Figure A.22. Low temperature (77 K) phosphorescence of PM_th:Gd(HFA)$_2$ in 2-MeTHF.
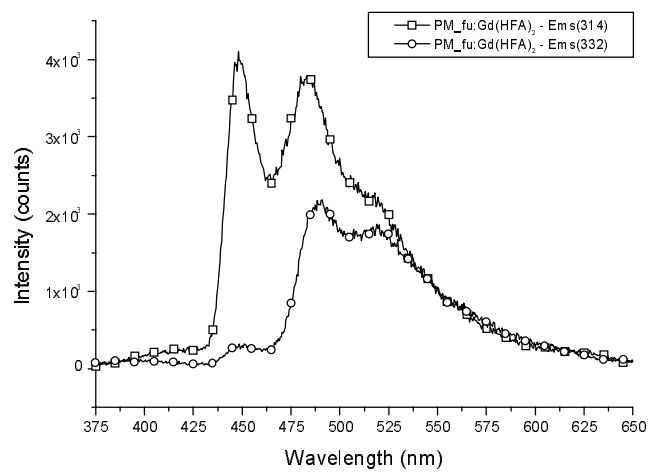
Figure A.23. Low temperature (77 K) phosphorescence of PM_fu:Gd(HFA)$_2$ in 2-MeTHF.
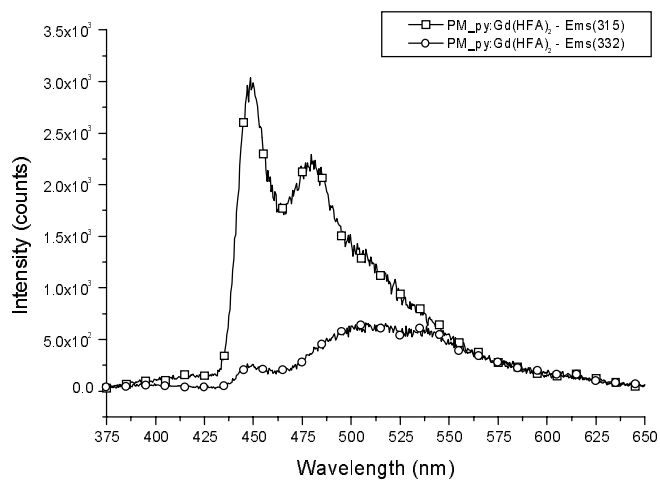
Figure A.24. Low temperature (77 K) phosphorescence of PM_py:Gd(HFA)$_2$ in 2-MeTHF.
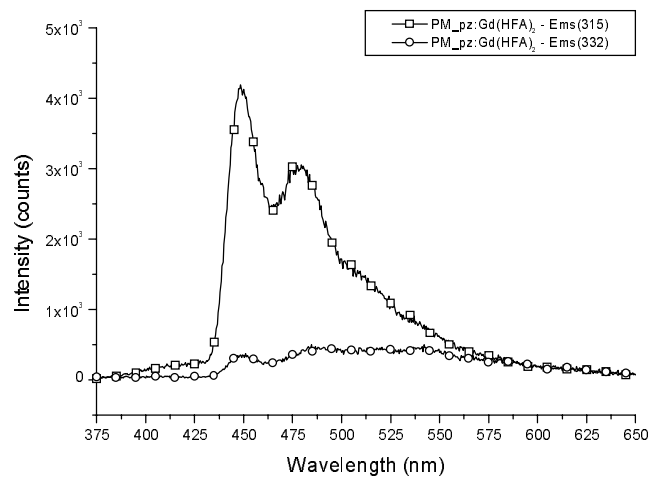
Figure A.25. Low temperature (77 K) phosphorescence of PM_pz:Gd(HFA)$_2$ in 2-MeTHF.
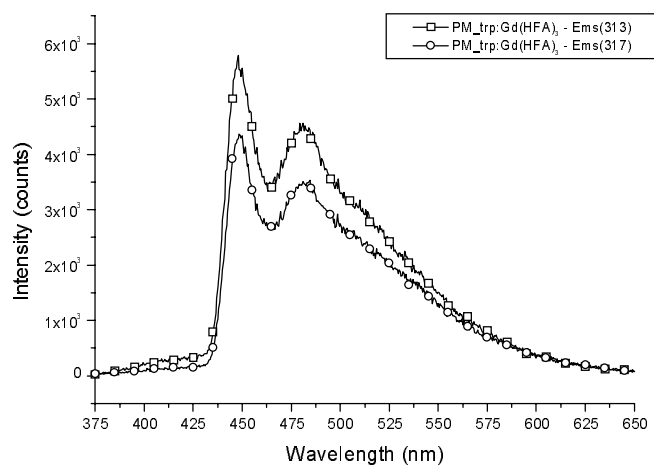
Figure A.26. Low temperature (77 K) phosphorescence of PM_trp:Gd(HFA)$_3$ in 2-MeTHF.
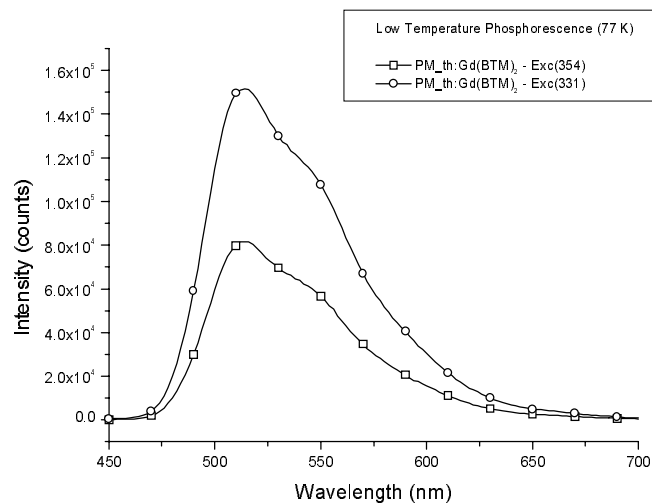
Figure A.27. Low temperature (77 K) phosphorescence of PM_th:Gd(BTM)$_2$ in 2-MeTHF.
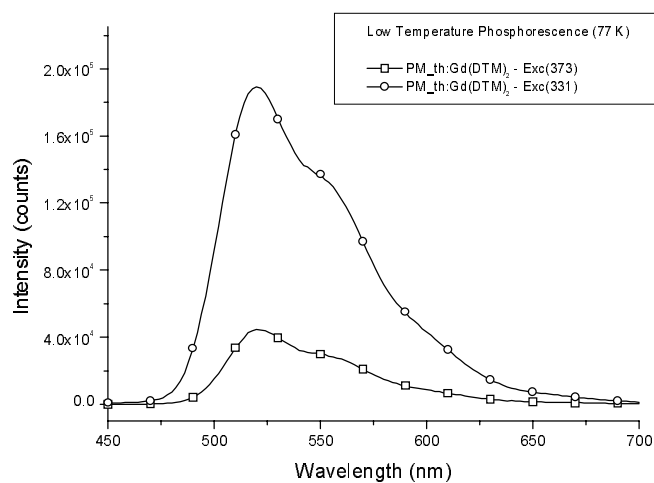
Figure A.28. Low temperature (77 K) phosphorescence of PM_th:Gd(DTM)$_2$ in 2-MeTHF.
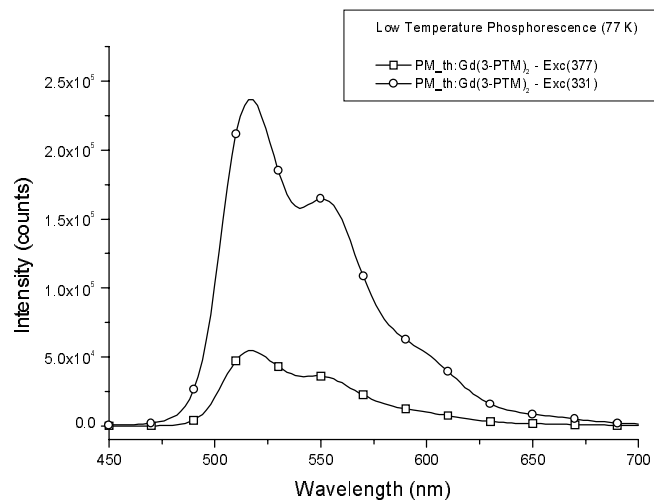
Figure A.29. Low temperature (77 K) phosphorescence of PM_th:Gd(3-PTM)$_2$ in 2-MeTHF.
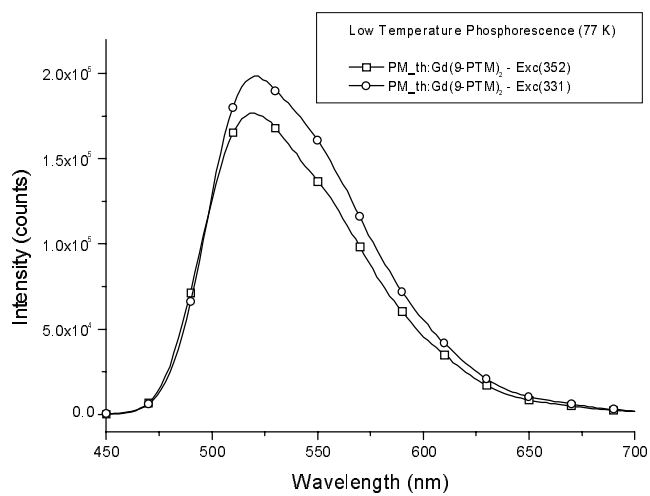
Figure A.30. Low temperature (77 K) phosphorescence of PM_th:Gd(9-PTM)$_2$ in 2-MeTHF.
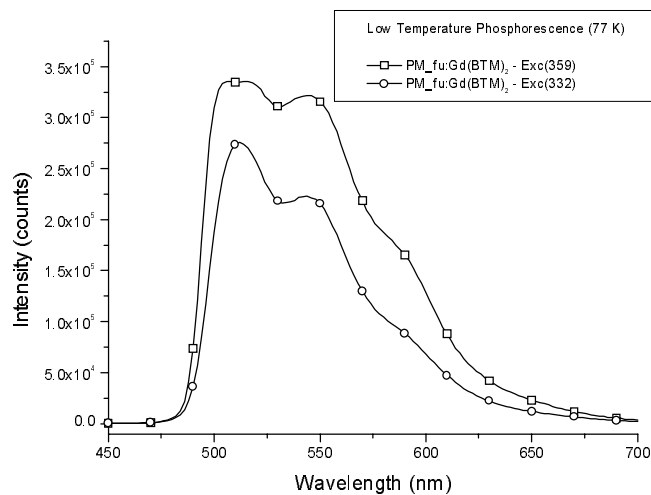
Figure A.31. Low temperature (77 K) phosphorescence of PM_fu:Gd(BTM)$_2$ in 2-MeTHF.
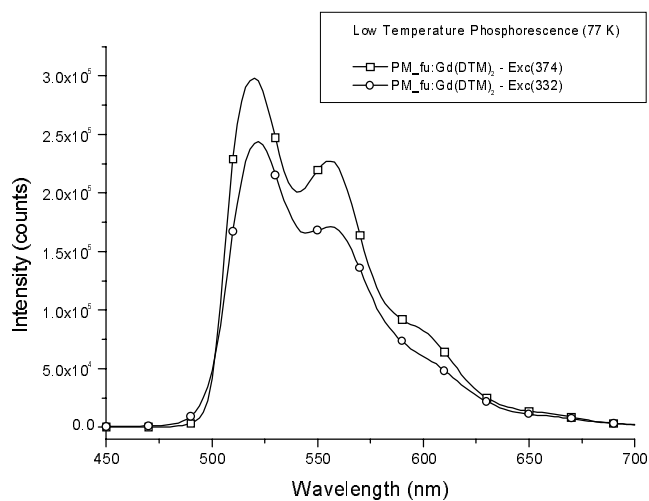
Figure A.32. Low temperature (77 K) phosphorescence of PM_fu:Gd(DTM)$_2$ in 2-MeTHF.
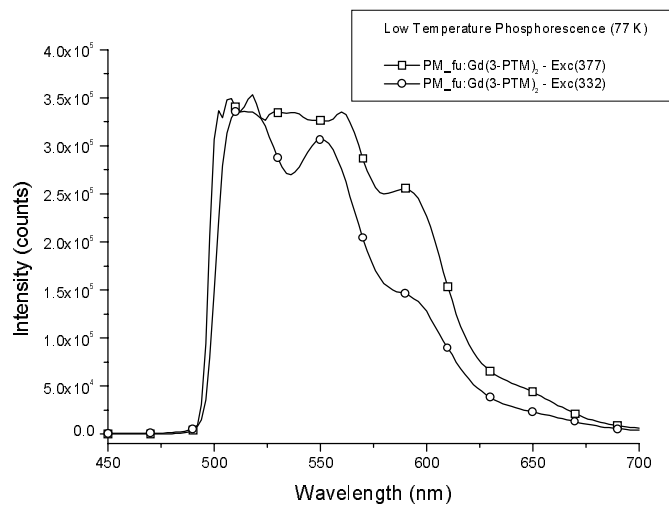
Figure A.33. Low temperature (77 K) phosphorescence of PM_fu:Gd(3-PTM)$_2$ in 2-MeTHF.
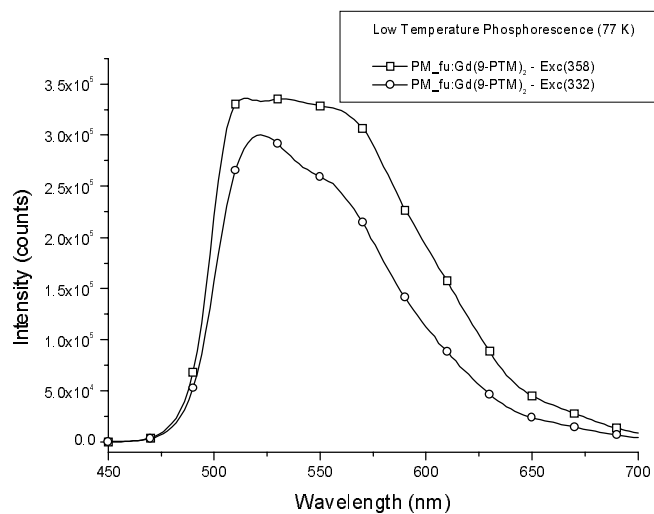
Figure A.34. Low temperature (77 K) phosphorescence of PM_fu:Gd(9-PTM)$_2$ in 2-MeTHF.
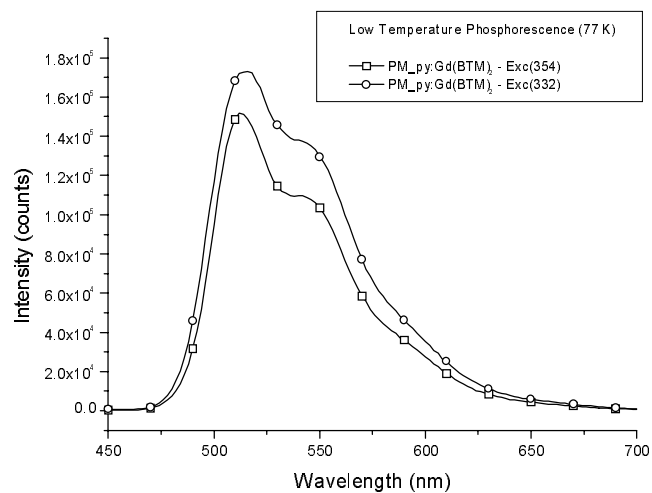
Figure A.35. Low temperature (77 K) phosphorescence of PM_py:Gd(BTM)$_2$ in 2-MeTHF.
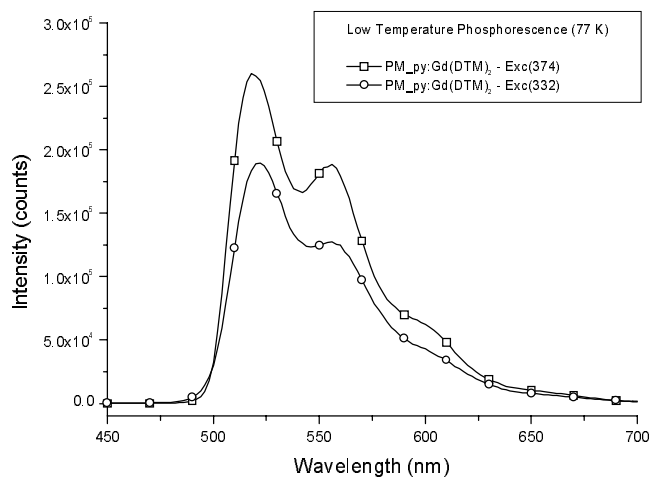
Figure A.36. Low temperature (77 K) phosphorescence of PM_py:Gd(DTM)$_2$ in 2-MeTHF.
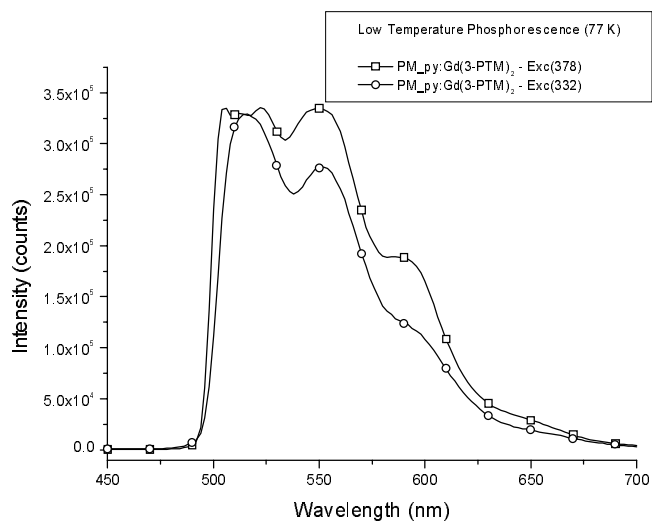
Figure A.37. Low temperature (77 K) phosphorescence of PM_py:Gd(3-PTM)$_2$ in 2-MeTHF.
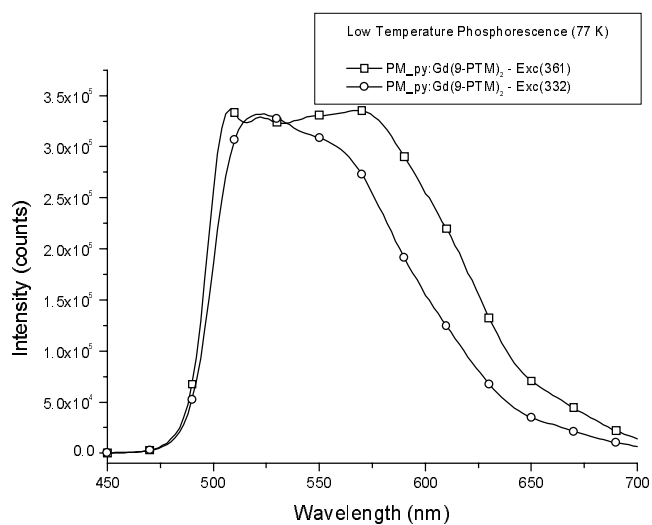
Figure A.38. Low temperature (77 K) phosphorescence of PM_py:Gd(9-PTM)$_2$ in 2-MeTHF.
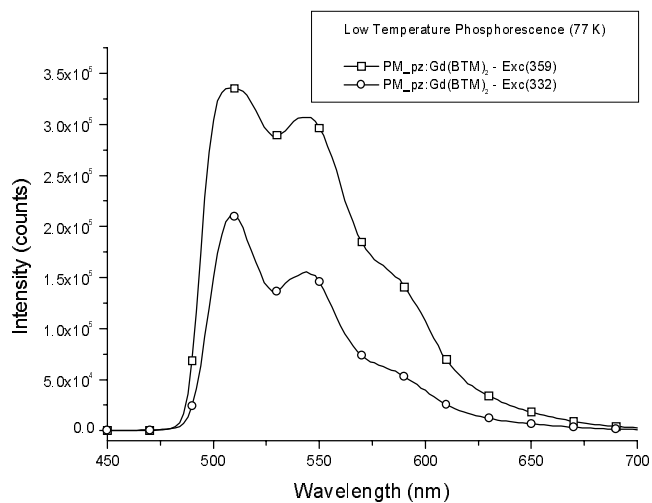
Figure A.39. Low temperature (77 K) phosphorescence of PM_pz:Gd(BTM)$_2$ in 2-MeTHF.
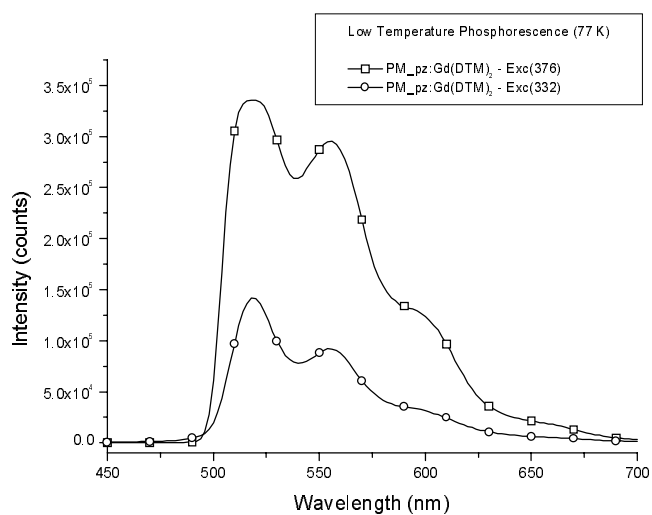
Figure A.40. Low temperature (77 K) phosphorescence of PM_pz:Gd(DTM)$_2$ in 2-MeTHF.
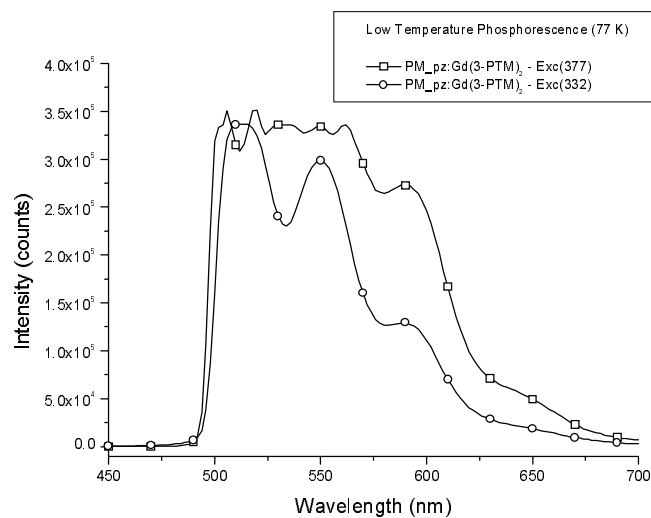
Figure A.41. Low temperature (77 K) phosphorescence of PM_pz:Gd(3-PTM)$_2$ in 2-MeTHF.
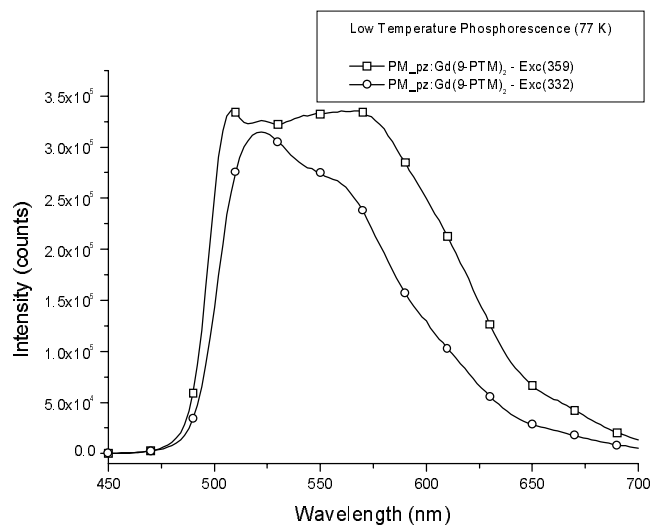
Figure A.42. Low temperature (77 K) phosphorescence of PM_pz:Gd(9-PTM)$_2$ in 2-MeTHF.
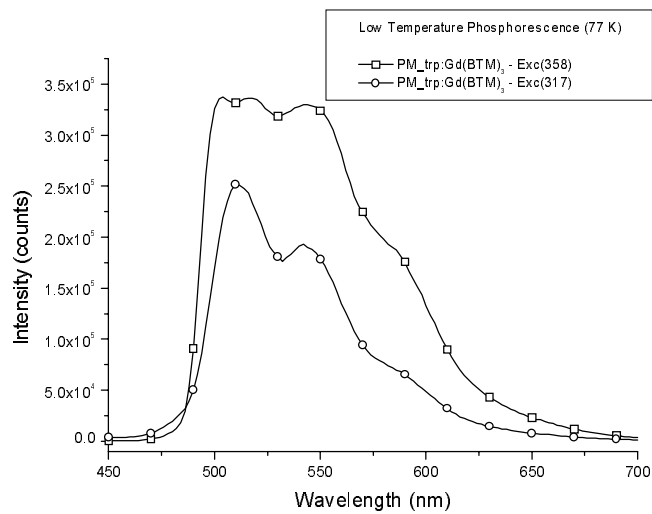
Figure A.43. Low temperature (77 K) phosphorescence of PM_trp:Gd(BTM)$_3$ in 2-MeTHF.
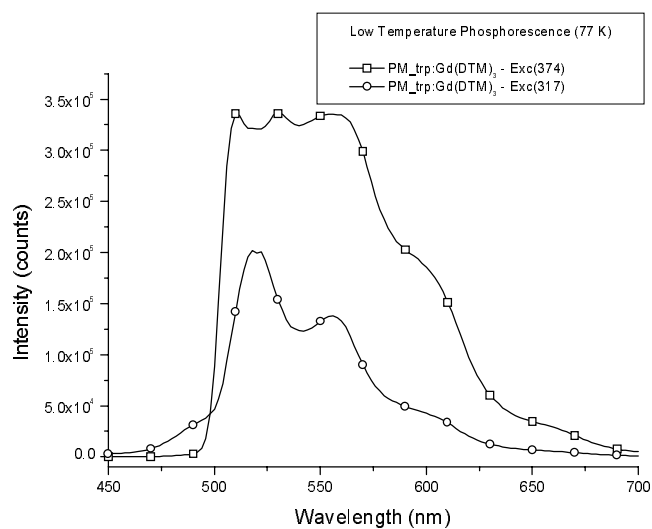
Figure A.44. Low temperature (77 K) phosphorescence of PM_trp:Gd(DTM)$_3$ in 2-MeTHF.
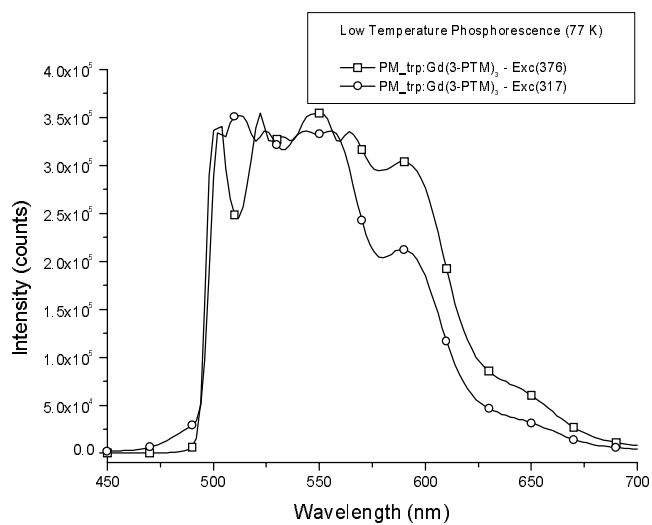
Figure A.45. Low temperature (77 K) phosphorescence of PM_trp:Gd(3 -PTM)$_3$ in 2-MeTHF.
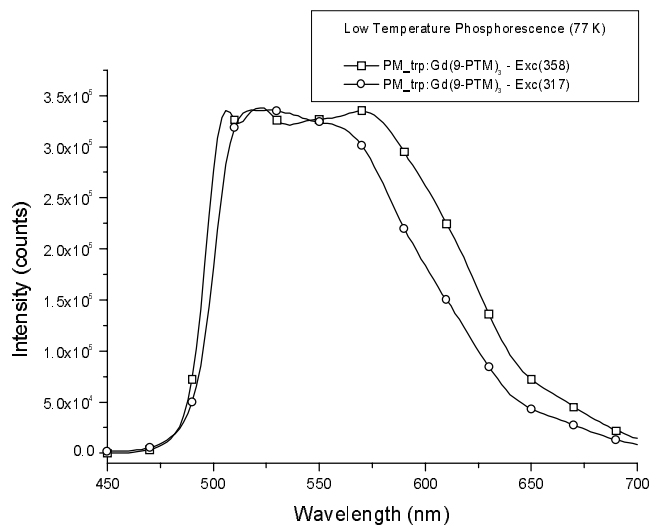
Figure A.46. Low temperature (77 K) phosphorescence of PM_trp:Gd(9 -PTM)$_3$ in 2-MeTHF.
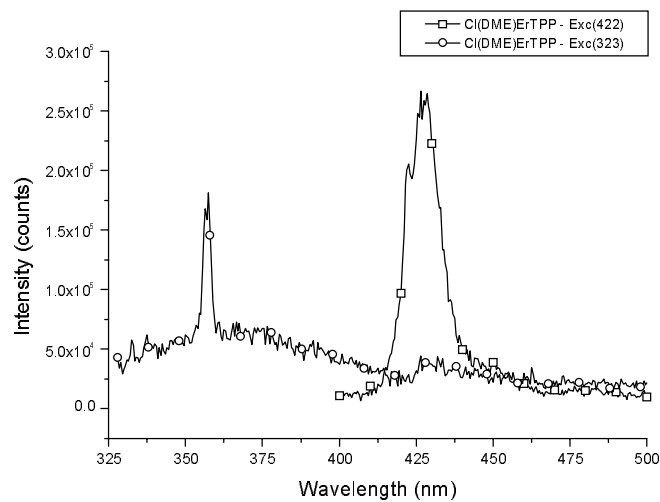
Figure A.47. Visible emission from Cl(DME)ErTPP at 1×10^{-5} M in anhydrous THF.
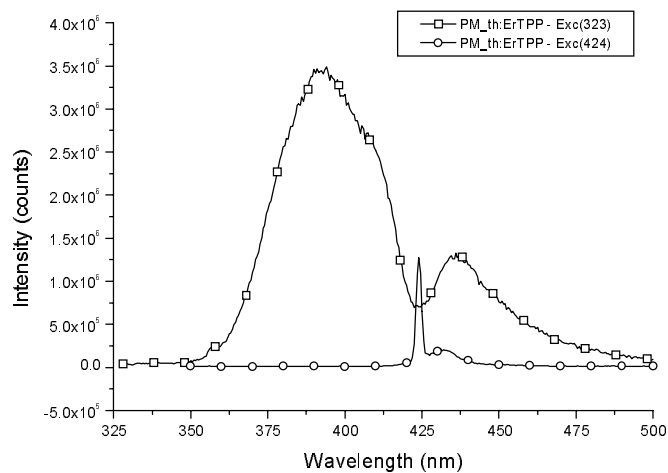
Figure A.48. Visible emission from PM_th:ErTPP at 1×10^{-5} M in anhydrous THF.
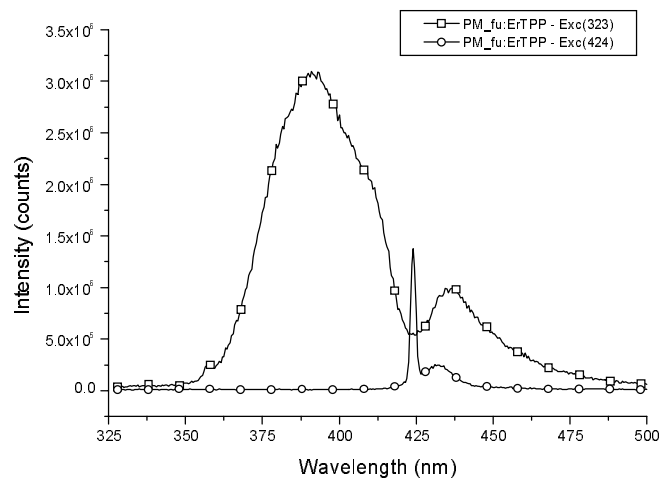
Figure A.49. Visible emission from PM_fu:ErTPP at $1x10^{-5}$ M in anhydrous THF.
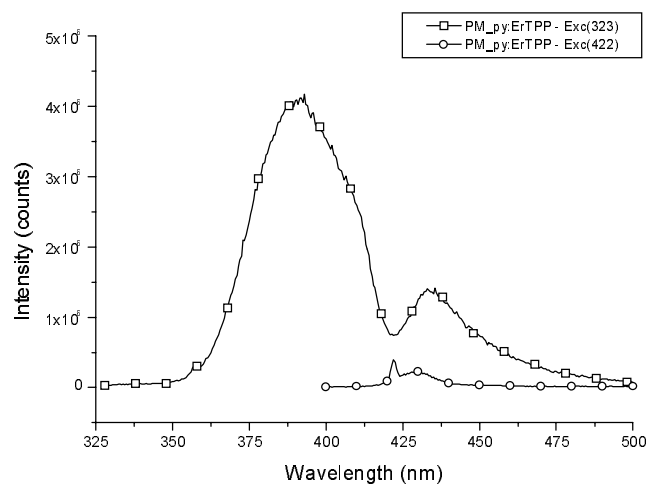
Figure A.50. Visible emission from PM_py:ErTPP at $1x10^{-5}$ M in anhydrous THF.
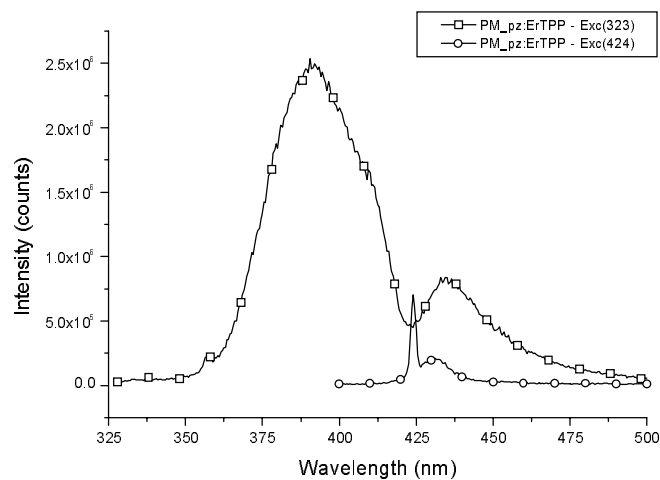
Figure A.51. Visible emission from PM_pz:ErTPP at 1×10^{-5} M in anhydrous THF.
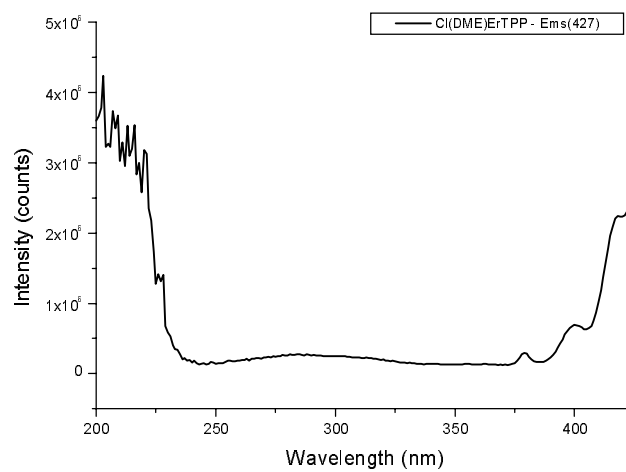
Figure A.52. Excitation spectrum of Cl(DME)ErTPP at 1×10^{-5} M in anhydrous THF.
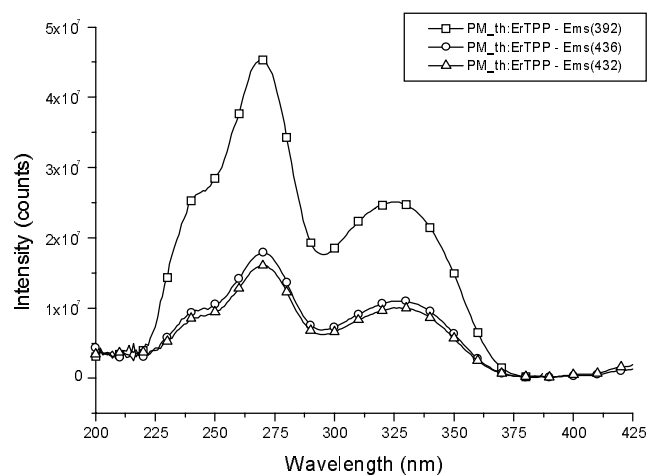
Figure A.53. Excitation spectrum of PM_th:ErTPP at $1x10^{-5}$ M in anhydrous THF.
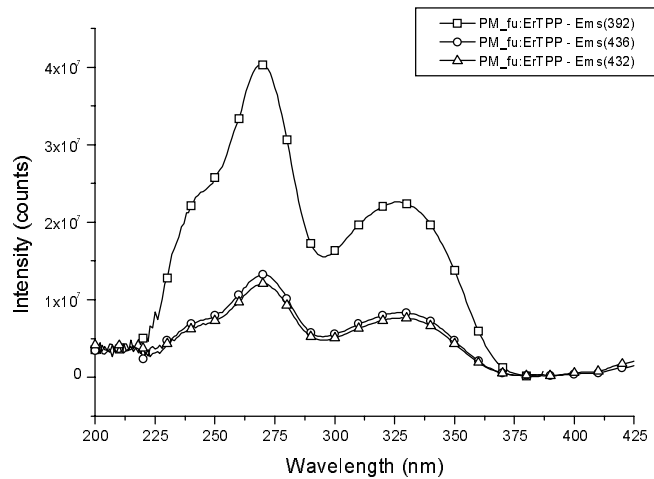
Figure A.54. Excitation spectrum of PM_fu:ErTPP at $1x10^{-5}$ M in anhydrous THF.
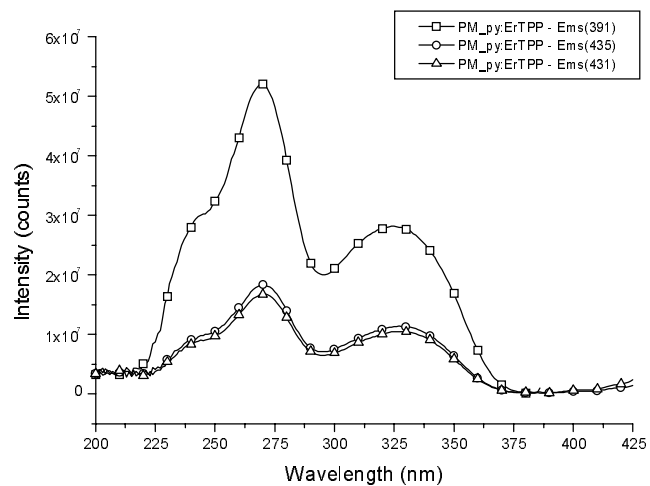
Figure A.55. Excitation spectrum of PM_py:ErTPP at 1x10^{-5} M in anhydrous THF.
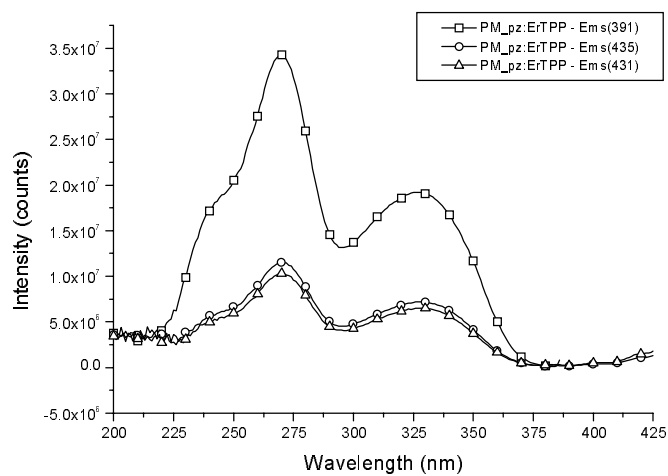
Figure A.56. Excitation spectrum of PM_pz:ErTPP at 1x10^{-5} M in anhydrous THF.

X-RAY CRYSTALLOGRAPHY

Cl(DME)ErTPP

Table A.1. Crystal data and structure refinement for C51 H41 Cl Er N4 O2.

Identification code	s_erporm
Empirical formula	C51 H41 Cl Er N4 O2
Formula weight	944.59
Temperature	133(2) K
Wavelength	0.71073 Å
Crystal system	Monoclinic
Space group	P2(1)/c
Unit cell dimensions	a = 12.191(3) Å α= 90°.
	b = 26.854(7) Å β= 111.459(4)°.
	c = 13.699(4) Å γ = 90°.
Volume	4173.5(19) Å^3
Z	4
Density (calculated)	1.503 Mg/m^3
Absorption coefficient	2.121 mm^{-1}
F(000)	1904
Crystal size	0.36 x 0.10 x 0.02 mm^3
Theta range for data collection	1.52 to 27.53°.
Index ranges	-14<=h<=15, -29<=k<=34, -17<=l<=17
Reflections collected	25531
Independent reflections	9388 [R(int) = 0.0788]
Completeness to theta = 27.53°	97.8 %
Transmission factors	min/max ratio: 0.614
Refinement method	Full-matrix least-squares on F^2
Data / restraints / parameters	9388 / 15 / 520
Goodness-of-fit on F^2	1.024
Final R indices [I>2sigma(I)]	R1 = 0.0565, wR2 = 0.1435
R indices (all data)	R1 = 0.0936, wR2 = 0.1623
Largest diff. peak and hole	3.399 and -1.083 e.Å^{-3}

Table A.2. Atomic coordinates (x 10^4) and equivalent isotropic displacement parameters ($Å^2$x 10^3) for C51 H41 Cl Er N4 O2. U(eq) is defined as one third of the trace of the orthogonalized U^{ij} tensor.

_____

	x	y	z	U(eq)
Er(1)	3655(1)	2031(1)	3739(1)	21(1)
Cl(1)	3096(2)	1297(1)	2405(2)	48(1)
O(1)	2674(4)	2483(2)	2126(4)	31(1)
O(2)	4995(5)	2190(2)	2813(4)	37(1)
N(1)	4038(5)	2874(2)	4254(4)	22(1)
N(2)	1914(5)	2277(2)	3921(4)	21(1)
N(3)	3378(4)	1442(2)	4883(4)	20(1)
N(4)	5491(5)	2021(2)	5117(4)	23(1)
C(1)	5109(6)	3103(3)	4489(5)	23(2)
C(2)	4938(6)	3629(3)	4244(6)	31(2)
C(3)	3763(6)	3714(3)	3915(5)	28(2)
C(4)	3198(6)	3248(2)	3925(5)	22(1)
C(5)	1984(6)	3189(3)	3651(5)	22(1)
C(6)	1286(6)	3662(3)	3442(6)	25(2)
C(7)	550(7)	3804(3)	2453(7)	41(2)
C(8)	-56(7)	4267(3)	2317(8)	54(3)
C(9)	109(7)	4572(3)	3130(7)	42(2)
C(10)	819(7)	4434(3)	4110(8)	43(2)
C(11)	1407(6)	3979(3)	4276(6)	33(2)
C(12)	1389(6)	2737(3)	3610(5)	22(1)
C(13)	119(6)	2685(3)	3250(5)	26(2)
C(14)	-96(6)	2192(3)	3371(5)	26(2)
C(15)	1013(6)	1952(2)	3838(5)	23(2)
C(16)	1187(6)	1468(3)	4251(5)	23(2)
C(17)	138(6)	1149(3)	4176(5)	26(2)
C(18)	17(6)	678(3)	3769(5)	29(2)
C(19)	-920(7)	372(3)	3736(6)	40(2)
C(20)	-1756(6)	546(3)	4100(6)	33(2)

C(21)	-1656(6)	1026(3)	4507(6)	33(2)
C(22)	-723(6)	1328(3)	4553(5)	27(2)
C(23)	2297(6)	1248(3)	4813(5)	23(2)
C(24)	2477(6)	818(3)	5468(6)	31(2)
C(25)	3653(6)	738(3)	5921(6)	30(2)
C(26)	4216(6)	1133(2)	5549(5)	23(1)
C(27)	5425(6)	1191(3)	5863(5)	23(1)
C(28)	6162(6)	780(3)	6548(5)	25(2)
C(29)	6265(6)	338(3)	6110(6)	31(2)
C(30)	6863(6)	-63(3)	6744(7)	39(2)
C(31)	7375(7)	-5(3)	7811(7)	43(2)
C(32)	7300(7)	441(3)	8260(6)	41(2)
C(33)	6699(6)	840(3)	7641(6)	30(2)
C(34)	6025(6)	1608(2)	5714(5)	21(1)
C(35)	7261(6)	1704(3)	6203(5)	26(2)
C(36)	7480(6)	2172(3)	5928(6)	28(2)
C(37)	6379(6)	2374(3)	5277(5)	22(1)
C(38)	6199(6)	2870(2)	4938(5)	23(2)
C(39)	7287(6)	3183(3)	5194(5)	26(2)
C(40)	8090(6)	3105(3)	4717(6)	35(2)
C(41)	9100(7)	3391(3)	4976(7)	43(2)
C(42)	9343(7)	3762(3)	5735(7)	40(2)
C(43)	8540(7)	3844(3)	6217(6)	42(2)
C(44)	7517(6)	3557(3)	5931(6)	35(2)
C(45)	1606(7)	2328(4)	1340(6)	44(2)
C(46)	3508(8)	2719(3)	1733(6)	44(2)
C(47)	4435(9)	2365(4)	1759(6)	54(3)
C(48)	5915(8)	1838(4)	2894(8)	60(3)
C(49)	3922(9)	4908(5)	4932(11)	80(3)
C(50)	4815(13)	4773(9)	5784(12)	241(12)
C(51)	5898(11)	4876(14)	5861(14)	370(20)

Table A.3. Bond lengths [Å] and angles [°] for C51 H41 Cl Er N4 O2.

_____

Er(1)-N(2)	2.322(6)
Er(1)-N(3)	2.337(5)
Er(1)-N(4)	2.342(6)
Er(1)-N(1)	2.368(6)
Er(1)-O(1)	2.419(5)
Er(1)-O(2)	2.444(5)
Er(1)-Cl(1)	2.602(2)
O(1)-C(45)	1.414(8)
O(1)-C(46)	1.460(9)
O(2)-C(47)	1.433(9)
O(2)-C(48)	1.439(10)
N(1)-C(1)	1.370(9)
N(1)-C(4)	1.386(8)
N(2)-C(15)	1.375(9)
N(2)-C(12)	1.385(9)
N(3)-C(26)	1.372(8)
N(3)-C(23)	1.386(8)
N(4)-C(34)	1.391(8)
N(4)-C(37)	1.394(8)
C(1)-C(38)	1.392(9)
C(1)-C(2)	1.447(9)
C(2)-C(3)	1.355(9)
C(3)-C(4)	1.431(10)
C(4)-C(5)	1.396(9)
C(5)-C(12)	1.406(10)
C(5)-C(6)	1.496(9)
C(6)-C(7)	1.377(10)
C(6)-C(11)	1.387(10)
C(7)-C(8)	1.422(11)
C(8)-C(9)	1.338(13)
C(9)-C(10)	1.357(12)
C(10)-C(11)	1.393(10)

C(12)-C(13)	1.449(9)
C(13)-C(14)	1.371(10)
C(14)-C(15)	1.422(9)
C(15)-C(16)	1.402(9)
C(16)-C(23)	1.416(9)
C(16)-C(17)	1.511(9)
C(17)-C(18)	1.369(10)
C(17)-C(22)	1.412(10)
C(18)-C(19)	1.394(10)
C(19)-C(20)	1.369(11)
C(20)-C(21)	1.394(11)
C(21)-C(22)	1.378(10)
C(23)-C(24)	1.431(10)
C(24)-C(25)	1.354(9)
C(25)-C(26)	1.454(9)
C(26)-C(27)	1.384(9)
C(27)-C(34)	1.393(9)
C(27)-C(28)	1.513(9)
C(28)-C(29)	1.357(10)
C(28)-C(33)	1.407(10)
C(29)-C(30)	1.407(10)
C(30)-C(31)	1.372(11)
C(31)-C(32)	1.363(12)
C(32)-C(33)	1.396(10)
C(34)-C(35)	1.430(9)
C(35)-C(36)	1.367(10)
C(36)-C(37)	1.420(9)
C(37)-C(38)	1.401(9)
C(38)-C(39)	1.499(9)
C(39)-C(40)	1.377(10)
C(39)-C(44)	1.379(10)
C(40)-C(41)	1.383(10)
C(41)-C(42)	1.392(11)
C(42)-C(43)	1.383(11)

C(43)-C(44)	1.394(10)
C(46)-C(47)	1.467(13)
C(49)-C(51)#1	1.319(10)
C(49)-C(50)	1.323(10)
C(50)-C(51)	1.315(11)
C(51)-C(49)#1	1.319(10)
N(2)-Er(1)-N(3)	76.01(18)
N(2)-Er(1)-N(4)	123.95(18)
N(3)-Er(1)-N(4)	77.41(18)
N(2)-Er(1)-N(1)	77.55(19)
N(3)-Er(1)-N(1)	120.59(18)
N(4)-Er(1)-N(1)	75.17(19)
N(2)-Er(1)-O(1)	77.83(17)
N(3)-Er(1)-O(1)	143.88(17)
N(4)-Er(1)-O(1)	138.52(18)
N(1)-Er(1)-O(1)	76.69(18)
N(2)-Er(1)-O(2)	144.79(19)
N(3)-Er(1)-O(2)	138.94(18)
N(4)-Er(1)-O(2)	78.26(18)
N(1)-Er(1)-O(2)	83.76(18)
O(1)-Er(1)-O(2)	68.90(17)
N(2)-Er(1)-Cl(1)	106.01(15)
N(3)-Er(1)-Cl(1)	83.90(14)
N(4)-Er(1)-Cl(1)	119.03(14)
N(1)-Er(1)-Cl(1)	154.93(14)
O(1)-Er(1)-Cl(1)	79.84(13)
O(2)-Er(1)-Cl(1)	79.67(14)
C(45)-O(1)-C(46)	114.8(6)
C(45)-O(1)-Er(1)	123.9(5)
C(46)-O(1)-Er(1)	112.1(4)
C(47)-O(2)-C(48)	111.3(6)
C(47)-O(2)-Er(1)	114.7(5)
C(48)-O(2)-Er(1)	119.7(5)

C(1)-N(1)-C(4)	106.2(6)
C(1)-N(1)-Er(1)	124.5(4)
C(4)-N(1)-Er(1)	123.6(4)
C(15)-N(2)-C(12)	106.0(5)
C(15)-N(2)-Er(1)	123.0(4)
C(12)-N(2)-Er(1)	124.0(4)
C(26)-N(3)-C(23)	106.2(5)
C(26)-N(3)-Er(1)	126.8(4)
C(23)-N(3)-Er(1)	125.0(4)
C(34)-N(4)-C(37)	106.3(5)
C(34)-N(4)-Er(1)	125.9(4)
C(37)-N(4)-Er(1)	125.3(4)
N(1)-C(1)-C(38)	125.1(6)
N(1)-C(1)-C(2)	109.8(6)
C(38)-C(1)-C(2)	125.0(6)
C(3)-C(2)-C(1)	106.7(6)
C(2)-C(3)-C(4)	107.6(6)
N(1)-C(4)-C(5)	126.2(6)
N(1)-C(4)-C(3)	109.5(6)
C(5)-C(4)-C(3)	124.2(6)
C(4)-C(5)-C(12)	126.0(6)
C(4)-C(5)-C(6)	115.4(6)
C(12)-C(5)-C(6)	118.5(6)
C(7)-C(6)-C(11)	118.3(7)
C(7)-C(6)-C(5)	122.9(7)
C(11)-C(6)-C(5)	118.7(6)
C(6)-C(7)-C(8)	119.5(8)
C(9)-C(8)-C(7)	120.9(8)
C(8)-C(9)-C(10)	120.2(8)
C(9)-C(10)-C(11)	120.3(8)
C(6)-C(11)-C(10)	120.7(8)
N(2)-C(12)-C(5)	125.9(6)
N(2)-C(12)-C(13)	109.5(6)
C(5)-C(12)-C(13)	124.6(6)

C(14)-C(13)-C(12)	106.2(6)
C(13)-C(14)-C(15)	107.5(6)
N(2)-C(15)-C(16)	123.8(6)
N(2)-C(15)-C(14)	110.4(6)
C(16)-C(15)-C(14)	125.6(6)
C(15)-C(16)-C(23)	125.3(6)
C(15)-C(16)-C(17)	119.8(6)
C(23)-C(16)-C(17)	114.7(6)
C(18)-C(17)-C(22)	118.6(6)
C(18)-C(17)-C(16)	120.9(6)
C(22)-C(17)-C(16)	120.5(6)
C(17)-C(18)-C(19)	121.5(7)
C(20)-C(19)-C(18)	119.9(7)
C(19)-C(20)-C(21)	119.5(7)
C(22)-C(21)-C(20)	120.8(7)
C(21)-C(22)-C(17)	119.7(7)
N(3)-C(23)-C(16)	125.2(6)
N(3)-C(23)-C(24)	109.6(6)
C(16)-C(23)-C(24)	125.0(6)
C(25)-C(24)-C(23)	108.0(6)
C(24)-C(25)-C(26)	106.3(6)
N(3)-C(26)-C(27)	126.0(6)
N(3)-C(26)-C(25)	110.0(6)
C(27)-C(26)-C(25)	124.0(6)
C(26)-C(27)-C(34)	127.0(6)
C(26)-C(27)-C(28)	115.7(6)
C(34)-C(27)-C(28)	116.9(6)
C(29)-C(28)-C(33)	119.2(7)
C(29)-C(28)-C(27)	119.6(6)
C(33)-C(28)-C(27)	121.1(6)
C(28)-C(29)-C(30)	120.5(7)
C(31)-C(30)-C(29)	120.1(8)
C(32)-C(31)-C(30)	120.1(8)
C(31)-C(32)-C(33)	120.4(7)

C(32)-C(33)-C(28)	119.7(7)
N(4)-C(34)-C(27)	124.8(6)
N(4)-C(34)-C(35)	108.5(6)
C(27)-C(34)-C(35)	126.5(6)
C(36)-C(35)-C(34)	108.3(6)
C(35)-C(36)-C(37)	106.9(6)
N(4)-C(37)-C(38)	125.1(6)
N(4)-C(37)-C(36)	109.8(6)
C(38)-C(37)-C(36)	124.7(6)
C(1)-C(38)-C(37)	125.6(6)
C(1)-C(38)-C(39)	118.1(6)
C(37)-C(38)-C(39)	115.9(6)
C(40)-C(39)-C(44)	118.0(7)
C(40)-C(39)-C(38)	121.7(6)
C(44)-C(39)-C(38)	120.3(6)
C(39)-C(40)-C(41)	120.9(7)
C(40)-C(41)-C(42)	121.1(7)
C(43)-C(42)-C(41)	118.4(7)
C(42)-C(43)-C(44)	119.7(8)
C(39)-C(44)-C(43)	121.9(7)
O(1)-C(46)-C(47)	110.0(7)
O(2)-C(47)-C(46)	108.5(7)
C(51)#1-C(49)-C(50)	121.1(4)
C(49)-C(50)-C(51)	119.4(4)
C(49)#1-C(51)-C(50)	119.4(4)

_____

Symmetry transformations used to generate equivalent atoms:

#1 -x+1,-y+1,-z+1

Table A.4. Anisotropic displacement parameters ($\mathring{A}^2$x 10^3) for C51 H41 Cl Er N4 O2. The anisotropicdisplacement factor exponent takes the form: $-2\pi^2[$ h^2 $a^{*2}U^{11}$ + ... $+ 2$ h k a* b* U^{12}].

	U^{11}	U^{22}	U^{33}	U^{23}	U^{13}	U^{12}
Er(1)	26(1)	21(1)	15(1)	0(1)	8(1)	0(1)
Cl(1)	90(2)	27(1)	30(1)	-8(1)	23(1)	-9(1)
O(1)	37(3)	36(3)	17(2)	6(2)	6(2)	0(2)
O(2)	39(3)	49(4)	29(3)	2(3)	19(2)	3(3)
N(1)	23(3)	30(3)	13(3)	-2(2)	7(2)	1(2)
N(2)	28(3)	20(3)	14(3)	1(2)	5(2)	-1(2)
N(3)	23(3)	21(3)	15(3)	-2(2)	6(2)	-1(2)
N(4)	29(3)	22(3)	20(3)	1(2)	11(2)	3(2)
C(1)	22(3)	26(4)	20(4)	1(3)	8(3)	-1(3)
C(2)	32(4)	24(4)	39(4)	3(3)	16(3)	-3(3)
C(3)	28(4)	26(4)	30(4)	-1(3)	12(3)	1(3)
C(4)	27(4)	20(4)	18(3)	1(3)	8(3)	1(3)
C(5)	28(4)	23(4)	15(3)	2(3)	6(3)	2(3)
C(6)	18(3)	25(4)	32(4)	0(3)	10(3)	-1(3)
C(7)	36(4)	32(5)	41(5)	-2(4)	-1(4)	0(3)
C(8)	34(5)	35(5)	68(7)	31(5)	-11(4)	-3(4)
C(9)	32(4)	25(4)	65(6)	4(4)	15(4)	3(3)
C(10)	45(5)	27(5)	70(6)	2(4)	36(5)	3(4)
C(11)	31(4)	34(4)	36(4)	-1(4)	15(3)	2(3)
C(12)	22(3)	27(4)	14(3)	0(3)	3(3)	-2(3)
C(13)	23(4)	26(4)	21(4)	3(3)	0(3)	1(3)
C(14)	24(4)	23(4)	27(4)	3(3)	5(3)	0(3)
C(15)	25(4)	23(4)	21(4)	-2(3)	8(3)	1(3)
C(16)	24(4)	25(4)	22(4)	0(3)	10(3)	-2(3)
C(17)	28(4)	25(4)	23(4)	7(3)	6(3)	0(3)
C(18)	32(4)	26(4)	28(4)	1(3)	9(3)	-5(3)
C(19)	44(5)	28(4)	46(5)	-3(4)	15(4)	-11(4)
C(20)	30(4)	31(4)	39(5)	5(3)	15(3)	-8(3)

C(21)	30(4)	37(5)	36(4)	10(4)	16(3)	8(3)
C(22)	31(4)	25(4)	25(4)	2(3)	10(3)	-3(3)
C(23)	27(4)	25(4)	19(3)	0(3)	10(3)	-2(3)
C(24)	30(4)	31(4)	33(4)	4(3)	14(3)	-4(3)
C(25)	32(4)	26(4)	34(4)	9(3)	14(3)	4(3)
C(26)	32(4)	18(4)	19(3)	2(3)	10(3)	3(3)
C(27)	27(4)	24(4)	15(3)	-1(3)	5(3)	2(3)
C(28)	26(4)	21(4)	28(4)	4(3)	9(3)	-3(3)
C(29)	35(4)	27(4)	25(4)	0(3)	3(3)	-1(3)
C(30)	31(4)	28(4)	52(6)	-1(4)	10(4)	0(3)
C(31)	37(5)	31(5)	50(6)	16(4)	2(4)	-1(4)
C(32)	51(5)	39(5)	25(4)	5(4)	5(4)	-6(4)
C(33)	38(4)	25(4)	24(4)	1(3)	6(3)	-5(3)
C(34)	27(4)	22(4)	13(3)	-1(3)	7(3)	3(3)
C(35)	28(4)	24(4)	26(4)	5(3)	9(3)	6(3)
C(36)	23(4)	33(4)	29(4)	0(3)	11(3)	-2(3)
C(37)	21(3)	24(4)	23(4)	1(3)	11(3)	2(3)
C(38)	22(3)	27(4)	21(4)	-3(3)	10(3)	-5(3)
C(39)	27(4)	26(4)	25(4)	0(3)	10(3)	-4(3)
C(40)	31(4)	41(5)	40(5)	-9(4)	20(4)	-9(3)
C(41)	25(4)	59(6)	48(5)	1(4)	17(4)	-5(4)
C(42)	23(4)	47(5)	46(5)	1(4)	8(4)	-11(4)
C(43)	40(5)	44(5)	38(5)	-8(4)	10(4)	-11(4)
C(44)	30(4)	45(5)	32(4)	3(4)	13(3)	-9(4)
C(45)	46(5)	55(6)	21(4)	-5(4)	-1(4)	-1(4)
C(46)	56(6)	51(6)	29(4)	7(4)	19(4)	-12(5)
C(47)	72(6)	74(7)	22(4)	13(4)	25(4)	-5(5)
C(48)	46(6)	89(8)	59(7)	-13(6)	34(5)	7(5)

Table A.5. Hydrogen coordinates (x 10^4) and isotropic displacement parameters ($\mathring{A}^2$x 10^3) for C51 H41 Cl Er N4 O2.

_____

	x	y	z	U(eq)
H(2)	5534	3867	4302	37
H(3)	3383	4027	3714	33
H(7)	447	3595	1867	49
H(8)	-584	4360	1639	65
H(9)	-273	4887	3020	50
H(10)	916	4649	4687	52
H(11)	1896	3884	4966	39
H(13)	-450	2941	2983	31
H(14)	-849	2039	3178	31
H(18)	584	556	3502	35
H(19)	-979	44	3462	48
H(20)	-2399	340	4076	39
H(21)	-2237	1148	4755	40
H(22)	-659	1654	4836	32
H(24)	1878	622	5567	37
H(25)	4033	476	6389	36
H(29)	5931	298	5370	37
H(30)	6914	-374	6433	47
H(31)	7781	-275	8238	52
H(32)	7660	480	8999	49
H(33)	6653	1150	7957	37
H(35)	7831	1480	6644	31
H(36)	8227	2331	6133	34
H(40)	7949	2851	4203	42
H(41)	9637	3333	4630	52
H(42)	10044	3955	5919	48
H(43)	8685	4094	6739	50
H(44)	6962	3622	6254	42

H(45A)	1217	2615	912	67
H(45B)	1088	2184	1670	67
H(45C)	1773	2077	894	67
H(46A)	3867	3013	2171	53
H(46B)	3090	2835	1004	53
H(47A)	4087	2082	1284	65
H(47B)	5020	2530	1522	65
H(48A)	5593	1567	2389	90
H(48B)	6230	1701	3606	90
H(48C)	6547	2006	2741	90
H(49)	3138	4848	4890	96
H(50)	4675	4603	6336	289
H(51)	6545	4796	6483	440

TpErTPP

Table A.6. Crystal data and structure refinement for C53 H37 B Er N10.

Identification code	m_erporm
Empirical formula	C53 H37 B Er N10
Formula weight	992.00
Temperature	133(2) K
Wavelength	0.71073 Å
Crystal system	Orthorhombic
Space group	P2(1)2(1)2(1)
Unit cell dimensions	a = 9.0579(16) Å α= 90°.
	b = 23.340(4) Å β= 90°.
	c = 23.820(4) Å γ = 90°.
Volume	5035.8(15) Å^3
Z	4
Density (calculated)	1.308 Mg/m^3
Absorption coefficient	1.711 mm^{-1}
F(000)	1992
Crystal size	0.40 x 0.15 x 0.05 mm^3
Theta range for data collection	1.22 to 27.57°.
Index ranges	-11<=h<=10, -28<=k<=30, -23<=l<=30
Reflections collected	30688
Independent reflections	11336 [R(int) = 0.0608]
Completeness to theta = 27.57°	98.8 %
Transmission factors	min/max ratio: 0.729
Refinement method	Full-matrix least-squares on F^2
Data / restraints / parameters	11336 / 0 / 586
Goodness-of-fit on F^2	1.035
Final R indices [I>2sigma(I)]	R1 = 0.0469, wR2 = 0.0927
R indices (all data)	R1 = 0.0627, wR2 = 0.1039
Largest diff. peak and hole	1.528 and -1.095 e.Å^{-3}

Table A.7. Atomic coordinates (x 10^4) and equivalent isotropic displacement parameters (Å^2x 10^3) for C53 H37 B Er N10. U(eq) is defined as one third of the trace of the orthogonalized U^{ij} tensor.

	x	y	z	U(eq)
Er(1)	6517(1)	4516(1)	914(1)	21(1)
N(1)	7868(5)	4366(2)	72(2)	23(1)
N(2)	8218(4)	5269(2)	894(2)	23(1)
N(3)	7771(5)	4457(2)	1786(2)	23(1)
N(4)	7302(5)	3551(2)	969(2)	22(1)
N(5)	4365(6)	4251(2)	284(2)	31(1)
N(6)	2966(5)	4434(2)	401(2)	30(1)
N(7)	4998(5)	5404(2)	805(2)	31(1)
N(8)	3498(5)	5394(2)	794(2)	33(1)
N(9)	4367(6)	4404(2)	1582(2)	28(1)
N(10)	2985(5)	4585(2)	1440(2)	30(1)
C(1)	7818(6)	3877(3)	-249(3)	27(1)
C(2)	8141(6)	4022(3)	-823(3)	30(2)
C(3)	8460(7)	4582(3)	-841(2)	31(1)
C(4)	8304(7)	4798(2)	-284(2)	26(1)
C(5)	8671(6)	5359(2)	-128(2)	26(1)
C(6)	9241(7)	5757(3)	-562(3)	31(2)
C(7)	10689(8)	5718(3)	-747(3)	48(2)
C(8)	11255(10)	6113(4)	-1129(3)	62(2)
C(9)	10376(12)	6536(4)	-1331(3)	63(3)
C(10)	8927(10)	6586(4)	-1154(3)	56(2)
C(11)	8358(10)	6193(3)	-766(3)	44(2)
C(12)	8679(6)	5573(2)	429(2)	23(1)
C(13)	9170(7)	6126(3)	589(3)	27(2)
C(14)	9028(6)	6169(3)	1146(3)	26(1)
C(15)	8458(7)	5632(2)	1343(2)	25(1)
C(16)	8264(6)	5486(3)	1907(2)	26(1)
C(17)	8527(8)	5955(2)	2333(2)	29(1)

C(18)	7497(8)	6390(3)	2386(3)	44(2)
C(19)	7708(10)	6834(3)	2761(3)	48(2)
C(20)	8969(11)	6841(3)	3090(3)	55(3)
C(21)	9984(9)	6424(3)	3041(3)	49(2)
C(22)	9795(8)	5966(3)	2655(3)	39(2)
C(23)	8000(6)	4935(3)	2116(2)	23(1)
C(24)	8088(7)	4766(3)	2696(3)	30(2)
C(25)	8002(7)	4198(3)	2713(3)	32(2)
C(26)	7771(7)	3992(3)	2152(2)	24(1)
C(27)	7634(7)	3420(3)	1994(2)	24(1)
C(28)	7751(7)	2977(3)	2442(2)	26(1)
C(29)	6597(8)	2606(2)	2556(2)	33(1)
C(30)	6725(9)	2176(3)	2963(3)	39(2)
C(31)	8043(8)	2120(3)	3245(3)	42(2)
C(32)	9199(8)	2479(3)	3144(3)	39(2)
C(33)	9061(7)	2910(3)	2739(3)	34(2)
C(34)	7459(6)	3216(3)	1441(2)	23(1)
C(35)	7552(7)	2625(3)	1291(3)	27(1)
C(36)	7484(6)	2597(2)	725(2)	23(1)
C(37)	7367(6)	3177(3)	524(3)	22(1)
C(38)	7531(6)	3324(2)	-41(2)	22(1)
C(39)	7495(6)	2827(3)	-448(2)	25(1)
C(40)	6233(6)	2490(2)	-479(2)	26(1)
C(41)	6211(6)	2009(2)	-824(3)	30(2)
C(42)	7452(7)	1872(3)	-1137(3)	30(2)
C(43)	8691(7)	2208(3)	-1111(2)	28(1)
C(44)	8727(6)	2684(2)	-773(2)	26(1)
C(45)	4251(8)	3960(3)	-201(3)	37(2)
C(46)	2804(7)	3952(3)	-395(3)	37(2)
C(47)	2014(7)	4253(3)	3(3)	33(2)
C(48)	5346(7)	5958(3)	714(3)	39(2)
C(49)	4121(8)	6294(3)	643(3)	49(2)
C(50)	2967(7)	5923(3)	698(3)	45(2)
C(51)	4264(8)	4221(3)	2110(3)	41(2)

C(52)	2823(8)	4286(3)	2319(3)	44(2)
C(53)	2059(7)	4504(3)	1881(3)	40(2)
B(1)	2599(7)	4842(3)	871(4)	31(2)

_____

Table A.8. Bond lengths [Å] and angles [°] for C53 H37 B Er N10.

_____

Er(1)-N(2)	2.337(4)
Er(1)-N(4)	2.366(4)
Er(1)-N(3)	2.371(4)
Er(1)-N(1)	2.375(5)
Er(1)-N(7)	2.500(5)
Er(1)-N(9)	2.528(5)
Er(1)-N(5)	2.538(5)
N(1)-C(1)	1.375(8)
N(1)-C(4)	1.376(7)
N(2)-C(15)	1.380(7)
N(2)-C(12)	1.381(7)
N(3)-C(23)	1.380(7)
N(3)-C(26)	1.392(8)
N(4)-C(37)	1.374(7)
N(4)-C(34)	1.376(7)
N(5)-C(45)	1.345(8)
N(5)-N(6)	1.367(7)
N(6)-C(47)	1.351(7)
N(6)-B(1)	1.506(9)
N(7)-C(48)	1.350(8)
N(7)-N(8)	1.359(6)
N(8)-C(50)	1.343(8)
N(8)-B(1)	1.537(8)
N(9)-C(51)	1.332(8)
N(9)-N(10)	1.364(7)
N(10)-C(53)	1.355(7)
N(10)-B(1)	1.522(9)
C(1)-C(38)	1.406(8)
C(1)-C(2)	1.439(8)
C(2)-C(3)	1.338(8)
C(3)-C(4)	1.428(8)
C(4)-C(5)	1.402(8)

C(5)-C(12)	1.417(8)
C(5)-C(6)	1.481(8)
C(6)-C(11)	1.382(9)
C(6)-C(7)	1.387(9)
C(7)-C(8)	1.395(9)
C(8)-C(9)	1.356(11)
C(9)-C(10)	1.383(12)
C(10)-C(11)	1.400(10)
C(12)-C(13)	1.419(8)
C(13)-C(14)	1.336(8)
C(14)-C(15)	1.436(8)
C(15)-C(16)	1.398(8)
C(16)-C(23)	1.400(9)
C(16)-C(17)	1.510(8)
C(17)-C(22)	1.382(9)
C(17)-C(18)	1.385(9)
C(18)-C(19)	1.381(10)
C(19)-C(20)	1.385(11)
C(20)-C(21)	1.344(11)
C(21)-C(22)	1.418(9)
C(23)-C(24)	1.439(9)
C(24)-C(25)	1.330(8)
C(25)-C(26)	1.435(9)
C(26)-C(27)	1.393(8)
C(27)-C(34)	1.411(8)
C(27)-C(28)	1.490(8)
C(28)-C(29)	1.384(9)
C(28)-C(33)	1.390(8)
C(29)-C(30)	1.401(8)
C(30)-C(31)	1.376(10)
C(31)-C(32)	1.363(10)
C(32)-C(33)	1.400(9)
C(34)-C(35)	1.427(8)
C(35)-C(36)	1.350(8)

C(36)-C(37)	1.441(8)
C(37)-C(38)	1.397(8)
C(38)-C(39)	1.513(8)
C(39)-C(40)	1.390(8)
C(39)-C(44)	1.400(8)
C(40)-C(41)	1.391(8)
C(41)-C(42)	1.386(8)
C(42)-C(43)	1.372(9)
C(43)-C(44)	1.373(8)
C(45)-C(46)	1.390(8)
C(46)-C(47)	1.380(9)
C(48)-C(49)	1.369(9)
C(49)-C(50)	1.365(9)
C(51)-C(52)	1.405(9)
C(52)-C(53)	1.353(10)
N(2)-Er(1)-N(4)	121.26(14)
N(2)-Er(1)-N(3)	75.29(17)
N(4)-Er(1)-N(3)	75.64(17)
N(2)-Er(1)-N(1)	75.78(16)
N(4)-Er(1)-N(1)	75.60(16)
N(3)-Er(1)-N(1)	118.96(15)
N(2)-Er(1)-N(7)	74.81(15)
N(4)-Er(1)-N(7)	163.71(15)
N(3)-Er(1)-N(7)	113.79(17)
N(1)-Er(1)-N(7)	108.54(17)
N(2)-Er(1)-N(9)	126.74(17)
N(4)-Er(1)-N(9)	95.65(16)
N(3)-Er(1)-N(9)	79.15(16)
N(1)-Er(1)-N(9)	155.90(16)
N(7)-Er(1)-N(9)	74.16(16)
N(2)-Er(1)-N(5)	132.66(17)
N(4)-Er(1)-N(5)	91.79(16)
N(3)-Er(1)-N(5)	150.71(17)

N(1)-Er(1)-N(5)	81.94(17)
N(7)-Er(1)-N(5)	73.59(16)
N(9)-Er(1)-N(5)	75.86(16)
C(1)-N(1)-C(4)	105.9(5)
C(1)-N(1)-Er(1)	125.1(4)
C(4)-N(1)-Er(1)	124.1(4)
C(15)-N(2)-C(12)	105.0(4)
C(15)-N(2)-Er(1)	123.3(4)
C(12)-N(2)-Er(1)	127.0(4)
C(23)-N(3)-C(26)	105.8(4)
C(23)-N(3)-Er(1)	121.6(4)
C(26)-N(3)-Er(1)	126.5(4)
C(37)-N(4)-C(34)	105.3(5)
C(37)-N(4)-Er(1)	125.1(4)
C(34)-N(4)-Er(1)	128.1(4)
C(45)-N(5)-N(6)	105.2(5)
C(45)-N(5)-Er(1)	133.7(4)
N(6)-N(5)-Er(1)	121.0(4)
C(47)-N(6)-N(5)	110.5(5)
C(47)-N(6)-B(1)	125.4(5)
N(5)-N(6)-B(1)	123.7(5)
C(48)-N(7)-N(8)	104.2(5)
C(48)-N(7)-Er(1)	133.0(4)
N(8)-N(7)-Er(1)	122.6(3)
C(50)-N(8)-N(7)	110.3(5)
C(50)-N(8)-B(1)	127.0(5)
N(7)-N(8)-B(1)	122.7(5)
C(51)-N(9)-N(10)	105.6(5)
C(51)-N(9)-Er(1)	132.9(4)
N(10)-N(9)-Er(1)	121.3(4)
C(53)-N(10)-N(9)	109.4(5)
C(53)-N(10)-B(1)	127.0(5)
N(9)-N(10)-B(1)	123.6(5)
N(1)-C(1)-C(38)	124.8(5)

N(1)-C(1)-C(2)	109.1(5)
C(38)-C(1)-C(2)	126.1(6)
C(3)-C(2)-C(1)	107.8(6)
C(2)-C(3)-C(4)	107.0(5)
N(1)-C(4)-C(5)	126.2(5)
N(1)-C(4)-C(3)	110.1(5)
C(5)-C(4)-C(3)	123.5(5)
C(4)-C(5)-C(12)	125.2(5)
C(4)-C(5)-C(6)	118.9(5)
C(12)-C(5)-C(6)	115.5(5)
C(11)-C(6)-C(7)	118.9(7)
C(11)-C(6)-C(5)	120.3(6)
C(7)-C(6)-C(5)	120.6(6)
C(6)-C(7)-C(8)	120.8(7)
C(9)-C(8)-C(7)	119.8(8)
C(8)-C(9)-C(10)	120.7(8)
C(9)-C(10)-C(11)	119.7(8)
C(6)-C(11)-C(10)	120.1(8)
N(2)-C(12)-C(5)	124.8(5)
N(2)-C(12)-C(13)	110.3(5)
C(5)-C(12)-C(13)	125.0(5)
C(14)-C(13)-C(12)	107.8(6)
C(13)-C(14)-C(15)	107.1(6)
N(2)-C(15)-C(16)	125.1(5)
N(2)-C(15)-C(14)	109.9(5)
C(16)-C(15)-C(14)	124.9(5)
C(15)-C(16)-C(23)	125.9(5)
C(15)-C(16)-C(17)	116.7(5)
C(23)-C(16)-C(17)	117.0(5)
C(22)-C(17)-C(18)	119.7(6)
C(22)-C(17)-C(16)	121.2(6)
C(18)-C(17)-C(16)	119.1(6)
C(19)-C(18)-C(17)	121.1(7)
C(18)-C(19)-C(20)	119.3(7)

C(21)-C(20)-C(19)	120.4(7)
C(20)-C(21)-C(22)	121.3(8)
C(17)-C(22)-C(21)	118.3(7)
N(3)-C(23)-C(16)	124.5(5)
N(3)-C(23)-C(24)	109.5(5)
C(16)-C(23)-C(24)	125.6(5)
C(25)-C(24)-C(23)	107.4(6)
C(24)-C(25)-C(26)	108.2(7)
N(3)-C(26)-C(27)	125.2(5)
N(3)-C(26)-C(25)	108.9(5)
C(27)-C(26)-C(25)	125.8(6)
C(26)-C(27)-C(34)	125.9(6)
C(26)-C(27)-C(28)	117.8(5)
C(34)-C(27)-C(28)	116.2(5)
C(29)-C(28)-C(33)	118.4(6)
C(29)-C(28)-C(27)	121.4(6)
C(33)-C(28)-C(27)	120.2(6)
C(28)-C(29)-C(30)	121.4(7)
C(31)-C(30)-C(29)	118.6(7)
C(32)-C(31)-C(30)	121.4(6)
C(31)-C(32)-C(33)	119.7(7)
C(28)-C(33)-C(32)	120.5(6)
N(4)-C(34)-C(27)	125.6(5)
N(4)-C(34)-C(35)	110.6(5)
C(27)-C(34)-C(35)	123.6(6)
C(36)-C(35)-C(34)	107.1(6)
C(35)-C(36)-C(37)	106.8(6)
N(4)-C(37)-C(38)	126.3(6)
N(4)-C(37)-C(36)	110.1(5)
C(38)-C(37)-C(36)	122.9(5)
C(37)-C(38)-C(1)	125.8(5)
C(37)-C(38)-C(39)	115.3(5)
C(1)-C(38)-C(39)	118.8(5)
C(40)-C(39)-C(44)	119.4(5)

C(40)-C(39)-C(38)	119.1(5)
C(44)-C(39)-C(38)	121.4(5)
C(39)-C(40)-C(41)	120.0(5)
C(42)-C(41)-C(40)	119.5(5)
C(43)-C(42)-C(41)	120.5(6)
C(42)-C(43)-C(44)	120.6(6)
C(43)-C(44)-C(39)	119.9(6)
N(5)-C(45)-C(46)	111.4(6)
C(47)-C(46)-C(45)	104.7(6)
N(6)-C(47)-C(46)	108.1(6)
N(7)-C(48)-C(49)	112.3(6)
C(50)-C(49)-C(48)	104.2(6)
N(8)-C(50)-C(49)	109.0(6)
N(9)-C(51)-C(52)	111.4(7)
C(53)-C(52)-C(51)	104.0(6)
C(52)-C(53)-N(10)	109.5(6)
N(6)-B(1)-N(10)	111.3(5)
N(6)-B(1)-N(8)	108.9(5)
N(10)-B(1)-N(8)	108.4(5)

_____

Symmetry transformations used to generate equivalent atoms:

Table A.9. Anisotropic displacement parameters $(\text{Å}^2 \text{x } 10^3)$ for C53 H37 B Er N10. The anisotropic displacement factor exponent takes the form: $-2\pi^2[\,h^2\,a^{*2}U^{11} + ... + 2\,h\,k\,a^*\,b^*\,U^{12}\,]$.

	U^{11}	U^{22}	U^{33}	U^{23}	U^{13}	U^{12}
Er(1)	15(1)	24(1)	25(1)	-2(1)	-2(1)	1(1)
N(1)	17(2)	25(3)	26(3)	-3(2)	-1(2)	-1(2)
N(2)	16(2)	30(2)	24(2)	0(2)	-4(2)	2(2)
N(3)	19(2)	25(3)	26(2)	-3(2)	-3(2)	2(2)
N(4)	19(2)	23(2)	23(3)	-4(2)	-2(2)	-3(2)
N(5)	16(3)	33(3)	43(3)	-2(3)	-10(2)	5(2)
N(6)	16(2)	33(3)	41(3)	2(3)	-3(2)	1(2)
N(7)	13(2)	31(3)	49(4)	-8(3)	-4(2)	2(2)
N(8)	21(2)	28(3)	49(3)	-5(2)	1(3)	2(2)
N(9)	23(3)	34(3)	27(3)	-3(2)	-1(2)	3(2)
N(10)	17(2)	35(3)	38(3)	-8(3)	3(2)	1(2)
C(1)	17(3)	40(4)	23(3)	1(3)	0(3)	5(3)
C(2)	24(3)	33(3)	31(4)	-3(3)	-3(3)	2(2)
C(3)	34(3)	36(3)	22(3)	3(3)	2(3)	6(3)
C(4)	21(3)	30(3)	28(3)	1(2)	-7(3)	0(3)
C(5)	16(3)	26(3)	37(3)	0(2)	0(3)	0(2)
C(6)	40(4)	27(3)	26(3)	-6(3)	-11(3)	0(3)
C(7)	46(5)	50(4)	47(5)	11(3)	12(3)	2(4)
C(8)	60(6)	75(6)	50(5)	13(4)	20(4)	-7(5)
C(9)	92(7)	56(6)	40(5)	16(4)	-8(5)	-18(5)
C(10)	67(6)	51(5)	51(5)	15(4)	-23(4)	1(4)
C(11)	46(4)	40(4)	45(4)	13(3)	-13(4)	-8(4)
C(12)	14(3)	21(3)	33(3)	0(2)	-3(2)	4(2)
C(13)	17(3)	31(4)	33(4)	-3(3)	-2(3)	0(3)
C(14)	17(3)	27(3)	35(4)	-4(3)	-4(3)	3(2)
C(15)	20(3)	25(3)	29(3)	-5(2)	-3(3)	1(3)
C(16)	24(3)	31(3)	25(3)	-9(3)	-6(2)	1(3)
C(17)	29(3)	26(3)	32(3)	-6(2)	1(3)	-6(3)

C(18)	35(4)	52(5)	44(5)	-7(4)	3(3)	8(4)
C(19)	56(5)	41(5)	46(5)	-13(4)	14(4)	3(4)
C(20)	101(8)	30(4)	33(4)	-9(3)	14(4)	-10(4)
C(21)	66(6)	45(5)	36(4)	-7(3)	-8(4)	-23(4)
C(22)	42(4)	36(4)	40(4)	-5(3)	-6(3)	-5(3)
C(23)	17(3)	31(3)	22(3)	-6(3)	-4(2)	1(2)
C(24)	33(4)	31(3)	27(3)	-10(3)	2(3)	-2(3)
C(25)	36(4)	36(4)	24(4)	1(3)	-1(3)	0(3)
C(26)	22(3)	32(4)	18(3)	-1(3)	0(3)	-1(3)
C(27)	20(3)	26(3)	27(3)	3(3)	1(2)	-1(3)
C(28)	25(3)	29(4)	22(3)	-3(3)	-2(3)	1(3)
C(29)	30(3)	35(3)	33(3)	-2(3)	-3(3)	5(3)
C(30)	52(5)	29(3)	35(4)	2(3)	6(4)	-6(3)
C(31)	63(5)	33(4)	31(4)	12(3)	5(3)	12(3)
C(32)	36(4)	42(4)	38(4)	14(3)	-3(3)	7(3)
C(33)	30(3)	35(4)	35(4)	4(3)	-1(3)	6(3)
C(34)	13(3)	30(3)	26(3)	1(3)	0(2)	0(2)
C(35)	21(3)	28(3)	32(4)	3(3)	-1(3)	1(3)
C(36)	20(3)	22(3)	28(3)	-1(2)	-3(2)	-2(2)
C(37)	12(3)	23(3)	32(3)	-1(3)	-2(2)	2(2)
C(38)	14(3)	25(3)	27(3)	-3(3)	1(2)	0(2)
C(39)	20(3)	31(3)	23(3)	2(3)	0(2)	2(3)
C(40)	22(3)	36(3)	20(3)	-1(2)	0(2)	3(3)
C(41)	22(3)	30(3)	38(4)	1(3)	-1(3)	-4(2)
C(42)	38(4)	27(3)	26(3)	-5(3)	-2(3)	11(3)
C(43)	24(4)	35(3)	26(3)	-2(2)	3(3)	7(3)
C(44)	20(3)	30(3)	27(3)	-1(2)	-2(2)	2(3)
C(45)	28(4)	40(4)	42(4)	-7(3)	-8(3)	0(3)
C(46)	32(4)	38(4)	42(4)	-10(3)	-15(3)	-5(3)
C(47)	25(3)	29(3)	44(4)	4(3)	-10(3)	-1(3)
C(48)	21(3)	38(4)	57(5)	3(3)	-1(3)	0(3)
C(49)	24(4)	32(4)	92(6)	6(4)	1(4)	2(3)
C(50)	23(3)	37(4)	74(6)	2(4)	-1(3)	11(3)
C(51)	27(4)	59(5)	38(4)	-4(4)	4(3)	-2(3)

C(52)	35(4)	64(5)	32(4)	0(4)	16(3)	-1(3)
C(53)	20(3)	55(4)	44(4)	-11(4)	7(3)	-1(4)
B(1)	17(3)	43(4)	33(4)	-1(4)	0(3)	-4(3)

_____

Table A.10. Hydrogen coordinates (x 10^4) and isotropic displacement parameters (Å^{2}x 10 ^{3}) for C53 H37 B Er N10.

_____

	x	y	z	U(eq)

_____

	x	y	z	U(eq)
H(2)	8131	3767	-1133	35
H(3)	8738	4795	-1164	37
H(7)	11303	5418	-611	57
H(8)	12254	6087	-1248	74
H(9)	10758	6800	-1597	75
H(10)	8321	6885	-1295	67
H(11)	7364	6226	-643	52
H(13)	9535	6415	344	32
H(14)	9261	6494	1369	32
H(18)	6630	6382	2162	52
H(19)	6997	7131	2792	57
H(20)	9117	7142	3352	66
H(21)	10845	6436	3268	59
H(22)	10523	5675	2620	47
H(24)	8189	5015	3009	36
H(25)	8080	3967	3041	38
H(29)	5699	2644	2353	40
H(30)	5920	1929	3043	46
H(31)	8150	1824	3516	51
H(32)	10094	2437	3347	47
H(33)	9868	3160	2667	40
H(35)	7645	2311	1541	33
H(36)	7509	2259	502	28

H(40)	5385	2588	-265	31
H(41)	5353	1776	-845	36
H(42)	7443	1542	-1371	36
H(43)	9533	2111	-1330	34
H(44)	9588	2917	-761	31
H(45)	5057	3782	-388	44
H(46)	2439	3778	-728	44
H(47)	979	4320	-2	39
H(48)	6330	6099	701	46
H(49)	4083	6694	573	59
H(50)	1952	6022	672	54
H(51)	5064	4067	2320	50
H(52)	2466	4196	2684	53
H(53)	1033	4588	1881	48

Sean Owen Clancy   Aaron Wayne Harper

ABSTRACT

DESIGN AND SYNTHESES OF POLYMERIC MATERIALS FOR VISIBLE AND NEAR-INFRARED EMITTING APPLICATIONS

Several classes of polyphenylene-type polymeric materials were synthesized according to several different design parameters, with the end results of each being able to sensitize small molecule organics or lanthanide chelates as dopants which emit energy in the visible and/or near-infrared regions of the electromagnetic spectrum. The goal of this research was to create materials that would emit in the near-infrared. The first group of materials was *para-para* linked polyphenylene-type polymers doped with several small molecule organic dyes. The second group was *para-para* and *para-meta* linked polyphenylene-type polymers doped with a series of Coumarins and a couple metalloporphines. The third group was *para-meta* linked polyphenylene-type polymers with pendant terpyridine groups. The fourth group was *para-meta* linked polyphenylene-type polymers with various pendant *beta*-diketonates to which europium complexes were bound. The fifth group was *para-meta* linked polyphenylene-type polymers with various pendant *beta*-diketonates to which erbium-porphyrinate complexes were bound.

The first and second groups served as preliminary studies on the energy transfer properties of polymers to organic dyes. With a better understanding of how doped conjugated polymers behaved, other polymers were designed with specific structural properties that lead to the desired photophysical properties. This

elaboration of structure-property relationships also lead to the pendant groups to which the lanthanides would be datively or covalently bonded to the polymer, as was studied with the third and fourth groups, respectively. Upon this foundation, the fifth group of materials reached the goal of having polymeric-materials that emitted energy in the near-infrared region of the electromagnetic spectrum.